
Dissertation zur Erlangung des Doktorgrades
der Fakultät für Chemie und Pharmazie
der Ludwig-Maximilians-Universität München

**Formulation and Characterization of siRNA containing
Polyplexes as Dry Powder for Pulmonary Delivery**



Tobias Wolfgang Mathias Keil

aus

Gräfelfing, Deutschland

2020

Erklärung:

Diese Dissertation wurde im Sinne von § 7 der Promotionsordnung vom 28. November 2011 von Frau Prof. Dr. Olivia Merkel betreut.

Eidesstattliche Versicherung

Diese Dissertation wurde eigenständig und ohne unerlaubte Hilfe erarbeitet.

München, 21.07.2020

Tobias Keil

Dissertation eingereicht am: 08.06.2020

1.Gutachterin / 1. Gutachter: Prof. Dr. Olivia Merkel

2.Gutachterin / 2. Gutachter: Prof. Dr. Wolfgang Frieß

Mündliche Prüfung am: 03.07.2020

Für meine Eltern und Marlene

„Wer am Ende ist, kann von vorn anfangen,
denn das Ende ist der Anfang von der anderen Seite.“

- Karl Valentin

Index

I	Introduction	1
	1. Spray Drying	
	2. Small Interfering RNA	
	3. Spray Drying of Small Interfering RNA	
II	Aims of Thesis	11
III	Dry Powder Inhalation of siRNA	13
IV	Characterization of Spray Dried Powders with Nucleic Acid-containing PEI Nanoparticles.....	17
	1. Abstract	
	2. Introduction	
	3. Materials and Methods	
	4. Results and Discussions	
	5. Conclusion	
	6. Acknowledgements	
	7. Supplementary Data	
V	Evaluation of Tubing Material on Adsorption of DNA-PEI Polyplexes.....	43
	1. Abstract	
	2. Graphical Abstract	
	3. Introduction	
	4. Materials and Methods	
	5. Results and Discussion	
	6. Conclusion	
	7. Acknowledgements	
VI	T_H2-cell targeted pulmonary siRNA delivery for the treatment of asthma.....	57
	1. Abstract	
	2. Graphical/Visual Abstract and Caption	
	3. Introduction	
	4. T _H 2-cell Targeting	
	5. Optimization of Endosomal Release: Tf-Mel-PEI	
	6. Pulmonary Delivery of Nucleic Acids	
	7. Dry Powder Formulation	
	8. Conclusion	
	9. Funding Information	
	10. Acknowledgements	

VII	Successful Spray Drying of siRNA - evaluation of crystalline and amorphous substances on the drug quantity and quality of inhalable nano in microparticles.....	73
	1. Abstract	
	2. Introduction	
	3. Materials and Methods	
	4. Results and Discussion	
	5. Conclusion and Outlook	
	6. Acknowledgements	
	7. Supplementary Data	
VIII	New Characterization Technique of Polyplexes by TRPS.....	105
	1. Abstract	
	2. Introduction	
	3. Materials	
	4. Methods	
	5. Results and Discussion	
	6. Conclusions	
	7. Acknowledgements	
IX	Summary and Outlook	117
X	Publication List.....	121
XI	Reference List	123
XII	Acknowledgements.....	137

Chapter I)

Introduction

I Introduction

I.1. Spray Drying

For almost 150 years spray drying has been applied to dry substances. [1] From the first application in food industries to produce microparticle powders which were almost free of water and therefore easier and cheaper to transport, the technique has also attracted interest in the pharmaceutical industry. [2] Developments which allowed the predictable tuning of particle size and shape as well as the amount of residual moisture makes it an important tool until today. Spray drying (SD) can be performed in three different fashions: Co-current, counter-current and combined flow (Figure I.1.) with different effects on product temperature and subsequently on moisture content: When operating in a co-current flow (Figure I.1.A) the liquid is sprayed in the same direction as the flow of drying air. Droplets are exposed to heat when the moisture content is the highest. Due to drying and water evaporation which generates a cooler surrounding, the product is treated with the most caution but the final product contains higher residual moistures as compared to the other two techniques: Counter current flow is optimal (Figure I.1.B) for generating powders with nearly no residual moisture. This is attributed to the fact that the droplets and eventually the powder are streaming against a flow of gas with increasing temperature. Although complete removal of water might be favorable for some substances, the process might also interfere with stability of others such as thermolabile products which are subjected to higher temperatures. In a combined flow (Figure I.1.C) both techniques are joined: the product solution is sprayed in upwards direction against a downstream flow of drying gas. The product is exposed to the hottest temperatures only for a short time allowing efficient water removal before being redirected by gravitational forces into a cooler zone. Hence, efficient drying is achieved with caution towards product thermo stability. [3, 4]

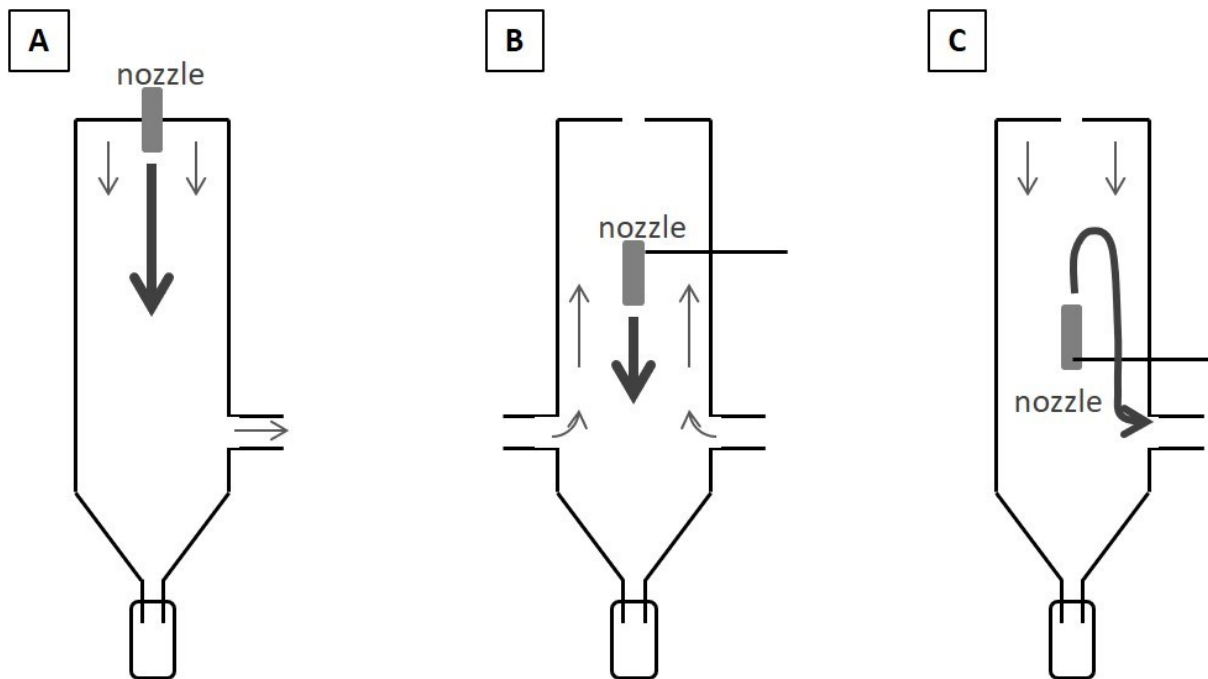


Figure I.1. Spray drying in **A)** Co-current flow, **B)** Counter-current flow and **C)** Combined; Big black arrows indicate flow of droplets; small grey arrows indicate flow of drying gas.

SD is characterized by three main steps: starting from the atomization of the liquid stream, the generated droplets are exposed to a drying gas heated above room temperature and are consecutively separated by a suitable device. Atomization is the process of generating a liquid/gas aerosol. This process allows for a vastly increased surface area of the liquid and a subsequently very efficient heat transfer from gas to droplets. As a consequence, water evaporates creating a cooled environment around the forming particle. This leads to a 'protective area' when using a co-current flow as described above. The particle temperature therefore never reaches the spray nozzle inlet temperature (T_{In}). The product temperature is considered to reach the temperature which is measured at the outlet point of the drying chamber, i.e. outlet temperature (T_{Out}). [2] In a combined flow, the product temperature is exposed to the heat only for a few milliseconds and does not reach T_{In} but is equal to T_{Out} . In a counter current flow however, water is nearly completely removed and the product temperature is equal to T_{In} .

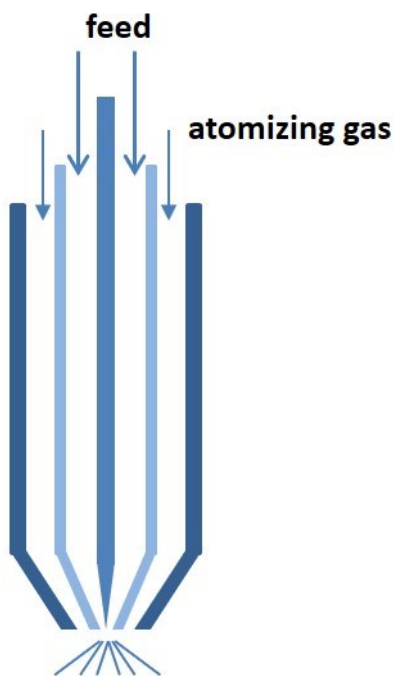


Figure I.2. Two fluid nozzle feeding and atomizing gas are guided independently and get into contact just after leaving the nozzle; frictional forces lead to the atomizing of the feeding solution.

Atomization can be achieved by different devices. Amongst the most popular devices are pneumatic nozzles. These devices use compressed carrier gas to create frictional forces which atomize the liquid into small droplets. In Figure I.2. a two-fluid nozzle is depicted. Here the liquid solution is pumped through the inner part of the nozzle and meets the atomizing gas at the outlet. As a consequence of interfering streams atomization takes place. Beside two fluid nozzles, three fluid nozzles (two atomizing gases, one feed solution) and four fluid nozzles (one atomizing gas, two feed solutions) are also available and allow for more sophisticated applications. Despite the broadened applicability introduced by the different nozzle types, the two-fluid nozzle is the most abundant one. Its application ranges from microencapsulation, preparation of granules, solid dispersions, self-emulsifying drug delivery systems, protein powders to dry powders for pulmonary administration [2, 4-11].

Especially with the appearance of inhalable insulin in 2016 as marketed under the trademark of Exubera™ by Pfizer, spray drying gathered particular attraction in the field of pulmonary delivery of therapeutic macromolecules. [11, 12] Although off market due to various problems, it was a milestone in the formulation of inhalable proteins as first-in-class. Insulin is a ~5.7 kDa heavy polypeptide consisting of ~51 amino acids arranged into two chains forming two nearly antiparallel α -helices in one chain, and one α -helix and one β -strand in the second. Preservation of these secondary structures as well as the quaternary structure is necessary to keep its biological activity. [13, 14] Loss of structure can be induced by self-interaction under certain conditions with deamidation as a result of acidification and oxidation processes. [13] Also, hydrogen bonds are necessary to preserve the protein structure. During spray drying, water is removed, reducing the amount of hydrogen bridges in a protein and thus affecting protein structure and activity. Hence, formulation plays a central role for structural conservation: in Exubera™, recombinant human insulin was formulated at a high concentration of 60% w/w in combination with mannitol, glycine and

sodium citrate. [15] Process parameters were chosen to generate particles which are of amorphous state. [16] This unordered and non-crystalline state owns most of the characteristics of a liquid but with a viscosity comparable to solids. Importantly, it was shown that amorphous products can stabilize proteins much better than their crystalline counter parts which is the most plausible reason for the generation of an amorphous matrix in the Exubera™ formulation. [8-10] For obtaining amorphous mannitol, the feeding rate and the aspirator has to be maximized in order to obtain a very quick drying process and hence a very humid product. [17] As mannitol is a not a good glass former, the addition of glycine in this formulation acts as glassy stabilizer and is aiding in forming an amorphous state [18]. However, as mentioned before, the obtained products contain comparably high percentages of residual moisture which results in an amorphous solid state which is less stable than a crystalline formulation. Instability is caused by the fact, that amorphous structures are thermodynamically labile and tend to rearrange into crystalline structures over storage, possibly destabilizing the protein structure. This process is particularly observed above the so-called glass transition temperature where the substance transits from a vitreous to a honey like state. Residual moisture in the product causes this transition temperature to decrease. [19] A decrease, however, in the glass transition temperature leads to a less stable formulation and recrystallization is likely to occur at lower temperatures, thereby impeding the performance of biopharmaceuticals in spray dried formulations. [20] Therefore, Exubera™ was subjected to a secondary drying step reducing the amount of water to approximately 1.5% and increasing the glass transition temperature. These steps enabled the formulation to stabilize insulin in an amorphous phase while increasing the shelf life at room temperature to 2 years. [11, 16, 18]

Although stabilization plays a key role in the formulation, the active ingredient most importantly needs to reach its site of action. Regarding drug delivery to the lung, as aimed for with the application of Exubera™, special interest needs to be paid to the aerosol characteristics of the formulation. The aerodynamic diameter, one of the most relevant parameters, differs from the geometric diameter and is considered as the diameter of a particle which has the same velocity as a sphere of unit density in an air stream. [21] The aerodynamic diameter depends on the shape, density and geometric diameter of particles. For successful lung targeting, microparticles need to be produced with a mass mean aerodynamic diameter (MMAD) of approximately 1 to 5 µm. Particles above 5 µm

undergo inertial impaction in the oropharynx and the conductive airways and are subject to mucociliary clearance. Particles between approximately 1 and 5 μm mostly deposit in the deep lung area due to sedimentation, whereas deposition of particles between 0.5 and 1 μm in size depends on diffusion and hence Brown motion. [21-23] While particles between 2 and 5 μm can reach deep lung areas and are preferred for local treatments, particles between 1 and 2 μm in size are probably most efficient in system delivery. [21] It has to be noted that for pharmaceutical application particles below 0.5 μm are considered to be exhaled but in fact literature shows an increasing lung deposition the smaller the particles get, e.g. 0.04 μm . [22, 24] Although delivery might be possible, generation of such small particles for inhalation and a mass relevant deposition of such is challenging and not profitable compared to the preparation and application of microparticles between 1 and 5 μm . For Exubera™ a MMAD of approximately 2 μm was reached enabling successful delivery to the lungs. This characteristic was mainly influenced by the powder itself and hence its preparation technique i.e. spray drying. [11] The development of Exubera™ is a very interesting story as it demonstrated successful delivery of a biopharmaceutical through the lungs for the first time in history.

1.2. Small Interfering RNA

First notion of a specific gene downregulation mechanism was observed in 1991 when Fire and colleagues introduced plasmid DNA of two genes in reverse orientation into the embryo of *Caenorhabditis elegans*. [25] Over nearly the following decade these mechanisms were investigated to fully understand that double stranded RNA is the key for downregulating homologous mRNA without altering the transcription rate of the latter (Figure 1.3.). [26-28] This process is known as RNA interference (RNAi). It was discovered that the introduced double stranded RNA is processed via so called Dicer enzymes into molecules of a size of ~21-25 base pairs with two-nucleotide 3' overhangs and 5' -phosphate termini. [29]

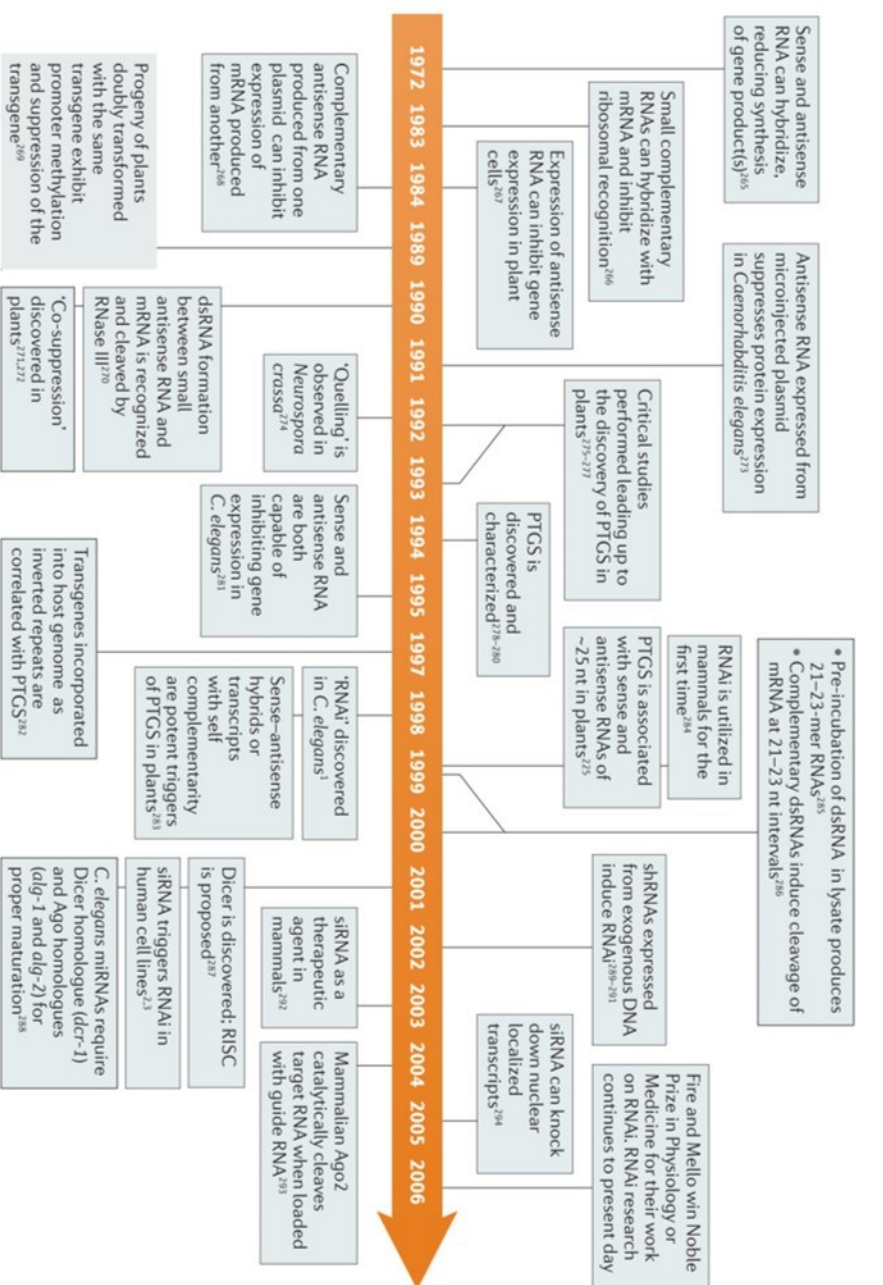


Figure 1.3. Early events in the discovery and elucidation of the RNAi pathway. A timeline of important developments leading up to the discovery of RNAi in animals is shown. Ago, Argonaute; dsRNA, double-stranded RNA; nt, nucleotide; PTGS, post-transcriptional gene silencing; RISC, RNA-induced silencing complex; shRNA, short hairpin RNA; siRNA, small interfering RNA. Reprint with permission from Springer Nature from [26].

These small interfering RNA's (siRNA) consist of a guide and a passenger strand and are incorporated into a ~100 kDa heavy multicomponent endonuclease complex called RNA-induced silencing complex (RISC) where upon activation the passenger strand is removed. The guide strand directs the complex to the homologous region of the mRNA by Watson-Crick base-pairing. [30] Ultimately, targeted mRNA is degraded by RISC's endonuclease activity preventing the translation to proteins (Figure I.4.). [31]

Until today, the application of siRNA is the most preferred way to induce RNAi. [26] Unfortunately, the development of new therapeutics based on this unique mechanism is rather slow: After the discovery of RNAi in 1998 it took >20 years for the first medicine to reach the market despite tremendous efforts. Reasons lie in the chemical structure of siRNA itself: great susceptibility to degradation by ubiquitously present nucleases, negative charge of phosphate groups hindering approximation towards negatively charged cell membranes and the hydrophilic structure hinder diffusion across cell membranes of this macromolecule. [32, 33]

Current available medicines are based on the delivery of siRNA rather than bigger double stranded RNA. Less than two years ago, in late 2018, the very first RNAi therapeutic, Patisiran, managed to overcome all these and regulatory hurdles and gained approval by FDA and EMA. [34] This drug tackles hereditary transthyretin-mediated amyloidosis (hATTR amyloidosis) by downregulating the transthyretin gene (TTR) protein which promotes the disease hallmarks as a cause of a mutated TTR. It is based on a lipid nanoparticle formulation consisting of four different components: DLin-MC3-DMA, PEG₂₀₀₀-C-DMG, 1,2-distearoyl-sn-glycero-3-phosphocholine (DSPC), and cholesterol. The latter two are responsible for the structural stabilization of the nanoparticle. PEGylation has often been described to enhance circulation time in the blood

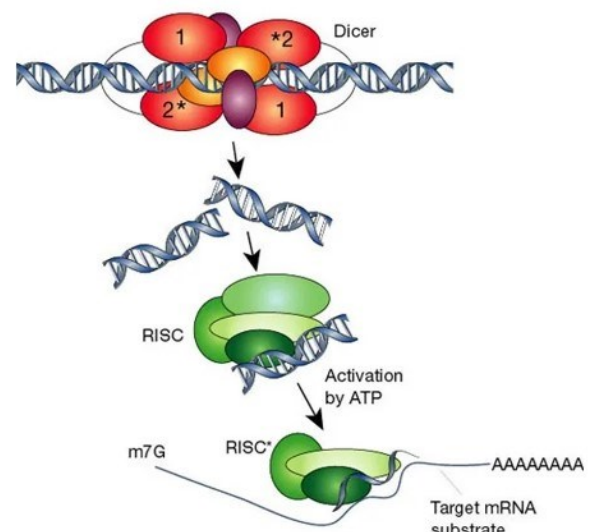


Figure I.4. RNA interference
Dicer enzyme processes RNA into ~21-25 bp long siRNA; after incorporation of siRNA into RNA-induced silencing complex (RISC) and subsequent activation by ATP, the complex is directed to the homologous mRNA target by the guide strand
Reprinted with permission from Springer Nature from [30].

and is the reason for the incorporation of PEG₂₀₀₀-C-DMG into the nanoparticle formulation. [35] DLin-MC3-DMA on the other hand, leads to the encapsulation of siRNA based upon its positive charged substructure. Furthermore, it is responsible for specific uptake into hepatocytes - the site where most of the TTR protein is synthesized - fusion with the endosomal membrane and the release of its siRNA content into the cytoplasm. The targeting effect of the formulation can be explained by the fact that upon intravenous injection of the formulation, particles are opsonized by apolipoprotein E (Apo E). This first defense mechanism to prevent foreign particles and substances to harm the body assists Patisiran in a particular manner: Upon transport into the liver, the Apo E decorated particles are recognized by Apo E receptors on the surface of hepatocytes. [36-38]. Uptake is initiated and after fusion of DLin-MC3-DMA with the endosome, siRNA is released to its site of action. [35] Through these formulation 'tricks', siRNA is protected from nucleases, the hydrophilic character of siRNA is masked and a passive targeting by receptor mediated uptake is introduced to increase specificity.

Another approach to overcome the before mentioned hurdles is chemical modification of siRNA. It was shown that 2'-deoxy-2'-fluoro and 2'-O-methyl modification of ribose moieties increased the stability against nucleases significantly without decreasing activity. In fact, the potency could not only be retained but even increased. [33, 39-42] Additionally, it was shown that phosphorothioate linkages at the 5'-end of guide and passenger siRNA strands increase the stability against nucleases. [43, 44] These findings were crucial for the development and approval of givosiran in late 2019. [45] This is the second approved siRNA therapeutic. Its activity relies on the modification of the ribose moieties and its liver targeting which is based upon the conjugation of three N-acetylgalactosamine (GalNac) to the passenger guide. The three GalNac ligands are recognized by liver asialoglycoprotein receptor and lead to a receptor mediated uptake and ultimately the downregulation of the targeted mRNA, specifically in the liver.

I.3. Spray Drying of small interfering RNA

Although production of complex compounds such as inhalable biopharmaceuticals and the first approvals of siRNA therapeutics were successful, only very few investigations have been directed to the production of inhalable siRNA therapeutics. (Web of Science search, 05.01.2020, 10.50 am, TI=(siRNA AND spray drying)) Of these publications, the focus was laid on the delivery of naked siRNA and nanocarrier based strategies.

The group of Jenny K. W. Lam directed their research towards pulmonary delivery of naked siRNA which showed successful transfection without further investigating the exact mechanism of uptake and endosomal release [46-49]: Chow et al. published a very interesting paper of naked siRNA as dry powder formulation for pulmonary delivery by spray drying with mannitol and L-leucine. However, characterization of aerodynamic properties was not performed according to state-of-the art. [50] Referring to the European as well as the US pharmacopoeia, the assessment of aerodynamic size distribution has to be determined by the amount of drug. [51, 52] Here however, the calculation of the aerodynamic diameter was executed by a surrogate parameter i.e. mannitol which does not show any pharmacological effect and hence relevance for the determination. Despite this flaw in experiment design, they showed that spray drying did not alter the integrity of siRNA under mild conditions (T-Out = 50°C) and that microparticle characteristics are less influenced by siRNA itself rather than the process and formulation parameters: as known from literature, -leucine led to a corrugated particle morphology and acted as a dispersion enhancer improving measured aerodynamic properties in that study. [53] Unfortunately, this publication did not just lack quantification of siRNA for determination of aerodynamic properties but also in regard to drug recovery after spray drying leaving uncertainties regarding dosing. The successive study by Chow and colleagues described the preparation of higher concentrated naked siRNA powders which were analyzed after spray drying and related to the amount of siRNA before spray drying. [54] However, no satisfying reasons for losses of over 25% were offered. Wu and colleagues investigated the effect of thermal and shear stress upon naked siRNA during spray drying. They showed that increasing T-Out from 60° to 125°C and increasing the atomizing gas flow rate from ~470 to 740 L/h led to an increase in decomposition of siRNA. [55] However, no variation of the excipient was investigated whether amorphous or crystalline forming substances are preferred.

This could have an effect on the amount of siRNA recovered after spray drying which varied from 80 - 94%, as described for formulations of biopharmaceuticals (see chapter I.1.). Additionally, the influence of the different process parameters on residual moisture, geometric and especially aerodynamic diameter were not investigated which are crucial for aerosol performance.

The group of Camilla Foged focuses on the formulation of a siRNA loaded nanocarrier systems based on poly(DL-lactide-co-glycolide acid) (PLGA). Jensen et al. published a paper in 2010 where the successful incorporation of siRNA loaded PLGA nanoparticles in different excipients, namely mannitol, lactose and trehalose, was shown. [56] Unfortunately, parameters which were examined for all three different formulations were only microparticle size, residual moisture content and yield. As expected, mannitol outperformed the other two subjects in all of these parameters and experiments were continued with the mannitol-based formulation only. Investigations on the solid state, quantities and in vitro performance of siRNA in all three excipients after spray drying were not performed. Despite this lack of information, Jensen showed that siRNA was recovered in an intact state although losses of 40% were detected. Again, the investigation of aerodynamic properties was not carried out according to the US or European pharmacopoeia but with an alternative technique leaving room for doubts. Additionally, PLGA nanocarriers were unable to downregulate mRNA levels as detected in the expression of the translated protein. Unfortunately, the investigation of excipients was not taken up once again in the successive study published in 2012. [57]

So far, intensive investigation of siRNA recovery after spray drying in combination with effects arising from excipients and subsequent effects on residual moisture in addition with the correct determination of aerodynamic properties has not been reported.

Chapter II)

Aims of Thesis

II Aims of Thesis

The aim of this thesis is to elucidate the effects of spray drying and its process parameters and excipients on siRNA formulations, drug yield and performance. Although spray drying of biopharmaceuticals is possible as shown in chapter I.1., much less is known about the effects of crystalline and amorphous structures upon spray drying on siRNA nanoparticle formulations, here polyplexes:

The aim to overcome the delivery hurdles described in I.2, is a combination of both explained concepts therein: instead of encapsulating siRNA into lipid nanoparticles we want to establish a delivery system comprising of positively charged polymers such as polyethyleneimine (PEI) which is able to encapsulate siRNA by electrostatic interactions into so called polyplexes. It was shown that PEI and its chemical modifications are able to successfully transfect cells with nucleic acids unlike PLGA based systems as shown in chapter I.3. [56, 58-62] Therefore, the aim is to establish analytics for a detailed determination of the composition changes during spray drying of polyplexes followed by an optimization of parameters such as inlet temperature and residual moisture content consequently. Also, establishing a method which follows European as well as United States requirements for the determination of aerodynamic properties are within the scope of this thesis.

The ultimate aim is a pulmonary T_H2 cell specific targeting by chemically linking transferrin to PEI or other polyamines resulting in a receptor mediated uptake in activated T_H2 cells supported by a local pulmonary application. Thereby, delivery of polyplexes is mainly restricted to the lung reducing the risk of uptake by other organs and hence reducing the risk of side effects. We hypothesize that receptor mediated uptake in combination with lung specific delivery show synergistic effects in the treatment of inflammatory T_H2 driven lung diseases.

Chapter III summarizes the needs for siRNA formulation and characterization.

Chapter IV is a proof of concept study where test substances namely PEI and bulk DNA are spray dried. Here analytical methods were established which are crucial for elucidating risks and determining the success of spray drying and consequently characteristics for dry powder inhalation.

Chapter V sheds light on the mechanism causing losses of PEI and DNA as observed in chapter IV. Here, the effect of pumping and tubing material on polyplex composition are highlighted.

Chapter VI summarizes the progress of our group for the development of a targeted delivery system for a pulmonary dry powder application.

Chapter VII deals with the preparation of polyplexes consisting of siRNA and a PEI based polymer i.e. PEG-PCL-PEI (PPP) via spray drying. Methods established in Chapter IV are applied and enabled efficient experimental set up.

Chapter VIII describes the establishment of a new uprising technique which is known as tunable resistive pulse sensing. This method allows particle by particle size, zeta potential and concentration measurements which is a mighty tool in the characterization of nanoparticles in general and polyplexes in specific but was not available for positively charged particles so far.

Chapter III)

Dry Powder Inhalation of siRNA

This Chapter was published in *Therapeutic Delivery*:

T.W.M. Keil, O.M. Merkel, Dry powder inhalation of siRNA, *Therapeutic delivery*, 10 (2019) 265-267.

III Dry Powder Inhalation of siRNA

Therapeutic RNA interference (RNAi) lately gathered a new wave of public interest due to the approval of the first small interfering RNA (siRNA) based drug (Patisiran) against hereditary transthyretin amyloidosis [63]. Exogenous double-stranded RNA can be used to trigger this interference by an intracellular complex known as RNA-induced silencing complex after 'dicing' the molecule to 21-23 nucleotides. Depending on the base pairing of this siRNA, the complex attaches to a specific messenger RNA (mRNA) and ultimately degrades it. Thus, a subsequent translation to the protein encoded by this particular mRNA is prevented. By choosing the siRNA sequence for subsequent base pairing, any possible mRNA/protein of interest can be downregulated, including mRNAs that cause a disease. The uptake of siRNA into the cytoplasm, however, is restricted by its chemical nature. High hydrophilicity and large size of siRNA compared to small molecules lead to a low uptake. To overcome these problems, vectors have been developed based on viral and non-viral delivery systems. Viral delivery systems such as adenoviruses, adenovirus associated viruses and lentiviruses, which are the most frequently tested viruses in literature, are able to successfully deliver siRNA. However, these vectors have great disadvantages such as high immunogenicity, high production costs and major hurdles for regulatory approval [64]. Non-viral systems, such as lipids or polymers, show lower immunogenicity, longer circulation times and lower costs, but also yield lower uptake efficiency. Nonetheless, when targeting inflammatory diseases in which additional immune response is counterproductive, these systems are favored and their shortcoming is addressed for example by adjusting administration route. In addition, non-viral systems can be modified due to their synthetic nature to optimize biocompatibility, internalization, transfection efficiency, circulation time

and active targeting and improve their overall performance [64, 65]. Lipid and polymer delivery systems can either form vesicle based nanoparticulate suspensions upon encapsulation or lipoplexes and polyplexes, respectively, upon complexation with charged substances [64, 66]. A benefit of nanoparticle formation is that siRNA is protected from RNases and, hence, is less susceptible to enzymatic degradation. RNases, which are ubiquitously present in eukaryotes, prokaryotes, bodily fluids and generally in every source of water, are one of the major risks in siRNA formulation. Therefore, it is of great interest to avoid sources of contamination and also the presence of water without which RNases lose their enzymatic activity. Hence, storage of siRNA-based medicines is best in solid formulations. Pulmonary delivery is an optimal way to treat lung diseases such as asthma, chronic obstructive pulmonary disease (COPD), cystic fibrosis, and lung cancer, avoiding the oral and intravenous route. Local administration onto the lung area is complemented by reduced doses, subsequently reduced systemic side effects, and circumvents the first pass metabolism [67]. For pulmonary delivery, drugs are delivered to the lung via liquid aerosol or dry powder formulations. Liquid aerosols generated by pressurized metered dose inhalers (pMDI) are mostly favored for small molecule delivery as they are easy to formulate. However, administration of pMDI needs some training for the patient to apply the medication correctly achieving best possible results. In detail, the timing of inhaling and the aerosol release needs to be coordinated and has to be done simultaneously. Otherwise drug deposition will take place in mouth and pharynx and not at the site of action within the lung, resulting in potential side effects [68]. On the other hand, dry powder inhalers (DPIs) release their drug formulation upon the patient's respiration. Hereby, coordination of breathing and drug release is not required, easing the handling of the device and increasing patients compliance [69]. Upon inhalation of the patient, the dry powder formulation is simultaneously released. Through the generated vacuum and the device's specific structure, possible agglomerates of particles are disaggregated [70]. However, these DPIs need certain respiration forces to trigger the release mechanism. In some cases, where airflow and, hence, respiration force is restricted, e.g. by the disease itself or the patient's anatomy (children), it is not strong enough to release the DPI's content. To overcome these problems, various DPIs were approved with different release mechanisms to fully adapt DPIs to the patient needs and therefore enable applicability [64, 69, 71, 72]. Advantages of DPIs over MDIs can be seen when water sensitive drugs are formulated such as siRNA related

medicines. In absence of water degradation caused by enzymatic and non-enzymatic reactions cannot take place [64]. For this purpose, dry powder formulations need to be produced with low residual moisture content, and the formulation itself needs to be protected from environmental humidity. For capsule driven DPIs, which are the most applied systems in early research stages due to easy filling and handling, typically a higher water resistive material is chosen for capsule production: i.e. instead of gelatin with about 10% residual moisture content, the most common capsule material, hydroxypropylmethylcellulose is used. This substance exhibits a residual moisture content of less than 1% and owns additional beneficial properties, e.g. less powder adhesion to the inner wall of the capsule, compared to gelatin [69, 73]. In addition, primary packaging materials such as aluminum films significantly restrict the diffusion of air and humidity through the packaging material into the dosage form preventing wetting of e.g. capsules and their powder content.

Techniques that are frequently reported in literature to produce dry powder formulations are spray drying (SD) and spray freeze drying (SFD) [74-77]. Hereby, siRNA nanoparticles are suspended in an aqueous excipient solution e.g. mannitol or trehalose, afterwards aerolized into small droplets and dried resulting in microparticles in which these nanoparticles are embedded. This procedure is necessary as particles between 1 and 1000 nm are not able to deposit in deep lung areas, because they are exhaled upon inhalation. Suitable aerodynamic sizes for lung deposition, which depend on geometric size and porosity, are between 1 and 5 μm [78]. Hence, nanoparticles need to be embedded into a microparticle which dissolves upon impaction on the lung fluid and releases its nanoparticle content. When using SD, microparticles are produced via gentle heating, whereas SFD techniques utilize the freezing of droplets in liquid nitrogen at first and subsequent removal of frozen water by lyophilization. Both preparation methods produce mostly microparticles in an amorphous state, which is favorable for stabilizing embedded nanoparticles. Whereas SD results in rather small geometric sizes with low porosity, SFD produces very voluminous particles with high porosity. These high volumes might cause powder packaging and/or application issues for SFD microparticles. On the other hand, higher temperatures necessary for SD are avoided [79]. Despite the different geometric sizes, both techniques are able to produce microparticles with an aerodynamic diameter between 1 to 5 μm , due to their different particle porosities. Beneficial for industrial particle production by SD is the short time of

drying which only takes minutes compared to several hours or days for SFD. Great advantage of both techniques is the ability to tune and design the microparticle by adjusting process parameters of the respective techniques: pump rate, airflow and solid concentration (for SD also aspiration rate and heat apply here) have a crucial effect on particle size and shape [53, 80]. In addition, microparticle morphology can be modified by excipients and further additives. Leucine for example is known to roughen the particle surface avoiding strong particle-particle interaction and improving aerodynamic properties [81]. As mentioned before, siRNA-based nanoparticles embedded in microparticles demonstrate increased siRNA stability due to the absence of water which avoids enzymatic degradation through RNases.

In summary, dry powder formulations therefore are a promising dosage form to locally deliver target specific siRNA enabling the therapy of several diseases such as asthma, cystic fibrosis or lung cancer. In literature, siRNA containing microparticles produced by SFD successfully demonstrated gene silencing activity in vivo [77]. Nevertheless, further research is required to realize this administration form for clinical application.

Chapter IV)

Characterization of Spray Dried Powders with Nucleic Acid-containing PEI Polyplexes

This chapter was published in the *European Journal of Pharmaceutics and Biopharmaceutics*:

T.W.M. Keil¹, D.P. Feldmann¹, G. Costabile, Q. Zhong, S. da Rocha, O.M. Merkel, Characterization of spray dried powders with nucleic acid-containing PEI nanoparticles, *European Journal of Pharmaceutics and Biopharmaceutics*, 143 (2019) 61-69.

First ideas for this research were brought up in a collaboration of Sandro da Rocha and Olivia M. Merkel. Daniel P. Feldmann started the project which he handed over to me after a few experiments and did parts of the writing. At that time Gabriella Costabile was my Postdoc and did supervision and proof reading. The main experimental data and writing was contributed by myself. ¹Both authors contributed equally to this work.

IV Characterization of Spray Dried Powders With Nucleic Acid Containing PEI Polyplexes

IV.1. Abstract

Localized aerosol delivery of gene therapies is a promising treatment of severe pulmonary diseases including lung cancer, cystic fibrosis, COPD and asthma. The administration of drugs by inhalation features multiple benefits including an enhanced patient acceptability and compliance. The application of a spray dried powder formulation has advantages over solutions due to their increased stability and shelf life. Furthermore, optimal sizes of the powder can be obtained by spray drying to allow a deep lung deposition. The present study optimized the parameters involved with spray drying polyplexes formed by polyethylenimine (PEI) and nucleic acids in inert excipients to generate a nano-embedded microparticle (NEM) powder with appropriate aerodynamic diameter. Furthermore, the effects of the excipient matrix used to generate the NEM powder on the biological activity of the nucleic acid and the ability to recover the embedded nanoparticles was investigated. The study showed that bioactivity and nucleic acid integrity was preserved after spray drying, and that polyplexes

could be reconstituted from the dry powders made with trehalose but not mannitol as a stabilizer. Scanning electron microscopy (SEM) showed trehalose formulations that formed fused, lightly corrugated spherical particles in the range between 1-5 μm , while mannitol formulations had smooth surfaces and consisted of more defined particles. After redispersion of the microparticles in water, polyplex dispersions are obtained that are comparable to the initial formulations before spray drying. Cellular uptake and transfection studies conducted in lung adenocarcinoma cells show that redispersed trehalose particles performed similar to or better than polyplexes that were not spray dried. A method for quantifying polymer and nucleic acid loss following spray drying was developed in order to ensure that equal nucleic acid amounts were used in all *in vitro* experiments. The results confirm that spray dried NEM formulations containing nucleic acids can be prepared with characteristics known to be optimal for inhalation therapy.

IV.2. Introduction

Pulmonary delivery remains one of the most logical routes for region-selective treatment of lung diseases. [82] Advantages such as a large surface area, low proteolytic activity, avoidance of the first pass effect and thin epithelium barriers all contribute to provide strong opportunities to enhance therapeutic efficacy through increasing drug bioavailability. [83] In addition, the use of dry powder inhalers to deliver a drug formulation presents its own set of advantages due to their ease of use and their relatively high patient compliance rate. [84] While numerous conventional treatments have been developed in order to target local lung diseases, one of the most promising strategies for treating severe lung diseases involves the use of gene therapy. Small interfering RNA (siRNA), e.g., can silence pathologic gene expression that underlays the disorder being treated. Lung diseases such as cystic fibrosis, pulmonary tuberculosis, viral infections, asthma, chronic obstructive pulmonary disease (COPD) and lung cancer have all been investigated as potential targets in which siRNA might prove to be a promising therapeutic. [85-88] Despite their potential, siRNA therapeutics face numerous challenges that limit their safe and efficient application in lung disease treatment. [89] To overcome these hurdles associated with the delivery of therapeutic siRNA, nanoparticles have long been the preferred approach for encapsulating and protecting nucleic acids. In the literature, a large variety of materials taking advantage of

nanof ormulation methods is reported to successfully deliver siRNA and achieve gene knockdown. [90]

Cationic polymers are a class of non-viral vectors that represent a large population of nanoparticles being developed as efficient delivery vehicles of siRNA. [91] Polyethylenimine (PEI) is one of the most widely studied gene delivery vectors due to its highly modifiable amine rich structure. The high incidence of positively charged amines renders PEI the ability to electrostatically interact with nucleic acids to form nanoparticles termed “polyplexes” and facilitate cellular internalization of siRNA. [92] In order to achieve local delivery of the gene therapy to the lungs, however, it is necessary to formulate the nanoscale polyplexes into a microparticle powder comprised of a suitable matrix with aerodynamic diameters within the range of 1 – 5 μm . [93] After their inhalation, the matrix of nano-embedded microparticles (NEMs) must then dissolve in the lung lining fluid and release the embedded polyplexes for cellular uptake.

Spray drying is a widely used processing technique employed by chemical, materials, cosmetic, food and pharmaceutical industries. [2] This rapid, continuous, reproducible and scalable technique is very appealing in both the industrial and laboratory setting as a method to produce dry powder formulations intended for inhalation. However, the use of the spray drying to process nucleic acid polyplexes into microparticle powder requires optimization of processing parameters such as the excipient selection and drying conditions in order to retain polyplex bioactivity, redispersibility, as well as stability. [94, 95]

The goal of this study was to optimize various spray drying parameters used to process PEI/bulk DNA (bdNA) polyplexes into NEMs, which will serve as a method development study for the formulation and analytics of siRNA polyplexes. The two well-known matrix stabilizing saccharides, mannitol and trehalose, were used in the spray drying process and the redispersibility of the corresponding NEM formulations was investigated. Additionally, various physical characteristics of the microparticles formed with the different excipients were examined. As polyplexes are a dynamic system made by electrostatic assembly which can be affected by shear forces, spraying could have a tremendous effect on the nanoparticle composition and concludingly their biological activity. This needs to be evaluated in order to achieve precise dosing and prevent overdosing as well as underdosing. [77, 96] Hence, an important goal of the work was to develop a method to quantify the

amount of polymer and nucleic acid that remained following spray drying. This method was established in a well-studied system of PEI and bDNA in order to proof its applicability, and to transfer it afterwards towards more complex systems containing nucleic acids e.g. siRNA and other amine-based polymers. Ultimately, the cellular internalization and transfection efficiency of the redispersed PEI/DNA polyplexes were assessed in lung adenocarcinoma A549 cells to pave the way for spray drying more sophisticated polyplex or micelleplex [97] formulations containing other polymers and/or siRNA with well-established analytics.

IV.3. Materials and Methods

IV.3.1. Materials

Hyperbranched polyethylenimine (PEI, 25k Da) was obtained from BASF (Ludwigshafen, Germany). RPMI-1640 medium with L-glutamine and sodium bicarbonate, Dulbecco's phosphate buffered saline (PBS), heat-inactivated fetal bovine serum (FBS), D-(+)-glucose, sodium bicarbonate, picrylsulfonic acid (TNBS) solution 5%, sodium pyruvate, 2-mercaptoethanol, dimethyl sulfoxide (DMSO, $\geq 99.7\%$), ethylenediaminetetraacetic acid (EDTA, 99.4–100.06%), trypan blue (0.4%, sterile filtered) and bulk DNA (bDNA) from salmon sperm (6,000kDa, Fisher Scientific) were purchased from Sigma-Aldrich (Munich, Germany). SYBR Gold dye was obtained from Life Technologies (Carlsbad, CA, U.S.A.).

IV.3.2. Preparation of polyplexes

To form polyplexes, 25k PEI was dissolved in water to yield a 1.0 mg/mL solution and was then filtered through a 0.22 μm filter for sterilization. This stock solution was then diluted to pre-calculated concentrations with sterile 5 or 10% solutions of mannitol or trehalose and an equal volume was added to a defined amount of bDNA to prepare polyplexes at various N/P ratios (the molar ratio of nitrogen in PEI to phosphate in bDNA). This solution was incubated for 20 minutes at room temperature to allow polyplex formation. The amount of 25k PEI required for a specific N/P ratio was calculated as follows (Eq. IV.1.):

$$m_{PEI} = \left(\frac{m_{DNA}}{330} \right) \cdot 43.1 \cdot N/P$$

where m_{PEI} is the mass of PEI in μg and m_{DNA} is the mass of bDNA in μg in each sample.

IV.3.3. Spray Drying

Spray drying was used to incorporate the polyplexes into nano-embedded microparticles (NEMs). First, polyplexes were formed at various N/P ratios as described above containing 20 μg of bDNA, and 2 mL of the solution was mixed with 8 mL of an aqueous solution of different matrix excipients before spray drying. The matrix excipients tested were 5 or 10% (w/v) solutions of mannitol or trehalose in RNase free DI-water. All powder formulations were prepared using a Büchi B-290 spray dryer (Büchi Labortechnik, Essen, Germany) equipped with a 2-fluid nozzle (Büchi Labortechnik). In brief, the spray dryer was pre-conditioned using distilled water, and all powder formulations were prepared at identical drying conditions using the following parameters: atomizing air flow = 473 L/h, aspiration = 70%, pump ratio = 5%, nozzle cleaner = 0, inlet temperature = 65 °C, outlet temperature = 38 ± 1 °C. Nitrogen was the atomizing gas, air was dehumidified with a DeltaTherm-dehumidifier (DeltaTherm, Munich, Germany) and dry microparticles loaded with polyplexes (white powder) were contained in the collection vessel at the end of the glass cyclone, from where they were collected using a spatula and stored in a desiccator at room temperature for further experiments.

For measurement of polyplex redispersibility, spray-dried samples were dissolved in 70 μL of water, and the resulting suspension of polyplexes in water/matrix solution was vortexed for 15 s before measuring z-average, PDI, and zeta (ζ) potential as described below.

IV.3.4. Hydrodynamic Diameter and Zeta (ζ) Potential Measurements

Hydrodynamic diameter measurements of freshly prepared or redispersed polyplexes were performed by dynamic light scattering (DLS) using a Zetasizer Nano ZS (Malvern Instruments Inc., Malvern, U.K.). To perform these measurements using attenuator levels between 6 and 8, the amount of spray-dried sample was adjusted adequately. Polyplexes prepared for spray drying were measured in their specific medium e.g. mannitol 10% where refractive index and viscosity were adjusted accordingly. For redispersed polyplexes, NEM were dissolved in a fashion to achieve equal excipient concentration as prior to spray drying. A total volume of 70 μL of each sample was added into a disposal cuvette (Brand GMBH, Wertheim, Germany) and the 173° backscatter angle measurement was read in triplicates with each run consisting of 15 scans. Results are represented as average size (nm) \pm standard deviation.

The particle size distribution was reflected in the PDI, which ranges from 0 for a monodisperse to 1.0 for an entirely heterogeneous dispersion. The samples were then diluted to 570 μL with filtered Nanopure water and transferred to a folded capillary cell (Malvern Instruments Inc., Malvern, U.K.), and ζ -potential measurements were taken. ζ -potential measurements were read in triplicates by laser Doppler anemometry (LDA), with each run consisting of 30-50 scans. Results are shown in $\text{mV} \pm$ standard deviation.

IV.3.5. Scanning electron microscopy

The surface morphology and geometric size of the NEMs was examined by scanning electron microscopy (SEM) using an JSM-6510LV LGS, 25kV (JEOL, Peabody, MA, U.S.A). For imaging, the NEM powder was sprinkled on a stub covered with double-sided carbon tape and sputter-coated with gold (Ernest Fullan) under vacuum for 40 s. The sizes of the microparticles were estimated from the SEM images processed with the Fiji distribution of ImageJ. [98] The histogram of the measured diameters was fit to a Gaussian distribution, from which average and standard deviation were calculated and outliers were shown.

IV.3.6. Residual water content

The residual water content of the NEM powder after spray drying was determined by coulometric measurement using an Aqua 40.00 Karl Fischer Titrator with corresponding software from Analytik Jena AG (Jena, Germany). The samples (approx. 15 mg) were loaded into 2R vials, placed into the heating chamber and measured at 150°C until the measurement drift reached the start drift $\leq +2 \mu\text{g}/\text{min}$ or until a final measurement time of 10 minutes. The start drift was established after approximately 1 hour of equilibration showing a rate of less than 10 $\mu\text{g}/\text{min}$. Hydranal Coulomat AG (Riedel-de Haën, Seelze, Germany) was used as reagent. Before each session, the titrator was calibrated with a 1% water standard. The moisture content was calculated as the % weight of water relative to the overall sample weight.

IV.3.7. Cascade impactor analysis

An 8-stage Andersen-Cascade-Impactor (ACI) (Thermo Andersen, Smyrna, GA, USA) fitted with a USP induction port and pre-separator operated with a flow rate of $28.3 \text{ L} \times \text{min}^{-1}$ at 25 °C and 75% relative humidity, was used to evaluate the aerosol properties of the NEM powder. Prior to each ACI test, 55 mg of the formulation was loaded into 4 hydroxypropylmethylcellulose capsules each. A Handihaler (Boehringer Ingelheim Pharma GmbH & Co. KG, Ingelheim, Germany) was used to discharge each capsule twice according to the manufacturer's manual with an interval of 5 seconds in between. To enable a total volume of 4L passing through the instrument, the application time was set to 8.5 seconds. After each test, the ACI was disassembled and the powder that had deposited on each stage was weighed independently. The amount of nucleic acid deposited on each stage was analyzed as described under IV.3.8., and the mass median aerodynamic diameter (MMAD) and geometric standard deviation (GSD) were calculated as described in the literature. [51] The fine particle fraction (FPF) was calculated as the fraction of all particles deposited with an aerodynamic diameter below 5 μm . [51]

IV.3.8. Polymer and nucleic acid quantification following spray drying

In order to quantify the PEI and bDNA content that was encapsulated into the microparticles following spray drying, heparin competition assays were performed in order to disassociate the PEI-bDNA polyplexes within the NEM powder. Subsequently, the bDNA that was released from the polyplexes was determined by a modified SYBR[®] gold assay [97] while the PEI concentration was determined by TNBS assay [99]. First, the batch of NEM powder was dissolved in 2 mL borax buffer 0.1 M (Sodium Borax Decahydrate, Sigma Aldrich, Germany) in a volumetric flask. Following procedure was executed in triplicates: According to the theoretical content of bDNA, a volume was chosen to achieve approximately 0.04 μg of bDNA per N/P ratio. This solution was diluted to a final volume of 150 μL per sample with HPW in a tube. Afterwards, 75 μL of a 58k IU heparin solution was added to each tube to achieve complete disassociation of polyplexes after 2hr. This solution was further diluted to 450 μL and distributed into a white 96 well plate (Thermo Scientific™ BioLite microwell plate, Thermo Scientific GmbH, Schwerte, Germany) in triplicates of 100 μL each.

For quantification of bDNA, 30 μL of a 4 \times SYBR[®] gold solution was added to each well and incubated for 5 min in the dark at room temperature. The fluorescence of each sample was quantified using a Synergy 2 multi-mode microplate reader (BioTek Instrument, Winooski, VT, U.S.A.) at excitation wavelength of 485/20 nm and emission wavelength of 520/20 nm and compared to a freshly prepared standard curve of free bDNA incubated with SYBR[®] gold dye.

For quantification of 25k PEI, 100 μL of batch dissolved solution in 2 mL borax was incubated with 30 μL of 3 mM TNBS solution in triplicates and absorbance at 405 nm was determined after a 1 h incubation with a quartz cuvette in a UV-1600PC spectrophotometer (VWR International GmbH, Darmstadt, Germany). The measured absorbance was compared to a freshly prepared standard curve of free 25k PEI incubated with TNBS reagent. To verify each quantification assay, internal standards were prepared freshly and analyzed in parallel. These standards consisted of bDNA and PEI of known amounts which were chosen according to the theoretical amount of bDNA or PEI being analyzed in the sample, respectively. These were 0.04 μg bDNA per well for nucleic acid quantification and 0.48 to 1.2 μg PEI for polymer quantification. Measurements with deviations of less than 10% of the internal standard were considered as precise and taken into account for further analysis.

IV.3.9. Cell culture

Human adenocarcinoma alveolar based lung cancer cells (A549) were obtained from ATCC (LG Promochem, Wesel, Germany) and cultured in RPMI-1640 medium with L-glutamine and sodium bicarbonate and supplemented with 10% heat inactivated fetal bovine serum and 1% penicillin/streptomycin (Corning Incorporated, Corning, NY, U.S.A.). Cells were grown in 75 cm^2 cell culture flasks (Thermo Fisher Scientific, Waltham, MA, U.S.A.) at 37 °C and 5% CO_2 and passaged every 2-3 days when they reached confluency.

IV.3.10. In vitro cellular uptake

In 24-well plates, (Corning Incorporated, Corning, NY, U.S.A) 50,000 A549 cells were seeded and incubated overnight at 37°C and 5% CO₂. For each experiment, were prepared freshly with YOYO-labeled bDNA or redispersed after spray drying. Negative controls consisted of blank/untreated cells. Unless otherwise stated, cells were transfected for 24 h in 37°C and 5% CO₂ with a volume of fresh or redispersed polyplexes that contained 0.5 µg of YOYO-labeled bDNA within a total volume of 500 µL of serum containing cell culture media. Cells were then washed with PBS, trypsinized and spun down at 400 rcf for 5 min. After centrifugation, the supernatant was decanted, and the cells were washed three times and resuspended in 250 µL PBS/2 mM EDTA. Samples were analyzed via flow cytometry (Applied Biosystems Attune® Acoustic Focusing Cytometer, Life Technologies), and the median fluorescence intensity (MFI) was measured using 488 nm excitation and a 530/30 nm bandpass emission filter set. Samples were run in triplicates, with each sample gated by morphology based on forward/sideward scattering for a minimum of 10,000 viable cells. Analysis and presentation of the data was performed by GraphPad Prism 5.0 software calculating mean values and standard deviation.

IV.3.11. In vitro transfection efficiency

In 24-well plates, 50,000 A549 cells were seeded and incubated overnight at 37°C and 5% CO₂. For each experiment, freshly prepared or redispersed polyplexes loaded with GFP plasmid (The Plasmid Factory, Bielefeld, Germany) were tested. Negative controls consisted of blank/untreated cells. Unless otherwise stated, cells were transfected for 48 h in 37°C and 5% CO₂ with a volume of fresh or redispersed polyplexes that contained 0.75 µg of GFP plasmid within a total volume of 500 µL of serum containing cell culture media. Cells were then washed with PBS, trypsinized and spun down at 400 rcf for 5 min. After centrifugation, the supernatant was decanted, and the cells were washed three times and resuspended in 250 µL PBS/2 mM EDTA. Samples were analyzed via flow cytometry (Applied Biosystems Attune® Acoustic Focusing Cytometer, Life Technologies), and the median fluorescence intensity (MFI) was measured using 488 nm excitation and a 530/30 nm bandpass emission filter set. Samples were run in triplicates, with each sample gated by morphology based on forward/sideward scattering for a minimum of 10,000 viable cells. Analysis and presentation

of the data was performed by GraphPad Prism 5.0 software calculating mean values and standard deviation.

IV.3.12. Statistics

All results are given as mean value \pm standard deviation (SD). One-way ANOVA and two-way ANOVA with Bonferroni post-test were performed in GraphPad Prism software (Graph Pad Software, La Jolla, CA).

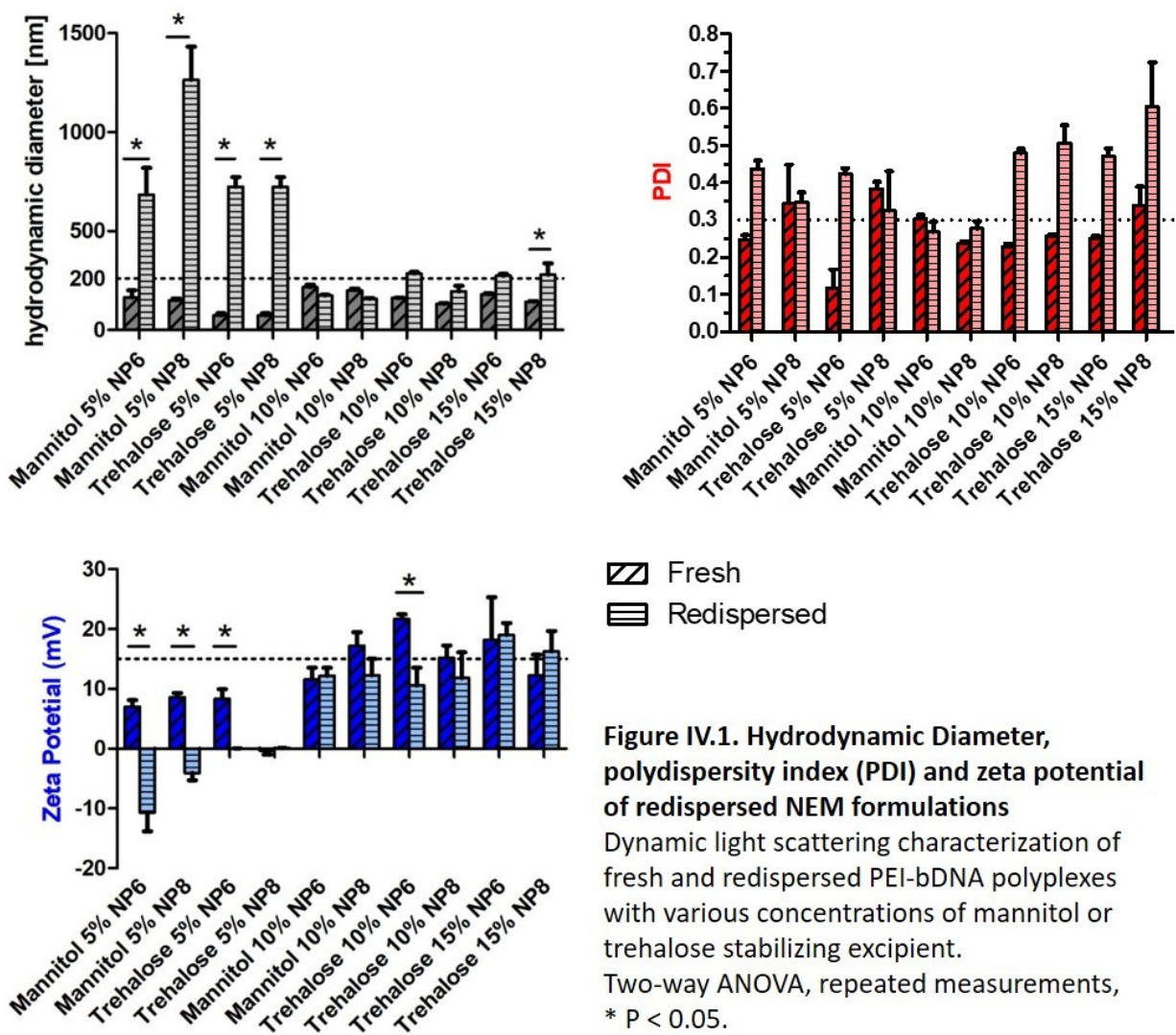
IV.4. Results and Discussion

In this proof-of-concept study, we investigated the preparation of nano-embedded microparticles (NEMs) from bulk DNA-loaded polyplexes that have aerosol diameters suitable for deep lung deposition through the use of spray drying. We subsequently studied the impact of spray drying parameters on their suitability for subsequent *in vitro* or *in vivo* transfection studies. The prototype polyplexes used here comprised of the well-studied polymer polyethylenimine (PEI) and double-stranded template DNA isolated from salmon sperm (bdDNA). The use of these popular DNA transfection components allowed for the optimization of excipient matrix and various spray drying parameters. The resulting DNA-loaded NEMs were then evaluated with respect to physiochemical and aerosol characteristics, and polyplex redispersibility, cellular uptake and transfection efficiency in a lung epithelial cell model.

IV.4.1. Dynamic light scattering measurements of spray dried PEI polyplexes

The bdDNA-loaded polyplexes were processed into NEMs to provide a vehicle for the protection and efficient delivery of nucleic acids to the lungs. To this extent, it is crucial that the microparticle scaffold aides in stabilizing the polyplexes during their storage and facilitates reconstitution into individual nanoparticles upon contact with the aqueous-based environment lining the lung epithelia. Here, PEI polyplexes were encapsulated into a microparticle powder with various excipient matrices via spray drying to generate a stable and inhalable powder. Mannitol and trehalose were selected as the stabilizing excipients based on their well-known ability to stabilize macromolecules. [100, 101] Previous studies conducted in the da Rocha lab reported optimal parameters for the generation of spray dried powder from PAMAM dendriplexes which we based our initial trials on. [102] These initial trials involved the use of aqueous 5% mannitol as the excipient matrix for the NEMs. Upon measuring redispersed PEI polyplexes via DLS, we found a 2-fold increase in particle diameter along with an increased overall negative surface charge at all N/P ratios that were tested (Figure IV.S1.). With the apparent increase in particle aggregation and negative surface charge, we hypothesized that the spray drying parameters being used were causing an unacceptable amount of polymer loss leading to a change of N/P ratio. It needs to be taken into consideration that polyplex suspensions at N/P higher than 2.5 contain a considerable amount of free polymer [103]. However, if free polymer is lost, a new equilibrium between

nucleic acid-bound and free polymer emerges [104]. Therefore, we modified the spray drying parameters and also investigated the use of the excipient trehalose at various concentrations on NEM redispersibility. Similar to our initial trials, the redispersed PEI polyplexes from NEM powder generated with 5% mannitol or 5% trehalose show a significant increase in particle diameter with reconstituted particles approximately >700 nm (Figure IV.1.). Moreover, the 5% excipient formulations also show decreased surface charges upon redispersion.



However, redispersed PEI polyplexes from the formulations with 10% mannitol and trehalose demonstrated no significant change in particle diameter and were all approximately 200 nm in size, and hence below our limit of 260 nm (dashed line Figure IV.1.). Literature suggests that smaller nanoparticles are likely phagocytosed by macrophages through their “secondary size” [105] which was defined as the size of their agglomerates on cell surfaces. Hence, we hypothesize that the smaller the particles, the more likely the endocytosis by lung epithelia rather than macrophage phagocytosis. We therefore assume that particles below this limit

allow macrophage escape to a greater extent than bigger particles and facilitate cell transfection. [91, 105] Additionally, these formulations maintained their positive surface charge, indicating that the particles retained their polymer/nucleic acid composition along with their colloidal stability. The 10% excipient requirement to generate reconstitutable NEMs is higher than amounts used to redisperse PLGA nanospheres [106] or PAMAM dendriplexes [107] in other studies. One possible hypothesis for the higher amount of excipient needed for the reconstitution of polyamine nanoparticles lies in the large amount of water in the polyplexes that is lost during the spray drying process which in turn may necessitate larger amounts of matrix excipients acting in a wick-like manner during redispersion. [108] The redispersed mannitol NEM formulations had the more monodisperse particle distributions of all the formulations tested. Specifically, the redispersed 10% mannitol formulation was the most monodisperse with PDI values of approximately 0.272 ± 0.02 , and hence below our limit of 0.3 (dashed line Figure IV.1.). The redispersed trehalose NEM formulations had more polydisperse particle distributions with PDI values all approximately 0.46 ± 0.10 . The PDI values reported here are well corroborated in various other studies investigating spray dried polymeric nanoparticles with mannitol or trehalose. [109] Due to their favorable characteristics upon redispersion, NEM formulations that were generated with 10% mannitol or trehalose were selected for further characterization studies.

IV.4.2. Aerodynamic diameter measurements of spray dried PEI polyplexes

A crucial characteristic for the deposition of particles in the lung is their aerodynamic behavior. In order to evaluate the aerodynamic behavior of the NEM formulations obtained, an 8-stage Andersen-Cascade-Impactor (ACI) was utilized to determine the mass median aerodynamic diameter (MMAD), geometric standard deviation (GSD), and fine particle fraction (FPF). The NEM formulations analyzed were comprised of 10% mannitol or trehalose and contained PEI polyplexes at N/P 6, 8 or 10. All the NEM formulations tested showed an MMAD in the ideal range for bronchial/alveolar targeting (1 - 5 μm) as shown in Figure IV.2. [110] However, NEM formulations containing 10% trehalose as an excipient showed a significantly lower MMAD of approximately $3.17 \pm 0.21 \mu\text{m}$ versus the 10% mannitol NEM formulations with approximately $4.67 \pm 0.13 \mu\text{m}$. Although not significant, GSD were slightly greater in trehalose formulations compared to mannitol formulations with $2.61 \pm 0.26 \mu\text{m}$ vs. $2.01 \pm 0.05 \mu\text{m}$. Also, not significantly different between both formulations is the FPF

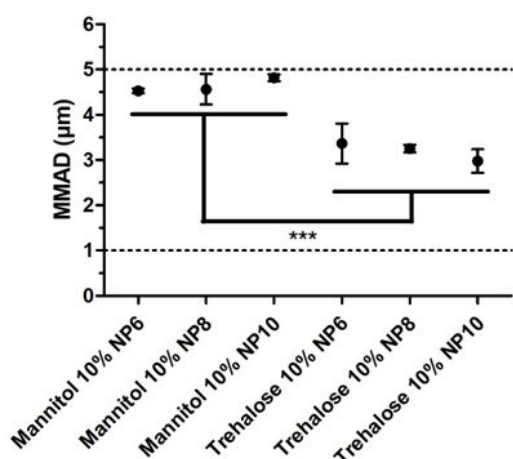


Figure IV.2. Aerodynamic diameter measurements.

Aerodynamic diameter of NEM formulations made with 10% mannitol or trehalose stabilizing excipient. Dotted lines represent optimal range of microparticle size (1 – 5 µm) to achieve deep lung deposition.

One-way ANOVA, *** P < 0.001.

which was calculated as $72.6 \pm 3.4\%$ for trehalose formulations and as $67.5 \pm 1.3\%$ for mannitol formulations (Figure IV.S2.). Aerosol performance strongly depends on MMAD, GSD and especially FPF representing the fraction reaching lower lung areas. By taking these findings into account we cannot state a significant difference between both formulations but acknowledge a trend for better performance with trehalose formulations as MMAD were smaller and FPF greater. Additionally, there was no significant difference between the various N/P ratios within each excipient group tested, indicating that the amount of PEI that was used in the original formulation had little effect on the resulting aerodynamic behavior of the NEM particle. The

larger microparticle diameters measured in the NEM formulations containing mannitol as an excipient may be explained by its crystalline nature upon drying. This is underlined by our XRD analysis where in the contrast to the amorphous halo of trehalose, mannitol showed distinct crystalline characteristics (Figure IV.S4.). Peaks at 14.6° and 16.8° strongly suggest the β polymorph as shown by Nunes et al. [111] Additionally, published results of the β polymorph of mannitol show comparable patterns with Figure IV.S4., confirming the crystalline structure of spray dried mannitol NEM. [112, 113] Amorphous sugars, such as trehalose (Figure IV.S3.), are well known to be excellent at stabilizing biomacromolecules while crystalline sugars, such as mannitol, may lead to phase separation and destabilization [114]. This phenomenon might explain slightly larger microparticle sizes in the formulations containing mannitol as an excipient.

IV.4.3. Scanning electron microscopy

In order to further characterize the NEM formulations, scanning electron microscopy was employed to visualize the microparticles that were formed. Imaging of spray-dried 10% mannitol NEM samples showed that the microparticles were predominantly spherical, with a smooth surface and diameters of approximately $2.8 \pm 2.1 \mu\text{m}$ (Figure IV.3.A.). Conversely, 10% trehalose microparticles are predominantly fused spheres with a corrugated surface and diameters of approximately $4.60 \pm 2.6 \mu\text{m}$ (Figure IV.4.B.). The fused nature of the trehalose particles visualized here may be attributed to “moisture bridges” forming between molecules of the trehalose. [115] The difference in the apparent microparticle diameter for these formulations when comparing the SEM images and their MMAD stems from the surface characteristics of the particles measured. Smoother particle surface increases the particle’s overall density and ultimately its aerosol performance. [116] Therefore, the smoother surface of the mannitol formulations may account for the slight increase in aerodynamic diameter shown in the ACI studies for this formulation.

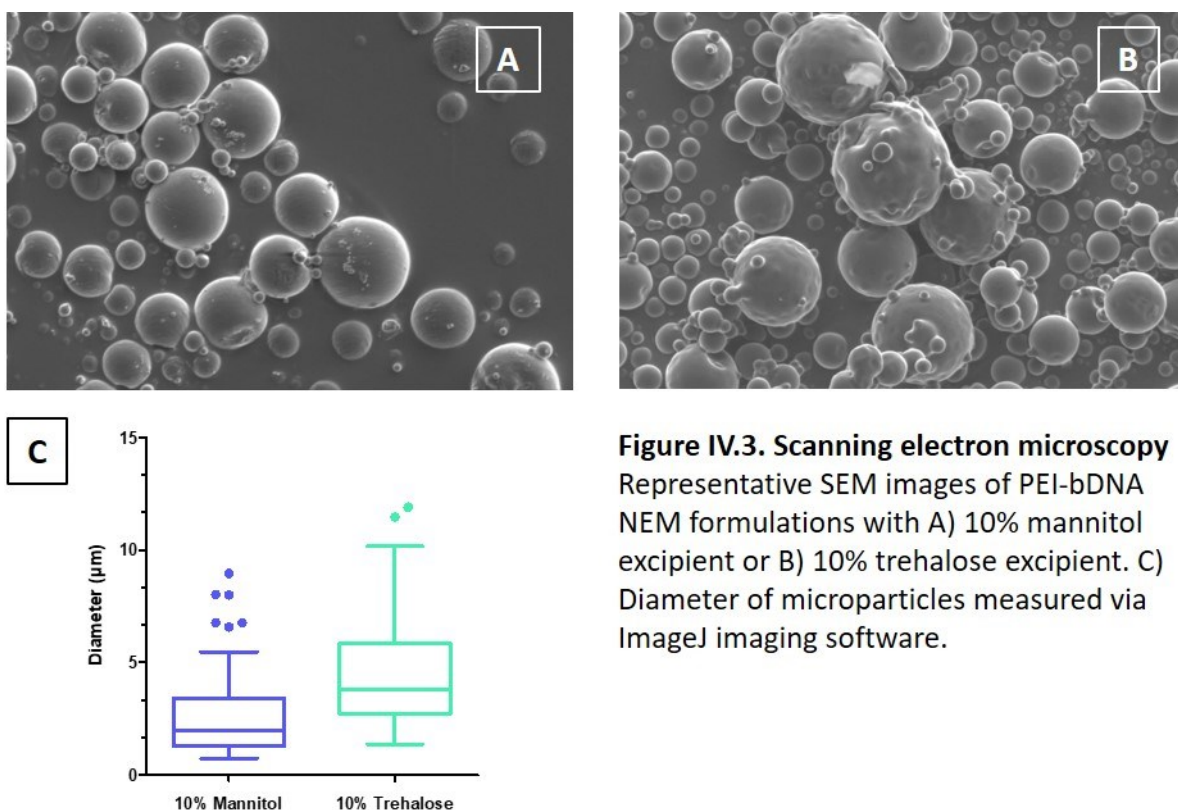


Figure IV.3. Scanning electron microscopy Representative SEM images of PEI-bDNA NEM formulations with A) 10% mannitol excipient or B) 10% trehalose excipient. C) Diameter of microparticles measured via ImageJ imaging software.

IV.4.4. Residual moisture content

It is well known that the residual moisture content following the generation of an inhalable powder plays one of the most crucial roles in determining its long-term stability, both physically and chemically. [117] Therefore, the residual moisture content of the NEM formulations was measured directly after the spray drying process. Immediately following the collection of the NEM powder, the 10% trehalose formulations showed a residual moisture content of 3.2% compared to 0.4% for the 10% mannitol

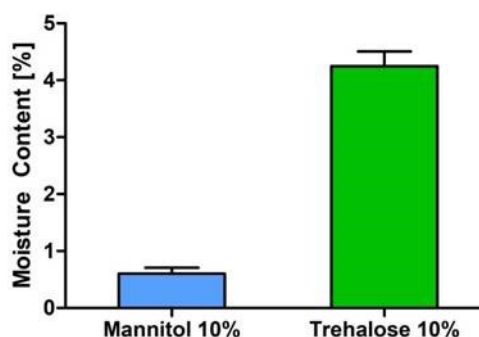


Figure IV.4. Moisture content analysis
Moisture content of NEM formulations made with 10% mannitol or trehalose stabilizing excipient directly after the spray drying process.

formulations (Figure IV.4.). One cause for the slightly higher moisture content in the trehalose NEM powder may be due to the hygroscopic nature of the material. [118] Empirically, we experienced an extremely low solubility of the 10% mannitol NEM powder, which made it difficult to continue characterization studies of these formulations. The lower residual moisture content of the 10% mannitol formulations reflects their low solubility and may be explained by the hydrophobic nature of crystalline mannitol. [119] Conversely, the higher moisture content and amorphous state of trehalose allows for the sufficient rehydration and buffering of the polyplexes in the NEM formulation.

IV.4.5. Quantification of polymer and nucleic acid content

One of the main disadvantages of spray drying at the laboratory scale is that the overall yield can vary from 20 -70% due to loss of product in the walls of the drying chamber [120]. Prior to any *in vitro* investigation of the NEM formulations' efficiency upon reconstitution, it was crucial to quantify the amount of polymer and nucleic acid that may have been lost during the spray drying process. Therefore, the 10% trehalose NEM powder was redispersed and the reconstituted polyplexes underwent a competition assay with the polyanion heparin in order to dissociate PEI from the bulk DNA, similar to our previous studies [95]. With the polyplex disassociated, we then utilized SYBR® gold fluorescent dye to assess the relative amount of free, uncondensed DNA (Figure IV.5.A.). As expected, there was about a 20 – 40% loss of bulk DNA in all of the formulations tested. While not statistically significant, there was

an increase in the overall retained amount of DNA as the N/P ratio increased, ultimately leveling off at an N/P ratio of 12. To quantify the amount of PEI that was lost following the spray drying process, a modified TNBS assay was conducted following the reconstitution of the 10% trehalose NEM formulation (Figure IV.5.B.). Here again, approximately 10 – 35% loss of PEI polymer was observed following the spray drying process. Interestingly, there was no observable trend in the overall amount of PEI lost following spray drying; however, there is a sharp increase in the amount of PEI retained in the NEM formulation at N/P ratio of 15 and higher, albeit not statistically significant. Following the quantification of the remaining PEI and bulk DNA in the spray dried microparticles, we were able to calculate the “redispersed” N/P ratio of the polyplexes within the 10% trehalose NEM formulation (Figure IV.5C). When these are compared to the “initial” N/P ratio, it becomes clear that the spray drying process effectively increases the N/P ratio of the polyplexes contained within each 10% trehalose formulation by approximately 20% through the combined loss of both the PEI and DNA in the final NEM formulation. To the best of our knowledge, we are the first to investigate the impact of spray drying on the composition of electrostatically assembled polyplexes, which has an important impact on their subsequent performance *in vitro* and *in vivo* as well as on toxicity, especially *in vivo* [121]. In comparison to recent literature, this could lead to new insights in the performance of spray dried polyplexes.

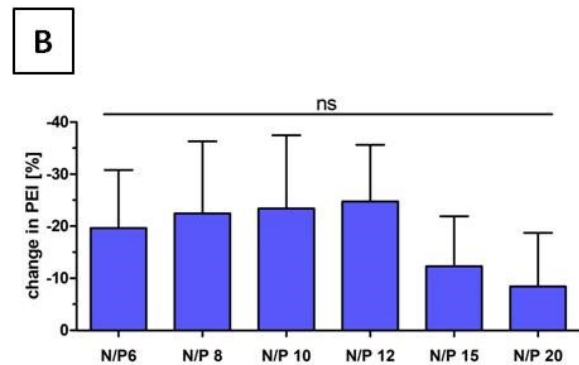
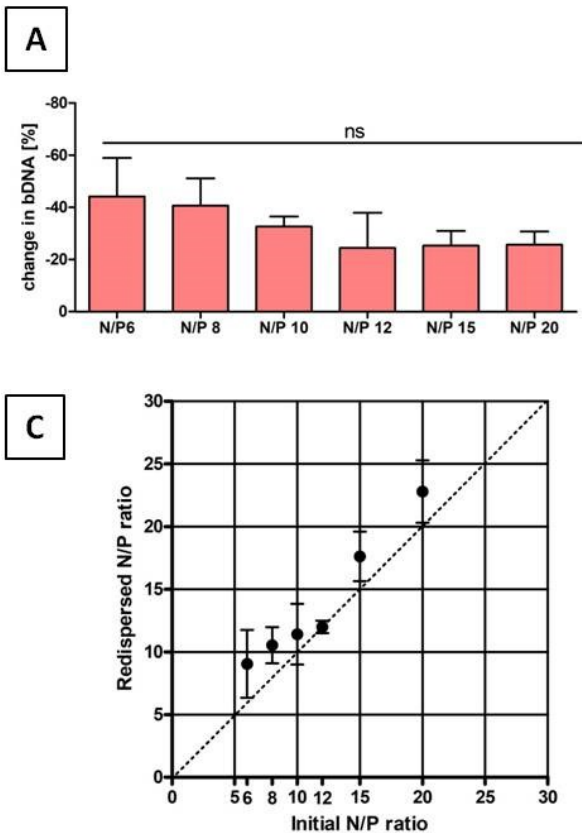


Figure IV.5. Polymer and nucleic acid quantification

Quantification of A) bulk DNA and B) PEI in the 10% trehalose NEM formulations following spray drying C) Comparing the redispersed N/P ratio with the initial N/P ratio of the PEI polyplexes loaded with bulk DNA.

Schulze et. al. showed increased transfection efficiency of PEI polyplexes containing an EGFP reporter plasmid after spray drying compared to their freshly prepared counterpart [96]. While the glucose-PVA ratio in spray dried polyplexes and the amount of PVA in freshly prepared polyplexes remains unclear, the group did not evaluate if the increase in EGFP expression is caused by a changed composition of polymer and/or nucleic acid content. Concentration of the nucleic acid content through intensive excipient loss for example might explain this phenomenon. Also decreased cytotoxicity of redispersed polyplexes in a dose escalation assay could be explained by a loss of polymer which, due to its cationic charge, is the root cause for cytotoxicity [96, 122]. In fact, a possible loss of polymer is supported by our findings. Hence, by applying our new developed method to this and other studies, we gain a better understanding of preparation and process effects on polyplex performance after spray drying.

IV.4.6. In vitro cellular uptake of redispersed polyplexes

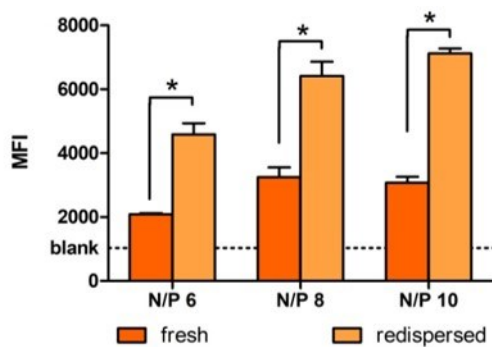


Figure IV.6. Cellular uptake of redispersed NEM formulations in A549 cells

Median fluorescence intensity (MFI) was determined by flow cytometry to evaluate the cellular uptake in a human non-small cell lung carcinoma cell line (A549) of fresh or redispersed PEI polyplexes from 10% trehalose NEM formulations at N/P ratios of 6, 8 and 10 with 0.5 μg of YOYO-1 labeled bulk DNA. Blank samples consisted of A549 cells treated with 5% glucose only. Data points indicate mean \pm SD (n=3). Two-way ANOVA, Bonferroni post-test, *** P < 0.001.

After quantifying the amount of bulk DNA in the 10% trehalose NEM formulation and ensuring that the polyplexes were able to be redispersed, the ability of the redispersed PEI/bDNA polyplexes to be delivered to cells was investigated. Therefore, YOYO-1 labeled DNA was used to form polyplexes with PEI at various N/P ratios and spray dried into NEM powder. An amount of each NEM powder correlating to 0.5 μg of YOYO-1 labeled DNA was then weighed out and lung adenocarcinoma A549 cells were treated for 24 h. Additionally, fresh polyplexes containing 0.5 μg of YOYO-1 DNA were transfected simultaneously. Following

transfection, cells were submitted to flow cytometry analysis and the level of per-cell fluorescence was quantified. Cells treated with vehicle only (5% glucose) were included as negative controls. As seen in Figure IV.6., a trend can be observed that freshly prepared

polyplexes with trehalose showed greater uptake efficiencies in comparison to freshly prepared polyplexes. However, this trend is statistically not significant, indicating a rather small effect of trehalose on uptake efficiencies. Also, redispersed polyplexes from the 10% trehalose NEM formulations show higher uptake efficiencies than their freshly prepared counterparts with trehalose. Again, this observation is statistically not significant but underlines and confirms our findings described above discussing the increase of N/P ratios (Figure IV.5.) and the hypothesized changed in vitro performance through spray drying. However, NEM with N/P ratio of 6 show a significant increase of MFI values compared to their freshly prepared counterparts which can be explained by a comparably strong increase from N/P ratio 6 to 8 after spray drying. However, this increased cell uptake could also be partly a result of the slightly agglomerated particles as reflected in the increased PDIs (Figure IV.1.).

IV.4.7. In vitro transfection efficiency redispersed polyplexes

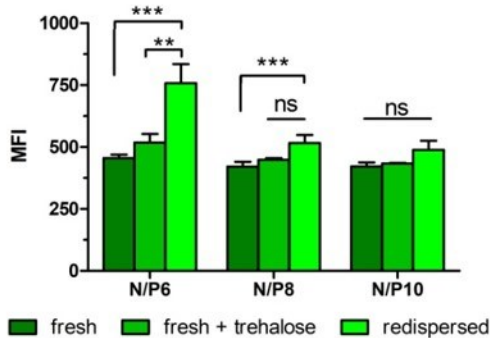


Figure IV.7. Transfection efficiency of redispersed NEM formulations in A549 cells

Median fluorescence intensity (MFI) was determined by flow cytometry to evaluate the transfection efficiency of pEGFP in a human non-small cell lung carcinoma cell line (A549) of fresh or redispersed PEI polyplexes from 10% trehalose NEM formulations at N/P ratios of 6, 8 and 10 with 0.75 µg of GFP plasmid in comparison to freshly prepared formulations in presence of trehalose. Blank samples consisted of A549 cells treated with 5% glucose only. Data points indicate mean ± SD (n=3). Two-way ANOVA, Bonferroni post-test, **P < 0.01, *** P < 0.001, ns = non-significant.

To further investigate the bioactivity of redispersed polyplexes and their transfection efficiency following spray drying, we utilized a GFP expressing plasmid. The GFP plasmid was complexed with PEI at various N/P ratios and formed polyplexes similar to those loaded with bulk DNA (Figure IV.S5.). Following spray drying using the same parameters outlined above, 10% trehalose NEM formulations were generated. Lung adenocarcinoma A549 cells were transfected with redispersed, fresh PEI/pEGFP polyplexes, or freshly prepared formulations in presence of trehalose for 48 h, and the level of GFP fluorescence per cell was quantified via flow cytometry (Figure IV.7.). Akin to the uptake studies, cells transfected with the redispersed polyplexes at the various N/P ratios exhibited similar, if not better gene transfection when

compared to the fresh polyplex counterparts. Interestingly, the presence of trehalose in freshly prepared particles did not show the same positive effect on transfection efficacy, especially at N/P 6. Therefore, trehalose potentially influencing the permeability of the cell membrane and thereby increasing polyplex uptake and gene transfection as observed previously [123] does not explain our observations. Importantly, due to the ability to quantify the amount of PEI and nucleic acid within each NEM formulation, we are able to ensure that the same quantity of plasmid DNA was used in the transfection for both fresh and redispersed polyplexes, however, according to Figure IV.5.C. the increased N/P ratio following spray drying could explain better transfection results. As hypothesized for the increased cellular uptake, faster sedimentation of larger particles may as well play a role, especially in the case of plasmid containing polyplexes at N/P 6 which showed stronger aggregation than higher N/P formulations (Figure IV.S5.) or bulk DNA containing polyplexes (Figure IV.1.). The results suggest, therefore, that the formulation of PEI/DNA polyplexes in the form of NEM does not negatively affect biological activity of the nucleic acid.

IV.5. Conclusion

Herein we demonstrate successful spray drying of PEI/DNA polyplexes into NEM powders intended for pulmonary gene delivery. Various spray drying processing parameters were optimized while the saccharides trehalose and mannitol were investigated as matrix excipients to stabilize the polyplexes in the resulting NEM formulations. The mannitol and trehalose NEMs were then characterized through various physical techniques, and the behavior of redispersed PEI-DNA polyplexes were compared to fresh unprocessed particles. Following these characterization studies, 10% trehalose was found to be an efficient stabilizer that preserved the size of the polyplexes following their resuspension. Microparticle powder analysis revealed fused, slightly corrugated particles with an aerodynamic diameter suitable for deep lung deposition. *In vitro* studies showed that the redispersed polyplexes maintained their uptake and transfection profiles in lung adenocarcinoma A549 cells when compared to fresh polyplexes. While previous studies describe spray drying of polymeric nanoparticles into NEMs, this study is, to the best of our knowledge, the first to quantify the extent of polymer and nucleic acid loss during the process and to recalculate the N/P ratio of the dried polyplexes accordingly. By quantifying the amount of DNA remaining in the resulting NEM powder, we were able to ensure that our

in vitro transfections were executed without bias due to equal DNA amounts transfected. However, as discussed, the increase of the N/P ratio may have a positive impact on uptake and transfection and would have to be accounted for when preparing new batches of NEMs. Taken together, this study serves as a proof-of-concept for the processing of polymeric nanoparticles loaded with nucleic acids into a dry powder that is suitable for inhalation therapy. After optimizing the analytics for precise analysis of the composition of a well-studied polyplex system, this study plants the basis for further studies with more complex polymers and siRNA. Along these lines, further optimization of the spray drying parameters to produce NEM powder from polymeric nanoparticles loaded with siRNA as well as formulation with biodegradable polymers is underway along with long term storage and stability studies of these NEM formulations.

IV.6. Acknowledgements

This work was supported by the European Research Council and Wayne State School of Medicine for GRA support of Daniel Feldmann. The authors thank Ahmed El Mahmoudi (Technical University of Munich) for expert spray lab support. Sandro da Rocha acknowledges the National Science Foundation under Grant No. 1643770.

IV.7. Supplementary Data

Figure IV.S1.A.

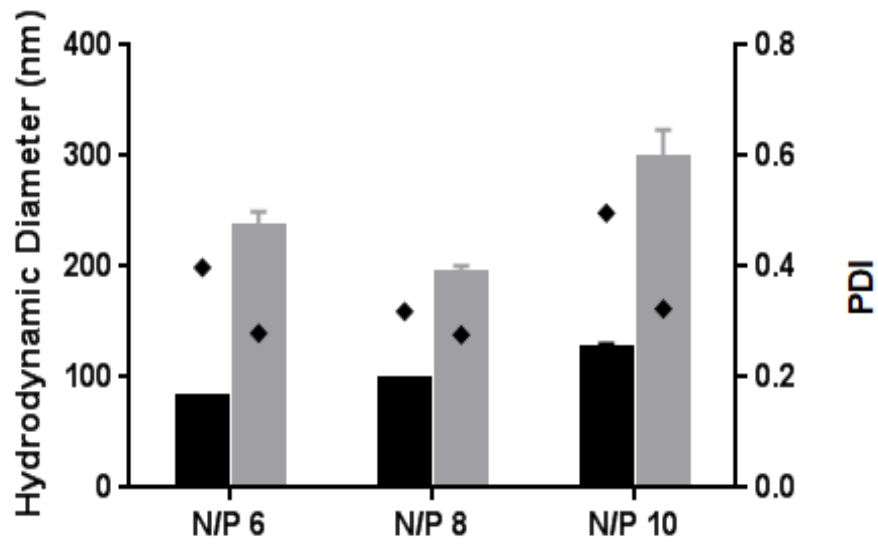


Figure IV.S1.B.

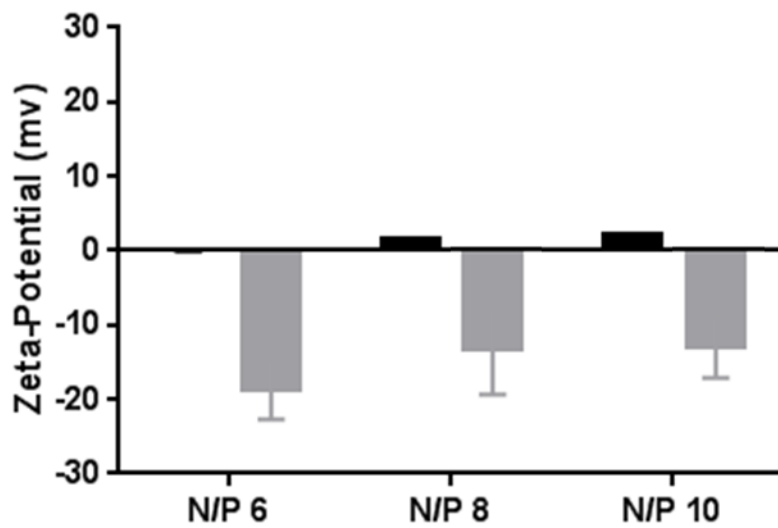


Figure IV.S1. A) Dynamic light scattering and B) Laser Doppler Anemometry characterization of fresh and redispersed PEI-bDNA polyplexes with 5% mannitol stabilizing excipient.

excipient	N/P ratio	MMAD [μm]	GSD [μm]	FPF [%]
Mannitol 10%	N/P 6	4.88	1.98	67.3
		4.59	2.01	67.5
		4.51	2.05	66.3
Mannitol 10%	N/P 8	4.19	2.21	62.8
		4.84	1.94	69.1
		4.66	2.00	67.3
Mannitol 10%	N/P 10	4.85	1.93	69.7
		4.73	1.97	68.4
		4.87	1.94	68.7
Trehalose 10%	N/P 6	2.78	2.53	78.6
		3.87	4.12	61.4
		3.64	2.47	65.7
		3.27	2.50	70.8
Trehalose 10%	N/P 8	3.13	2.64	72.3
		2.84	2.68	70.3
		3.33	2.45	74.5
		3.27	2.02	74.5
Trehalose 10%	N/P 10	3.05	2.39	75.0
		3.07	2.28	75.5
		2.60	2.82	80.2
		3.19	2.38	72.8

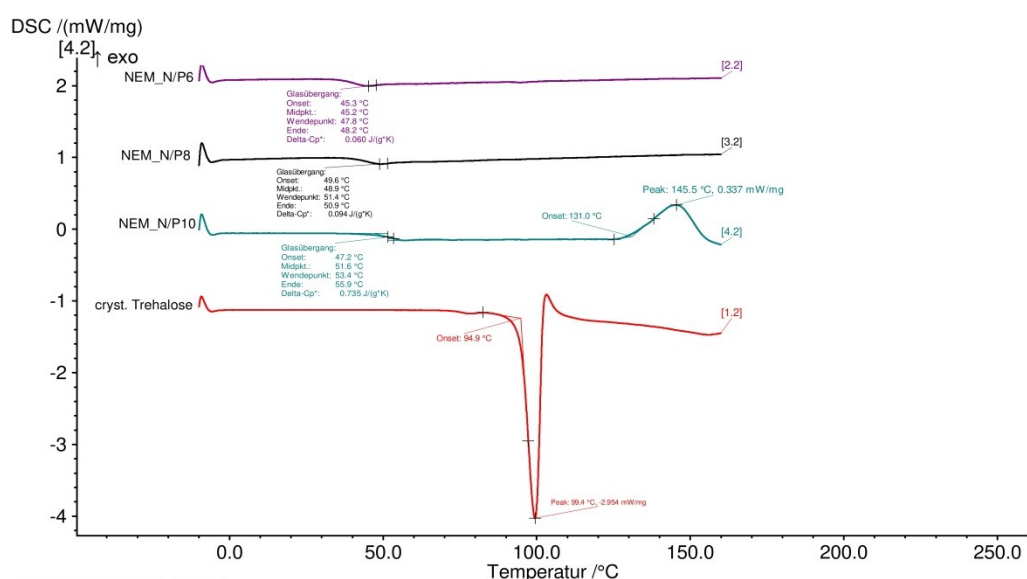
Figure IV.S2. Aerodynamic properties of mannitol and trehalose formulations. To evaluate effect of N/P ratio on aerodynamic properties of each formulation, One Way ANOVA analysis was performed with Bonferroni post-test, $p < 0.05$.

For inter-excipient analysis, statistics were executed with Two Way ANOVA and Bonferroni post-test, $p < 0.05$.

Differential Scanning Calorimetry (DSC)

For analysis, approximately 5 mg of crystalline trehalose dihydrate and NEM with N/P ratios of 6, 8 and 10, prepared of trehalose 10%, were weighed into concavus pans and closed. Another closed concavus pan was used as reference. Sample and reference pans were placed in the oven and cooled for 5 minutes at -10°C , followed by a temperature ramp of $8\text{K}/\text{min}$ until a temperature of 160°C was reached. After 5 additional minutes at 160°C , measurement stopped and the oven was cooled down for the next measurement. During isothermal and dynamic temperature phases, 50 and 200 points per minute were collected, respectively.

Crystalline trehalose showed its specific melting point at 99.4°C confirming literature values. However, no spray dried formulations exhibited a melting peak but rather glass transition points between 47.8° and 53.4° suggesting amorphous state of trehalose. In addition, the formulation containing polyplexes with a N/P ratio of 10 displayed an exothermal peak at 145.5°C . Common exothermal reactions in amorphous state formulations are



recrystallizations which might also explain this finding. However, not all formulations showed this recrystallization peak which is why we hypothesize that a certain amount of polymer is needed in order to trigger this reaction.

Figure IV.S3. Differential Scanning Calorimetry measurements of crystalline trehalose and NEM N/P6, 8 and 10 prepared of bDNA-PEI polyplexes in trehalose 10%

X-Ray Powder Diffraction (XRPD)

To identify crystalline structures of mannitol and trehalose, XRPD was executed with a 3,000 TT diffractometer (Seifert, Ahrensburg, Germany). The wavelength is 0.154178 nm and the device is equipped with a copper anode with a voltage of 40 kV and a current of 30 mA. The voltage of the scintillation detector was 1,000 V. Samples placed on the copper sample holder were analyzed in the range of 5-45° 2-theta in steps of 0.05° 2-theta.

The pattern of trehalose NEM show an amorphous halo, confirming the findings of the DSC measurements. In contrast, the pattern of the mannitol formulation shows distinct crystalline features. In comparison with literature, this pattern is very similar to the β polymorph and shows its specific peaks at 14.6° and 16.8° 2-theta. We therefore can confirm the crystalline structure of mannitol and further hypothesize that the state of mannitol after spray drying is dominated by the β polymorph as small amounts of different polymorphs cannot be excluded.

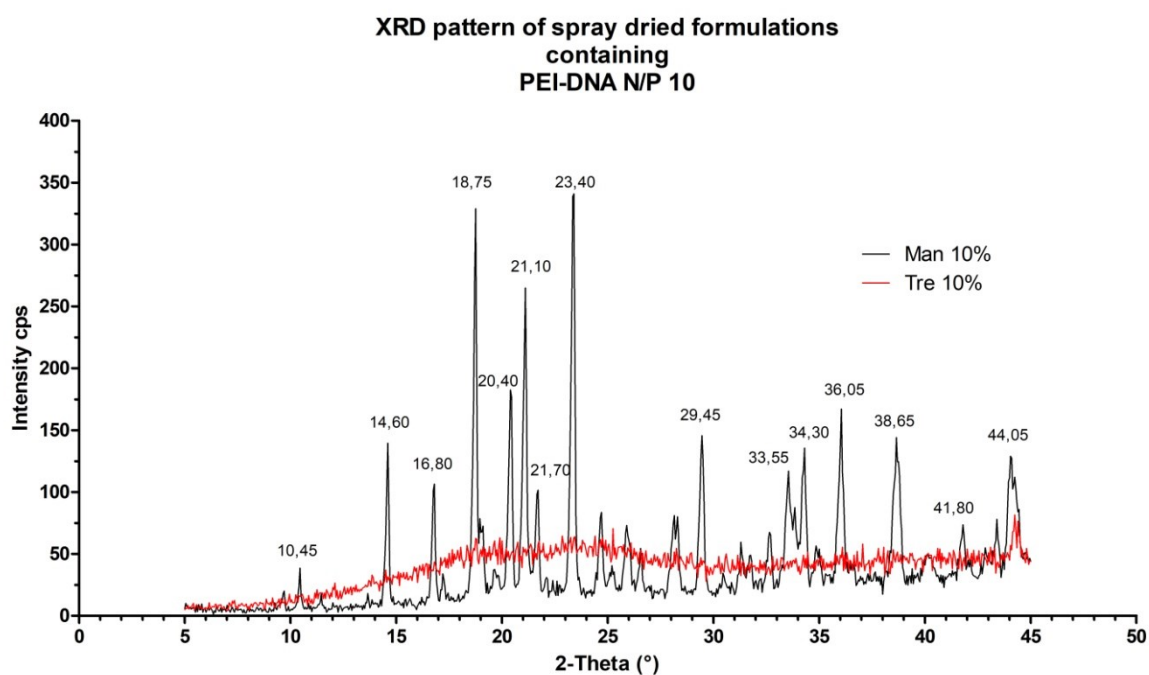


Figure IV.S4. XRD patterns of 10% Mannitol NEM and 10% Trehalose NEM

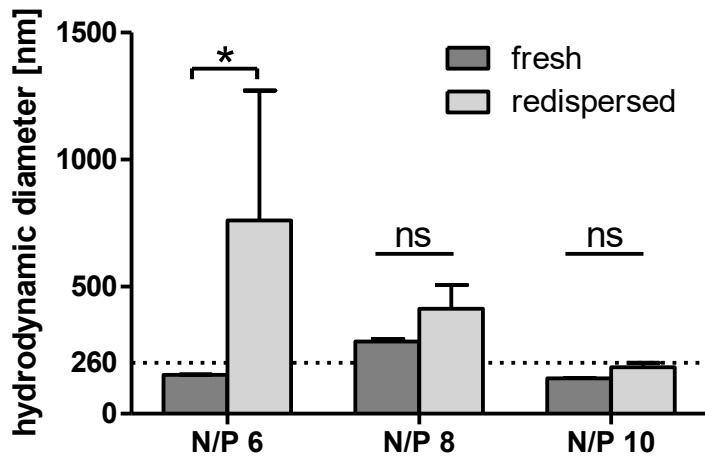


Figure IV.S5. Hydrodynamic diameters of freshly prepared and redispersed pEGFP/PEI polyplexes in presence of trehalose.

Chapter V)

Evaluation of Tubing Material on Adsorption of DNA-PEI Polyplexes

Tobias Keil¹, Natalie Deiringer¹, Wolfgang Frieß, Olivia M Merkel

¹Both authors contributed equally to this work.

This work is a collaboration between Wolfgang Frieß who brought up the idea of examining the adsorption effects of tubing material and Olivia Merkel who supervises the spray drying project of nucleic acids. Spray drying experiments, quantifications and related experiments of DNA and PEI were performed by myself. Characterization of the tubing material was done by Natalie Deiringer. The manuscript was written by both.

V Evaluation of adsorption of bDNA-PEI polyplexes to tubing materials

V.1. Abstract

Nucleic acids are a promising new drug class for potential treatment of a variety of diseases. But efficient delivery is still the major challenge impeding translation. Many nucleic acid formulations are based on polymeric components for nanoparticle delivery into cells. During various nanoparticle preparation processes such as microfluidic mixing, spray drying or final filling, pumping is a crucial step. Here, we studied the effect of peristaltic and syringe pumping on the component loss and overall loss of a binary polyplex formulation made of DNA and polyethyleneimine (PEI). We varied tubing length and material with a focus on subsequent spray drying. While significant losses were detected, no significant impact of the pump types used was observed. Interestingly, product loss increased with the length of silicon tubing. Losses of DNA were prevented by using Pumpsil tubings whereas comparable losses recorded after use of Silicon and Santoprene tubings. The following spray drying process did not affect DNA content but accounted for PEI loss. Characterization of the different tubing materials revealed similar hydrophobicity of all tubing materials and showed neutral surface charge for Pumpsil, negative surface charge for Santoprene and a positive surface charge for Silicon tubings. Hence, we hypothesize that adsorption of DNA onto

V.3. Introduction

Research on nucleic acids and their delivery has increased over the past decades to over 14 000 publications per year. The delivery of nucleic acids is hampered by its chemical nature: molecule size, negative charge and susceptibility to nucleases are the main challenges to be overcome. Several strategies have been developed including polymer based nanoparticle delivery. [124] Positively charged polymers such as polyethyleneimine (PEI) can interact with the negative phosphate groups of nucleic acids and form polyplexes of around 100 nm. These polyplexes can be taken up by the cells and finally transfect the cells with their cargo. [125] While polycationic materials such as PEI are often associated with cellular toxicity [103], they offer much higher encapsulation efficiency compared to nanoparticle formulations based on polymers such as PLGA [32, 126].

Pulmonary delivery has attracted great interest in the research community to tackle diseases such as asthma, chronic obstructive pulmonary disease and cystic fibrosis. Local treatment of these diseases is preferred over systemic parenteral application as less drug is required with lower risks for adverse effects due to direct tissue targeting. [67] It is known that only particles with an aerodynamic diameter between 1 and 5 μm are able to follow the airstream and deposit in the lower lung areas. While particles greater than 5 μm deposit in the throat or the upper airways, particles below 1 μm are often exhaled. [93] Therefore, polyplexes need to be formulated into microparticles with excipients suitable for inhalation for example by spray drying [96, 127]. During spray drying, solutions/suspensions can be sprayed via a nozzle into a drying chamber where heat is applied to dry the formulation gently.

We recently observed losses of around 30% bulk DNA (bDNA) and 20% PEI upon spray drying of model nanoparticles. [127] We assumed that these losses were attributed to the spray drying process and that the different extent to which the two nanoparticle components were lost was caused by particle instability. Comparable losses of nucleic acids and their formulations after spray drying were also reported by others [54-56]. However, further experiments to identify the root cause for the observed effects were not conducted so far. Considering that spray drying involves also pumping of the liquid feed, this study focused on pumping as an essential step in liquid product handling for filling, filtration, and transfer. While piston pumps have a high dosing accuracy, shed steel particles, drug aggregation and

shear are of concern. [128] Diaphragm pumps are similar to piston pumps in means of dosing accuracy and shear forces, but no shed steel particles are observed. [129, 130] Peristaltic pumps have lower dosing accuracy but they are well suited for shear sensitive products, and as single use systems the risk for cross contamination is minimized. [131] Syringe pumps are characterized by constant mean flow rate, high dosing precision and are also ideal for shear sensitive drugs but are limited in volume and thus not applicable for industrial production. [132]

In the last years substantial research was conducted on the use of pumps in fill and finish of biopharmaceutics focusing on the effect of shear stress on protein adsorption and aggregation [128-130, 133]. To the best of our knowledge, no reports are available investigating the behavior of nucleic acid nanoformulations upon pumping. In this study, peristaltic pumps were utilized because of their standard use in the pharmaceutical industry during fill and finish processes, liquid transfer and drug supply for spray dryers.

Due to our previous observations, this study aimed at gaining deeper insights into the impact of peristaltic pumping on polyplexes both with respect to loss and composition. Data sets were recorded for three different tubing materials, which are regularly used in pharmaceutical and food industry: high- and low-quality silicone tubings as well as a thermoplastic elastomer. The effects of only pumping or pumping and spray drying were evaluated based on polyplex size, PDI and the quantitative composition of the final product. Also, different tubing pretreatments and the addition of PS20 surfactant were tested to evaluate their effects on polyplex quality and quantity. These findings are of interest for spray drying polyplexes but are also important for any process utilizing peristaltic pumping in the field of nucleic acid nanoformulations.

V.4. Materials and Methods

V.4.1. Materials

Hyperbranched polyethyleneimine (PEI) (25 kDa) was obtained from BASF (Ludwigshafen, Germany). Bulk DNA sodium salt from salmon sperm (BP2514-250) (bDNA) and black 96 well plates (10307451) were purchased from Fisher Scientific (Schwerte, Germany). Heparin from porcine intestinal mucosa (H3393, >180 units/mg, grade I-A), picrylsulfonic acid (TNBS) (P2297), TRIS EDTA Buffer Solution 1x (93283) and polysorbate 20 (PS20) (P9416) were obtained from Sigma Aldrich (Munich, Germany), SYBR™ Gold dye from Life Technologies (Carlsbad, CA, U.S.A.), ethylene glycol from Grüssing (Filsum, Germany) and n-hexadecane from Merck (Darmstadt, Germany). Peroxide cured silicone tubings (inner diameter 2.0 mm, outer diameter of 4.0 mm) were bought from VWR International (228-0704, Germany), Pumpsil® tubing (inner diameter 1.6 mm) was a kind gift from Watson-Marlow (Rommerskirchen, Germany) and Santoprene® tubing (inner diameter 1.6 mm) was obtained from AET Lézaud (Wendel, Deutschland).

V.4.2. Polyplex Preparation

5 ml of polyplexes containing 10 µg of bDNA were prepared at an N/P ratio of 10 as described in [127]. For polyplex preparation, 10 µg of bDNA and the respective amount of PEI (13.1 µg) were diluted to 500 µL with HPW, each, and mixed together by pipetting. After 10 min incubation, polyplexes were further diluted with HPW to 5000 µL. After additional 10 min incubation, 70 µL were used for DLS analysis. The remainder was pumped at 1.2 ml/min and collected for further analysis. For experiments evaluating the effect of PS20 on adsorption effects, polyplexes were prepared as described above in a 0.02% PS20 HPW solution.

V.4.3. Spray Drying and Pumping

For spray drying experiments, polyplexes were prepared as described in 3.2 using 10% m/v trehalose instead of HPW. A B-290 spray dryer was used (Büchi Labortechnik, Essen, Germany) with a DeltaTherm-dehumidifier (DeltaTherm, Germany) at 1.2 ml/min feed rate (5% pump rate), equipped with a two-fluid nozzle at an airflow of 470 NL/h, aspirator preset to 70% and an inlet temperature of 65°C resulting in an outlet temperature of 40°C. Before drying the samples, the spray dryer was equilibrated for 20 min by feeding HPW. Samples were spray dried after pumping through the 60 cm silicone tubing using the built-in pump of the Büchi B-290 “PP60_SD”. Alternatively, 60 cm (“SP60_SD”) or very short 2 cm (“SP2_SD”) silicone tubing pieces were connected to the spray dryer using a syringe pump (KDS-220-CE, KD Scientific, Holliston, MA, USA). Additionally, samples were pumped through the silicone tubing only, without spray drying (“PP60”).

In another setup, Pumpsil® and Santoprene™ tubings were connected with a Masterflex L/S (7520-47), equipped with the Easy-Load II head module (77201-60, Cole-Parmer, Wertheim, Germany), because the thicker tubing did not fit the built-in pump. All Pumpsil® and Santoprene™ tubings had a length of 60 cm and were pre-rinsed with approximately 50 ml of 40°C HPW and air dried. One set of Silicon, Pumpsil® and Santoprene™ tubing was not pre-treated (NT), one was additionally autoclaved at 121°C for 15 minutes (AC) and one was additionally rinsed with RNase Zap before another HPW treatment. For the PS20 containing sample a not pre-treated set of tubings (NT-PS20) was used. All experiments were performed in triplicates.

V.4.4. Z-average, PDI and Zeta Potential Measurements

For Z-average, PDI and zeta potential measurements, 70 µL of freshly prepared or pump stressed polyplexes were placed into a disposable cuvette (Brand, Wertheim, Germany) or 700 µL of freshly prepared polyplexes into a folded capillary cell (DTS1070) and analyzed by a Zetasizer Nano ZS (Malvern Instruments, Malvern, U.K.) at 173° back scatter. Measurements were performed in triplicates with 15 sub-runs for size and PDI or up to 100 sub-runs for zeta potential.

V.4.5. bDNA Quantification

Nucleic acid quantification was performed as described elsewhere [127]. In short, 90 μL of sample was diluted to 150 μL , and 75 μL of a 2.33 mg/ml heparin solution in TRIS-EDTA-buffer was added. After 2h of incubation, samples were diluted 1:2 with HPW, 100 μL were pipetted into a black 96 well plate, 30 μL of a 4x SYBR gold solution was added an analysis was performed at 485 nm excitation of 520 nm emission with a FLUOstar® Omega microplate reader (BMG LABTECH, Ortenberg, Germany). Samples were analyzed in triplicates. To verify accuracy and precision of the analysis, an internal standard (iS) was prepared as described in V.5.1.

V.4.6. PEI Quantification

For polymer quantification, a TNBS assay as described previously was used [127]. In short, 9 standards ranging from 0 to 19.14 μg PEI/ ml were prepared. Of each sample, 100 μL were pipetted into a separate 0.5 ml vial. Subsequently, 30 μL of 0.088% (m/V) TNBS in 0.1 M borax buffer were added. Samples were incubated for 1 h and absorbance was measured with a quartz cuvette in a UV-1600PC spectrophotometer (VWR International, Darmstadt, Germany) at 405 nm. Again, an internal standard was prepared for verification. Analysis was performed in triplicates for calibration points, samples and internal standard. For samples containing PEI and bDNA, a calibration line was prepared with the corresponding amount of bDNA added.

V.4.7. Surface Potential Analysis

The surface potential of the tubing materials was estimated according to Altenor et al. [134] Tubing pieces of 0.5 cm were hardened in liquid nitrogen and milled with a Pulverisette 14 classic line (Fritsch, Idar-Oberstein, Germany) equipped with a 0.5 mm sieve ring operated at 10 000 rpm. Subsequently, 500 mg powdered tubing was dispersed in 50 ml 0.01 M NaCl, pH 5.8. After 24 h incubation, the pH value of each solution was measured using an Accumet AB-150 pH electrode (Fisher Scientific, Germany) and compared to the control buffer.

V.4.8. Surface Free Energy Determination

To estimate polar and dispersive parts of the three tubing materials, surface free energy was determined using a Krüss Drop Shape Analyzer DSA25 (Krüss, Hamburg, Germany). Contact angles of 2 µl of water, ethylene glycol or n-hexadecane were measured on the outer tubing wall. After 20 s of equilibration time, three measurements were performed. The drop shape was fitted by the Ellipse (Tangent-1) method with manual baseline adjustment. Surface free energy was calculated via the Owens-Wendt-Rabel-Kaelble analysis with the ADVANCE software v1.1.0.2 (Table V.1). Analysis was performed in triplicates.

Liquid	Surface tension	Polar component	Dispersive component
Water	72.8	51.0	21.8
Ethylene glycol	47.7	16.8	30.9
n-Hexadecane	27.6	0.0	27.6

Table V.1. Surface tensions and surface free energy components (mN/m) of the test liquids according to Ström et al. [135]

V.4.9. Data presentation, Graphics and Statistics

For spray drying experiments, results are calculated according to V.4.4. and V.4.5. and presented in µg. For tubing material evaluation, results are presented as adsorption and calculated according to following formula:

$$\text{adsorption} = \frac{\text{loss}}{l \cdot \pi \cdot d} \text{ (Eq. V.1.),}$$

Where loss is the difference between feed and calculated amount of bDNA or PEI according to 3.4 or 3.5 in mg, respectively, and l is the length and d the inner diameter of the tubing in m.

If not stated differently, data were processed by Graph Pad Prism5 software (Graph Pad Software, San Diego, CA, USA), presented as mean ± standard deviation and analyzed for statistical difference by One-Way ANOVA or Two-Way ANOVA with Bonferroni post-test p<0.05.

V.5. Results and Discussion

Upon spray-drying of polyplexes substantial material loss has been observed independent of the reduction in yield due to losses in the spray-dryer. We found up to 40% less DNA and 25% less PEI in the solid content for bDNA / PEI polyplexes spray dried with 10% trehalose [127]. To identify the root cause of the component loss, a 10% m/v trehalose solution containing polyplexes at N/P 10 was spray dried with the feed provided either via a syringe or a peristaltic pump using silicone tubing. In line with our previous work, spray drying with the peristaltic pump using a 60 cm tubing (PP60_SD) resulted in losses of approx. 33% bDNA and 28.0% PEI (Figure V.1.). Exchanging the peristaltic pump for a syringe pump (SP60_SD) to reduce shear forces did not significantly affect bDNA or PEI losses. Hence the kind of pump and shear forces seem to play only a minor role. Interestingly, spray drying with a much shorter tubing of only 2 cm (SP2_SD) resulted in 21.7% loss of PEI and no loss of bDNA. This difference between PEI and bDNA loss may be explained by the fact that polyplexes at an N/P ratio of 10 contain free unbound polymer. [103] This free PEI may be lost but not the intact polyplexes as indicated by an unchanged amount of nucleic acid. One pump cycle with a 60 cm long silicone tubing without spray drying (PP60) resulted in a bDNA loss (23.8%) similar to the one detected after spray-drying utilizing the same length of tubing independent of the type of pump. These findings highlight the effect of the tubing material on the bDNA content by adsorption rather than by spray drying or pumping. The bDNA loss within the 60 cm silicone tubing can be interpreted as adsorption of 1.25 ± 0.18 mg/m². Thus, the total loss is related to the tubing and depends on material, length and diameter.

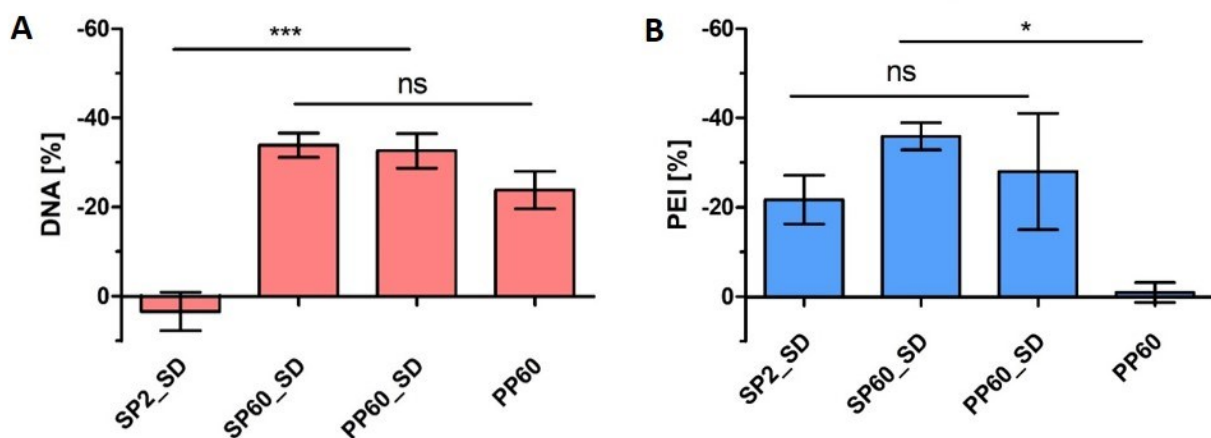


Figure V.1. Changes of (A) bDNA and (B) PEI in % after spray drying of polyplexes fed with a syringe pump equipped with a 2 cm (SP2_SD) or with a 60 cm silicon tubing (SP60_SD) or with a peristaltic pump with a 60 cm silicon tubing (PP60_SD) or polyplexes after only one peristaltic pump cycle through a 60 cm long silicon tubing without spray drying (PP60).

Spray drying however, evolved into the main reason for changes in the PEI content as spray dried samples (SP2_SD, SP60_SD, PP60_SD) showed PEI losses between 22 and 38% whereas the non-spray dried formulation (PP60) showed no change in PEI content (Figure V.1.B.).

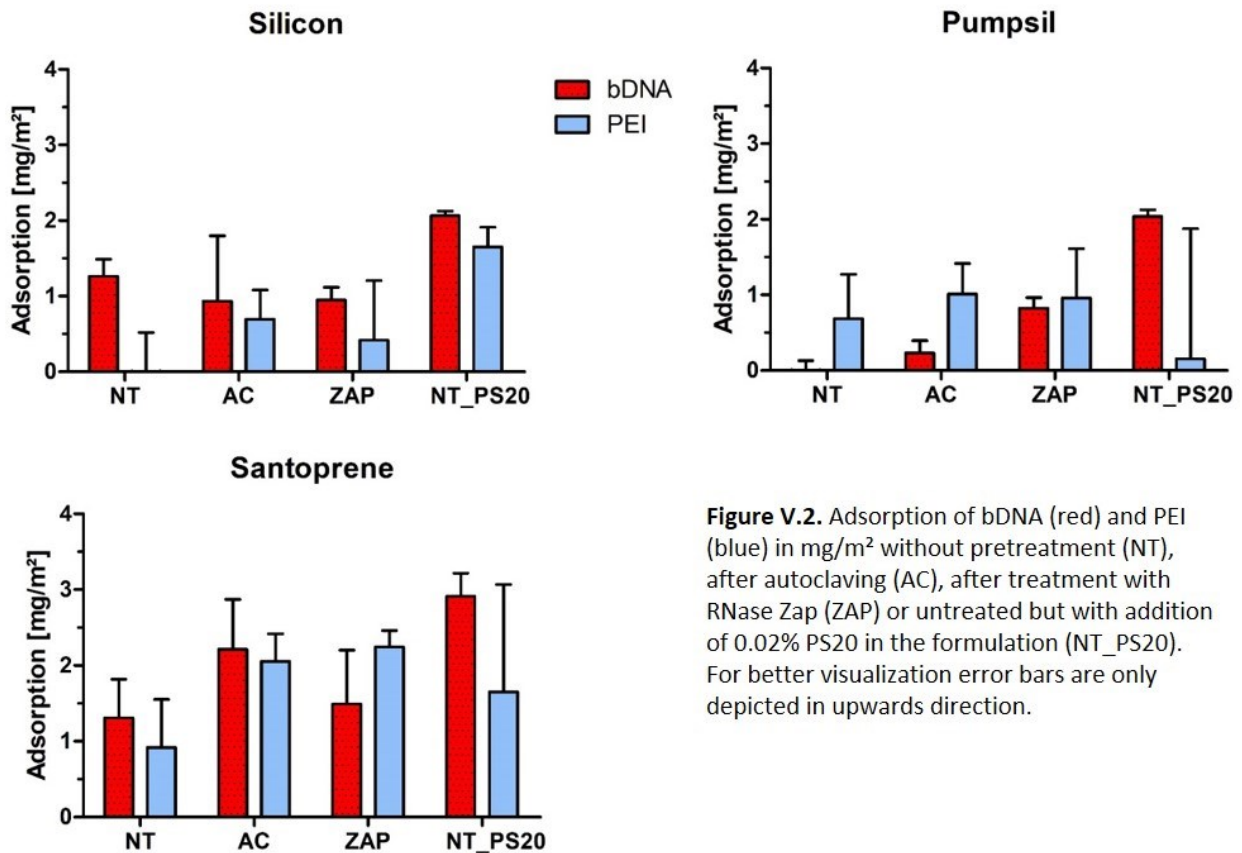


Figure V.2. Adsorption of bDNA (red) and PEI (blue) in mg/m² without pretreatment (NT), after autoclaving (AC), after treatment with RNase Zap (ZAP) or untreated but with addition of 0.02% PS20 in the formulation (NT_PS20). For better visualization error bars are only depicted in upwards direction.

To further elucidate the effect of adsorption to the tubing material, in addition to silicone tubing a high-quality low abrasion tubing (Pumpsil®) and a tubing consisting of thermoplastic vulcanizates (Santoprene™) were used for single pump cycles of polyplexes with a peristaltic pump without consecutive spray drying. Santoprene™ is a material which consists of an ethylene propylene diene monomer rubber embedded in a polypropylene matrix and is highly hydrophobic. Pumpsil® and Silicon tubings consist of methylated silicon oxide chains and might show slightly less hydrophobic properties. Furthermore, different pretreatment washing regimes were tested to investigate a potential effect of contaminants such as DNase. In addition, formulations containing PS20 as surfactant to reduce adsorption effects were evaluated. [136, 137] Adsorption of PEI and bDNA to silicone tubing did not change with pretreatment. Thus, contaminations from the tubing manufacturing and handling do not play a significant role in the observed losses of the polyplex components. PEI and bDNA adsorption could not be eliminated by addition of 0.02% PS20 to the formulation independent of the tubing material (Figure V.2.). PS20 can prevent adsorption events in the

biopharmaceutical field [138] But it can interact with the polyplexes and destabilize them as indicated by the higher standard deviations of z-average and pdi of the polyplexes in presence of PS20 (Figure V.3.). Less tightly packed polyplex offer a greater possibility for single constituting molecules to interact with the tubing material and could enhance adsorption effects.

The tubing material had a marked effect on component loss. No adsorption of bDNA was detected on untreated Pumpsil® whereas Santoprene™ and silicone tubings showed significant adsorption. This is surprising as Pumpsil® and silicone consist both of methylated silicon-oxide groups, but Santoprene™ is made of monomer rubber in a polypropylene matrix. Hence, differences were expected between the different chemical materials and not within one chemical material group, here the methylated silicon oxide chains. In contrast to bDNA adsorption, PEI adsorption was independent of the tubing material.

To better understand the adsorption of the polyplex components to the tubing surface and shed a light on the discrepancy between both methylated silicon oxide materials, we characterized surface charge and surface free energy of the tubing materials. Surface free energy can indicate the potential for hydrophobic (mostly van der Waals) and hydrophilic (hydrogen bonds and ionic) interactions. This is of special interest as the PEI-bDNA polyplexes own a positive surface charge of $+33.6 \pm 3.7$ mV and might be therefore prone to ionic interaction. All three tubing materials showed similar surface properties: low surface energy of approximately 20 mN/m with high dispersive and hardly any polar contribution (Figure V.4.A.). The values are in line with published data. Silicone and Pumpsil®, mainly consist of a structure based on poly(dimethylsiloxane) where the Si-O linkages seem to be shielded sufficiently by the methyl groups, resulting in an overall surface tension of 22.8 mN/m with polar components of 1.1 mN/m. [139, 140] Santoprene™ is a thermoplastic vulcanizate and consists of ethylene propylene diene monomer rubber particles embedded in polypropylene matrix absent of any polar groups. Literature claims an overall surface tension of 29 mN/m for the polypropylene matrix which is slightly higher than the values determined here (22.2 ± 3.22 mN/m). [141]

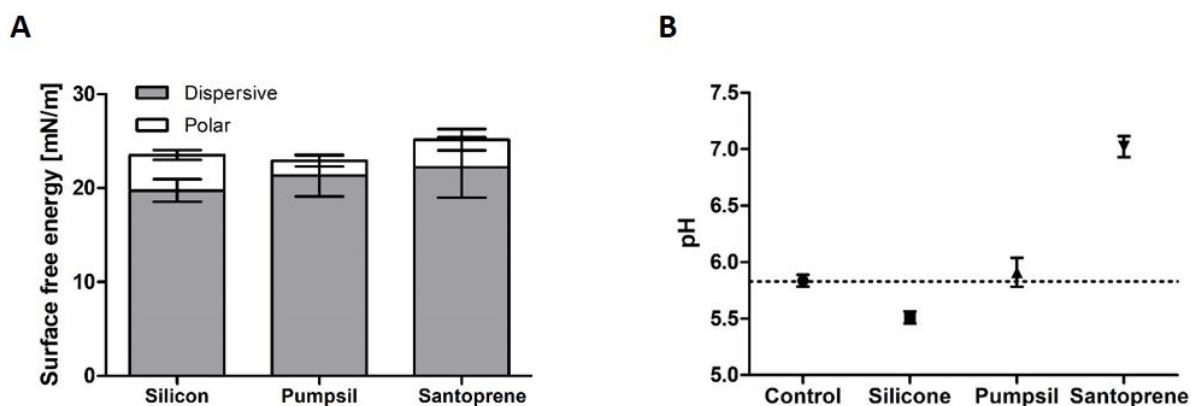


Figure V.4. A) Surface free energy of the tubing surfaces as obtained from the Owens-Wendt-Rabel-Kaelble analysis B) pH after 24 incubation of tubing material in 0.01 M NaCl; dotted line represents control

For surface charge determination the materials were shredded and incubated in buffer at the pH of the polyplex solution. [134] Pumpsil® did not show a shift of pH suggesting a net neutral surface charge (Figure V.4.B.). The regular quality silicone tubing, however, showed a slight decrease in pH indicating a positively charged surface, whereas Santoprene™ showed the opposite characteristics. Unfortunately, exact surface charge values cannot be obtained by this approach. The obtained relative estimations are in good agreement with literature values for the isoelectric points for silicone tubing or Santoprene™ like materials of around 5.2 and 3.5, respectively. [138] Thus, Pumpsil® will less likely interact via ionic interactions whereas Silicone is likely to interact with negatively charged molecules such as nucleic acids and Santoprene™ with positively charged molecules such as the positively charged polymer on its own or the whole polyplex with its positive surface charge. Linking the observation from material characterization to the adsorbed amounts no clear hypothesis was set up for the adsorption of bDNA, PEI and polyplex. But an interplay between mainly hydrophobic interactions and also contribution of electrostatic interactions is expected. Pumpsil® showed no significant difference in the composition of the dispersive and polar components compared to Santoprene™ and silicone tubing. But only Pumpsil® owns a neutral surface charge and shows no significant adsorption of bDNA after a single pump cycle. This leads to the assumption that both, electrostatic and hydrophobic interactions are required for adsorption of bDNA. In fact, literature claims hydrophobic as well as electrostatic interactions as main factors for adsorption of free and complexed DNA. It is known that DNA can adsorb nonspecifically to hydrophobic surfaces by contribution of electrostatic forces depending on surface charge density and hydrophobic interactions. [142-144]

Especially in these low ionic strength formulations, electrostatic interactions dominate the hydrophobic ones for DNA adsorption. [143] Although DNA owns negative charges due to phosphate groups it also owns hydrophobic regions provided by its nitrogenous bases which can interact with the hydrophobic surface. [145] It was shown, that the complexation of DNA with cationic agents leads to irreversible compaction on hydrophobic surfaces and in fact leads to even increased DNA adsorption of positively charge particles in comparison to free, negatively charged DNA. [146, 147] Upon pumping, attraction between polyplexes and the tubing material could lead to a reversible attachment of the whole polyplex on the surface. In case of such events, hydrophobic forces could drive a release of bDNA out of polyplexes and result in adsorption. Bengali et al. and Segura et al. presented that the adsorption of polyplexes for surface-mediated delivery of DNA showed higher immobilization of polyplexes on hydrophobic surfaces and a reduced DNA release compared to the hydrophilic analog. Release rate reduction was due to irreversible binding and aggregation of DNA complexes while hydrophilic surfaces showed rather reversible binding mechanisms. [148, 149]

V.6. Conclusion

This study showed that losses during spray drying of polyplexes have to be interpreted in the light of pumping. The drying process itself appears to lead to PEI loss, without losses of DNA. A DNA loss is based upon adsorption effects and depends on material and length of the tubing utilized to feed the liquid to the nozzle. Furthermore, we state that there is no difference between peristaltic and syringe pumps concerning the quality and quantity of polyplexes obtained after pumping despite their different pumping mechanisms. The addition of surfactants, here PS20, does not improve the performance but accounts for destabilization leading to increased adsorption effects. In the scope of this study, it was not possible to clearly identify the driving mechanism for adsorption as no distinct differences in surface characteristics were found for both silicone tubings despite differences in adsorbed mass. However, neutral surface charge seems to be favorable as no adsorption of DNA was observed on neutrally charged Pumpsil® but on positively and negatively charged Silicon and Santoprene, respectively. We showed adsorption effects for N/P 10 PEI-DNA polyplexes but the phenomenon observed is expected to also apply to other polyplex systems containing DNA or RNA. Depending on N/P ratio, polymer or lipid component, hydrophobicity and

surface charge, adsorption effects may vary quantitatively and need to be investigated for each system individually. Determining the amount of both the nucleic acid component and the carrier entities is crucial for product quality. Overall this study highlights that tubings strongly affect product recovery. Therefore, it is recommended to keep the contact area to polymeric tubing materials during production of nucleic acid delivery systems as little as possible for minimum product loss and quality assurance.

V.7. Acknowledgements

This project has received funding from the European Research Council (ERC) under the European Union's Horizon 2020 research and innovation programme (Grant agreement No. 637830). The authors also like to thank Christoph Zimmermann for his help of size and zeta potential measurements and Watson-Marlow for providing the tubing material.

Chapter VI)

T_H2-cell Targeted Pulmonary siRNA Delivery for the Treatment of Asthma

This chapter was published in WIREs interdisciplinary review:

T. W. M. Keil¹, D. Baldassi¹ and O. M. Merkel, T-cell targeted pulmonary siRNA delivery for the treatment of asthma, *Wiley Interdiscip. Rev.: Nanomed. Nanobiotechnol.*, 2020, e1634.

¹Both authors contributed equally to the manuscript draft

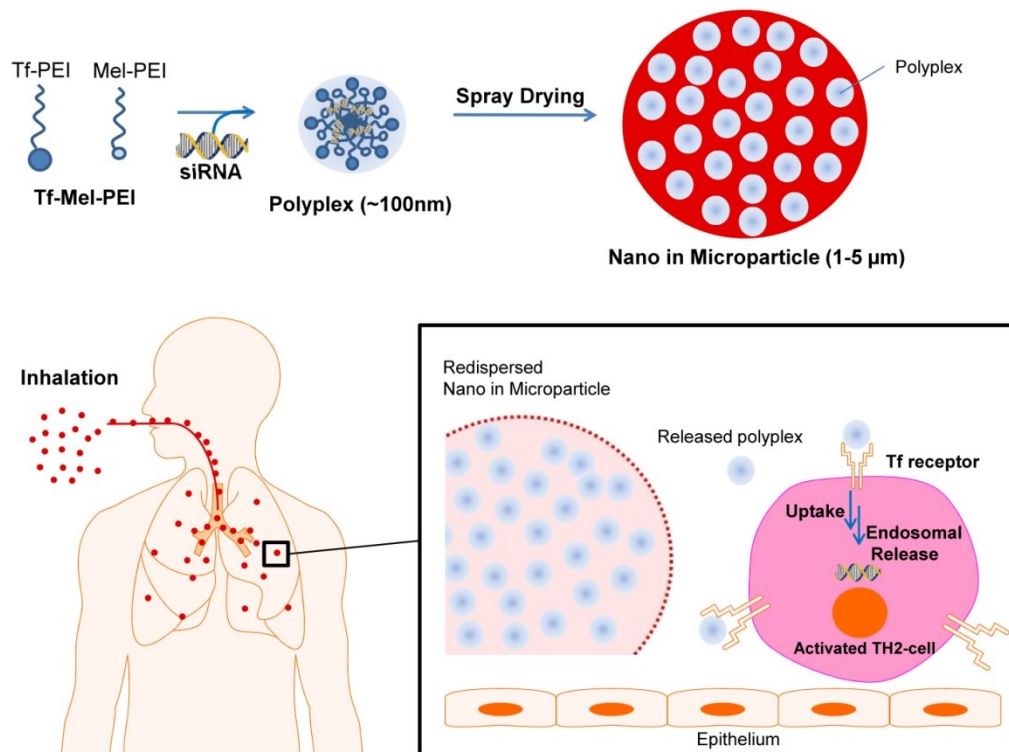
VI T_H2-Cell Targeted Pulmonary siRNA Delivery for the Treatment of Asthma

VI.1 Abstract

Despite the large number of drugs available for the treatment of asthma, in 5-10% of the patients this disease is not well controlled. While most treatments palliate symptoms, those suffering from severe and uncontrolled asthma could benefit more from a therapeutic approach addressing the root problem. An siRNA-based therapy targeting the transcription factor GATA3 in activated T helper cells subtype 2 (T_H2 cells), one of the key upstream factors involved in asthma, could therefore represent a promising strategy. However, the difficult-to-transfect cell type has not extensively been explored for nucleic acid therapeutics. In this regard, our group first identified a suitable pathway, i.e. transferrin receptor mediated uptake, to target efficiently and specifically activated T_H2 cells with a transferrin-polyethyleneimine (PEI) conjugate which forms polyplexes with siRNA. This system, despite efficient uptake in activated T cells *in vivo*, suffered from poor endosomal release and was later improved by a combination with a melittin-PEI conjugate. The new formulation showed improved endosomal escape and gene silencing efficacy. Additionally, in order to develop a clinically relevant dosage form for pulmonary delivery of siRNA we have lately focused on a dry powder formulation by spray drying for the production of inhalable nano-in-microparticles. In proof-of-concept experiments, DNA/PEI polyplexes were used in order to implement analytics and engineer process parameters to pave the way for spray drying also

siRNA containing polyplexes and more sophisticated systems in general. Ultimately, our efforts are devoted to the development of a novel treatment of asthma that can be translated from bench to bedside and are reviewed and discussed here in the context of the current literature.

VI.2. Graphical/Visual Abstract and Caption



Polyplexes made from siRNA complexed with Tf-PEI and Mel-PEI are shown to be specifically taken up by activated T cells facilitating endosomal release necessary for efficient gene silencing. By spray drying, dry powders are obtained for pulmonary delivery as therapeutic option in the treatment of asthma.

VI.3. Introduction

Amongst chronic inflammatory diseases of the airway, asthma is still considered a great medical and socioeconomic burden under which nearly 340 million people suffer worldwide [150]. The disease hallmarks, besides persistent lung inflammation, are shortness of breath, mucus hypersecretion, broncho obstruction with enhanced reactivity to spasmogens (airway hyperactivity) and airway remodeling [150-153]. The current asthma treatment algorithm is based on bronchodilating and anti-inflammatory agents (inhaled and/or systemic glucocorticoids) targeting symptoms only. However, in a small subset of patients these symptoms cannot be controlled even with high doses of the recommended drugs [154].

The origin of these symptoms, amongst others is the activation, infiltration and accumulation of T cells positive for the cluster of differentiation 4, also known as T helper cells (T_H2 cells), of subtype 2 ($CD4^+T_H2$ cells) into major airways and mucosa of small airways, and the subsequent release of proinflammatory cytokines (IL-4, IL-5, IL-9 and IL-13) [151-153, 155]. After it was found that the release of these interleukins is triggered by an upregulation of the GATA-binding protein 3 (GATA3) in T_H2 cells upon activation [156], GATA3, a transcription factor regulating T cell differentiation into T_H2 cells, emerged as a powerful therapeutic target [157]. Considering that the effect of silencing only single cytokines can be overcompensated by others [158], therapeutic downregulation of GATA3, preventing downstream release of all T_H2 cytokines and concomitant symptoms in parallel holds great promise.

A powerful tool for post-transcriptional gene silencing is RNA interference (RNAi): Fire and Mello who earned the Nobel Prize, discovered a nuclease complex known as RNA induced silencing complex (RISC) which recognizes and destroys target mRNAs. The target is specifically identified by small interfering RNAs (siRNA) which are RNA strands of 21-25 base pairs with base-complementarity to the target mRNA. Upon pairing of the activated RISC with single-stranded siRNA and the complementary mRNA site, cleavage of mRNA is initiated and the translation of the protein alongside the degraded mRNA is prevented [30]. Accordingly, targeting mRNA coding for GATA3 with siRNA could enable post-transcriptional gene silencing of the transcription factor which is overexpressed in activated T_H2 cells. Subsequently, downregulating the overexpressed level towards a more physiologic one could therapeutically be exploited towards a new asthma treatment without

general immunosuppressive side effects. Delivering siRNA exogenously into activated T_H2 cells, however, is not a simple task.

Considering the macromolecular nature of siRNAs which are highly negatively charged and the lack of nucleic acid specific active transporters on cell membranes in combination with ubiquitously present nucleases which quickly degrade siRNA in the body, intracellular siRNA delivery requires formulation of the latter. Compared to viral vectors, non-viral vectors are more advantageous regarding safety, manufacturability and immunogenicity [125]. Positively charged polymers are one class of non-viral vectors where polyethyleneimine (PEI) and its derivatives are the most studied representatives. These polymers form so called polyplexes on the nano-scale by electrostatic interaction with siRNA protecting it on the one hand from nucleases and enabling internalization and release into cells on the other [159]. However, in case of intracellular delivery into T cells, additional barriers, such as endosomal release, need to be considered [160].

In addition to avoiding nucleases which are present in high concentrations in blood but in very low concentrations in lung lining fluids, pulmonary administration of nucleic acids also avoids the rapid distribution within the body upon systemic delivery which comes with possible side effects [67]. Local pulmonary delivery can be achieved by inhaling particles (liquid or solid) of an aerodynamic size between 1 and 5 µm. Greater particles are deposited in the throat and upper airways unable to reach the area of interest. Smaller particles can undergo insufficient sedimentation and are exhaled. For optimal lung deposition, dry powder formulations are favored for siRNA delivery despite more complex formulation and preparation as compared with aerosolization [89]. The advantages can be easily explained by increased physical and chemical stability and the resulting prolonged shelf life due to the absence of water and nucleases [161]. Typical procedures to produce inhalable powders are spray drying or a combination of spray drying and lyophilization – spray freeze drying – of drug only or drug-excipient combinations [77]. For the latter, solutions or suspensions are sprayed into liquid nitrogen resulting in frozen particles which are lyophilized afterwards to remove residual water. However, this process requires high energy and time consumption due to long lyophilization cycles. A more straight forward process is spray drying where droplets are generated and dried by hot air [96]. This technique leads to microparticles where polyplexes or other nanoparticles are embedded in an excipient matrix resulting in

nano-in-microparticles which ideally resuspend into nanoparticles upon impaction on lung fluid.

This Focus Article highlights our previous and ongoing research regarding polyplexes designed for pulmonary delivery for the treatment of lung diseases in general, and of asthma specifically in the context of the current literature.

VI.4. T_H2-cell targeting

In the pathogenesis of asthma, T_H2 cells play a central role in orchestrating the allergic reaction. Upon activation and concomitant upregulation of GATA3, T_H2 cells secrete IL-4, IL-5, IL-9, IL-13 and tumor necrosis factor alpha (TNF α) [162, 163]. As shown in Figure VI.1., these cytokines stimulate different cell types resulting in further downstream effects and symptoms known for asthma. Although symptoms were shown to be reduced by i.v. application of antibodies against single interleukins in mice, their use is limited due to whole body distribution after systemic administration resulting in various side effects [164] and due to lack of compliance if administered clinically.

Rather than blocking or downregulating single cytokines, post-transcriptional interference with GATA3 expression has been reported to be a promising approach using intratracheal instillation with a bolus of GATA-3 shRNA lentiviral vector [165] or intranasal treatment with GATA-3 DNzyme [166]. In those experiments, however, the therapeutic nucleic acids were administered as unstable, free DNA and were not specifically targeted towards T_H2 cells.

The downregulation of GATA3 in activated T_H2 cells via pulmonary administration is therefore preferred as the secretion of T_H2 cytokines is ideally only downregulated in the activated T cells in the lung, preventing side effects of general immune suppression. However, the transfection of T cells is challenging since they do not express caveolin and are devoid of caveolae, preventing them from active endocytosis of nanoparticles. Primary T cells are thus known to be resistant to common non-viral delivery vectors [167].

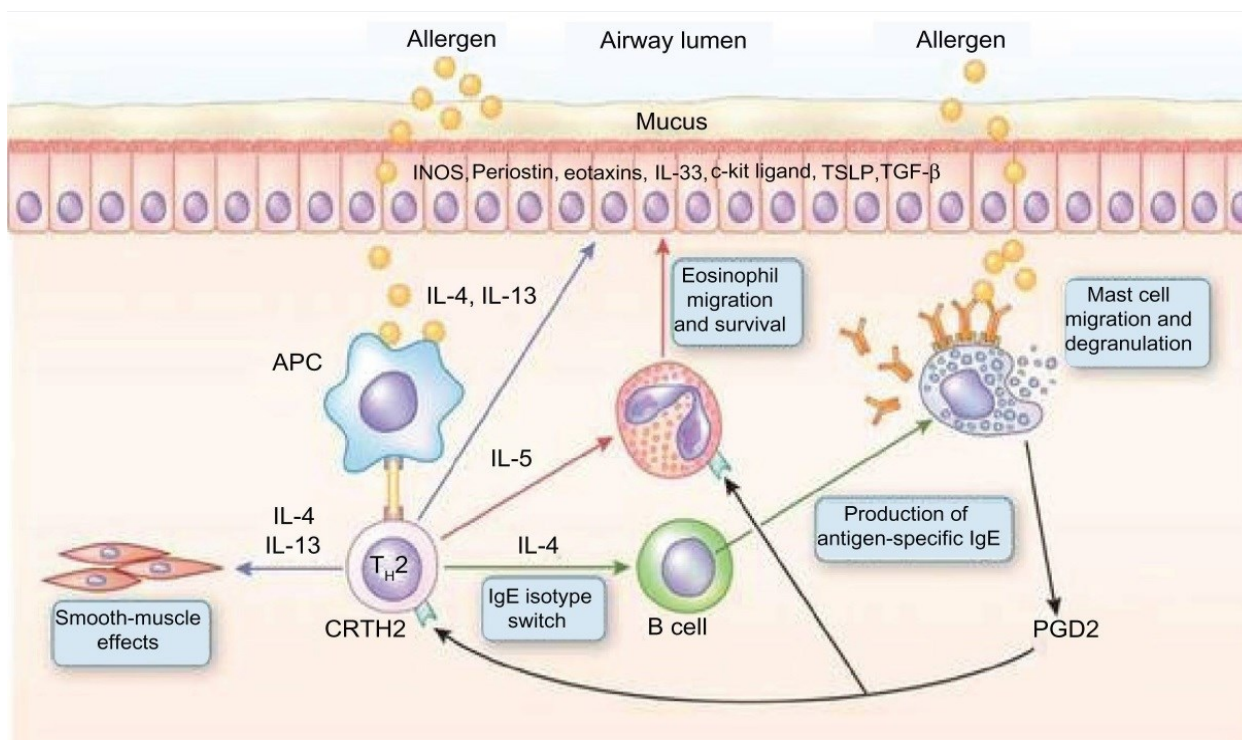


Figure VI.1. T helper-2 (T_H2) cells in asthma pathogenesis. Inhaled allergens are thought to be processed by two mechanisms in asthmatic airways. Allergens either: (1) activate mast cells through cross-linking with IgE on their cell surfaces through the high-affinity type 1 IgE receptor ($Fc\epsilon R1$) to release mediators that induce bronchoconstriction, such as histamine, cysteinyl leukotrienes, and prostaglandin D2 (PGD2) or (2) are processed by dendritic cells, which are induced to secrete the CC chemokine ligand (CCL) 17 and CCL22 by thymic stromal lymphopoietin (TSLP). Dendritic cells then attract and activate T_H2 cells by the binding of CCL17 and CCL22 with CC chemokine receptor 4 (CCR4) on the T_H2 cell surface. IL-33 is produced by airway epithelial cells and activates dendritic cells and T_H2 by inducing the release of tumor necrosis factor- α from mast cells. T_H2 secretes cytokines, including IL-4 and IL-13, which switch B cells to produce IgE, IL-5, which promotes the development and survival of eosinophils, and IL-9, which activates mast cells. Once IL-13 is produced, it can increase the survival and migration of eosinophils, and it promotes activation of macrophages to create an M2, or an allergic cell phenotype. Airway epithelial cells are stimulated, and through mediators such as periostin and transforming growth factor $\beta 1$ (TGF- $\beta 1$), they can increase airway inflammation and lead to the increased permeability of airway epithelial cells and mucous hypersecretion. IL-13 also has direct effects on airway smooth muscle, leading to increased contraction to agonists such as acetylcholine and decreased relaxation with beta-agonists. Reproduced with permission from Thomson, Patel & Smith [168], Copyright 2012 Dove Medical Press Ltd.

Since viruses efficiently transduce T cells, we sought to find a virus-like tool to target activated T_H2 cells specifically and efficiently in a receptor-mediated manner. While in the 1980s, an overexpression of transferrin receptor (CD71) in activated T cells was found whereas naïve T cells lacked the expression of CD71 [169, 170], this finding had so far not been exploited for nucleic acid delivery to T cells. This idea was picked up by our group in the early 2010s. First experiments were conducted to confirm differential receptor expression in

naïve vs. activated T cells and to test whether receptor mediated uptake was possible *ex vivo* in primary T cells exploiting transferrin (Tf) as a targeting ligand [171]. Therefore, in proof-of-concept experiments, low molecular weight (LMW) PEI was conjugated to Tf (Tf-PEI) and complexed with fluorescently labelled siRNA into polyplexes at different ratios. These formulations were initially only tested regarding intracellular delivery in primary T cells *ex vivo*. As seen in Figure VI.2.a., Tf-PEI polyplexes were significantly more efficiently taken up by activated T cells (ATCs) compared to blank, compared to unmodified PEI and even compared to the positive lipofectamine control. Also, no efficient uptake was observed in naïve T cells for either formulation (Figure VI.2.b.), which was expected based on the lack of caveolae in T cells [167]. The activation dependent expression of CD71 in both activated and naïve primary T cells was confirmed by anti-CD71 antibody binding assays (see Figure VI.2. insets). These results confirmed our hypothesis that specific targeting of activated T cells via transferrin is possible and further research was conducted.

While successful targeting of T cells was also shown by Ramishetti et al. after systemic administration of lipid nanoparticles which were surface functionalized with an CD4+ antibody [172], no differentiation between resting and activated T cells was made as the intention was to target and downregulate T cell specific genes systemically. In contrast, CD71 targeting results in the benefit of addressing only activated T cells which are strongly involved in asthma.

To test specificity of Tf-PEI polyplexes toward activated T cells in the complex environment of the lung, an *in vivo* biodistribution study was performed in a murine asthma model in comparison to healthy control groups: Mice were intratracheally administrated on four consecutive days with Tf-PEI or PEI polyplexes. After euthanizing animals, bronchoalveolar lavage (BAL) cells were collected to investigate the distribution of siRNA in different cells types (macrophages, eosinophils, type II pneumocytes, B and T cells). We observed a specific uptake in T cells in comparison to the other investigated cell types.

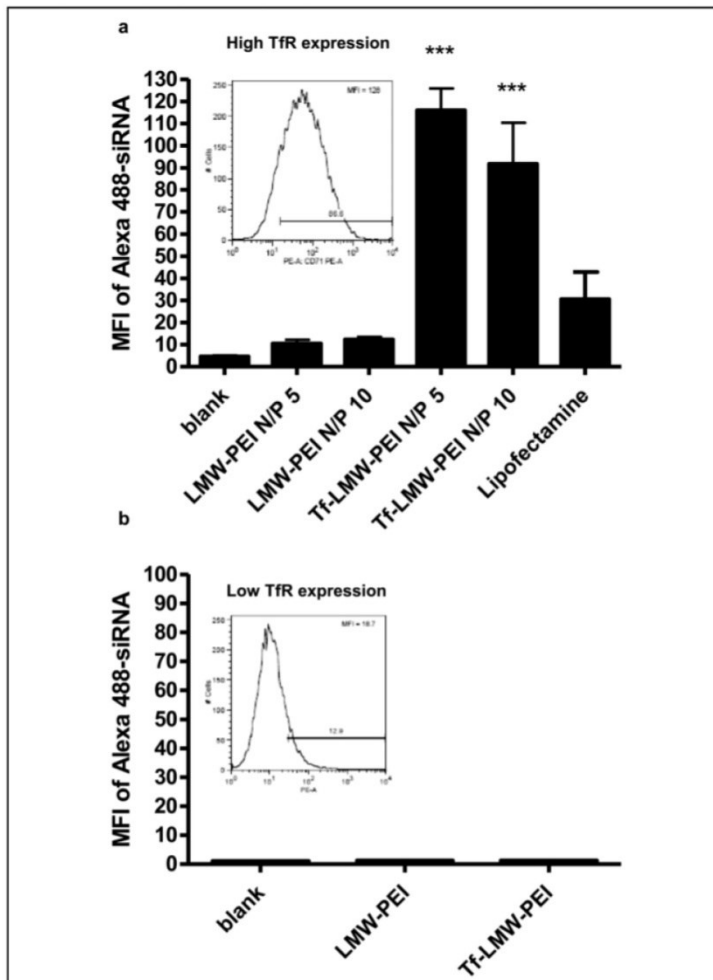


Figure VI.2. Specific Uptake of siRNA in activated T cells with a Tf-PEI conjugate. Uptake of Alexa488-labeled siRNA a) at different N/P ratios into fully activated T cells with high TfR expression (inset 2a), and b) lack of uptake into T cells with low TfR expression (inset 2b). The expression of Tf in T cells was confirmed by anti-CD71 antibody binding assay. The siRNA taken up into T cells was analyzed by flow cytometry. Lipofectamine was used as a positive control. Reproduced with permission from [171]. Copyright 2013 Elsevier B.V.

In line with the previous *ex vivo* study, the uptake in T_H2 cells was also significantly higher in asthmatic than in healthy mice [85]. In healthy animals, only macrophages took up siRNA independent of the formulation, and non-targeted PEI mediated uptake in type II epithelial cells and macrophages in both inflamed and healthy animals. However it has been described that macrophages do not express GATA3 [173], which leads us to hypothesize a lack of severe side effects due to nanoparticle delivery to macrophages. Type II pneumocytes, owever, do express GATA3 and are involved in T_H2 cytokine production. Therefore, non-specific delivery to lung epithelial cells is expected to have a positive, anti-inflammatory effect. Since GATA3 does however have a protective effect, for example in mammary luminal cells [174], we will investigate biodistribution of siRNA after pulmonary delivery to assess potential risks and side effects of the treatment.

VI.5. Optimization of Endosomal Release: Tf-Mel-PEI

After confirming effective targeting and uptake of Tf-PEI polyplexes in T_H2 cells in the lung, their therapeutic efficacy was tested *in vivo* by evaluating the knockdown of GATA3 and subsequent downstream effects. Despite significantly higher gene silencing rates of Tf-PEI compared to PEI *ex vivo* in primary T_H2 cells [85], a single treatment with Tf-PEI polyplexes did not result in significant gene silencing of GATA3 in lung tissue or of IL13 in pulmonary T cells, as determined by qRT-PCR and intracellular cytokine staining, respectively [175]. The reason for the lack of significant gene silencing was hypothesized to depend on the single administration and/or on insufficient endosomal escape of the nanocarrier after endocytosis.

Endosomal escape represents a crucial factor and is considered the rate-limiting step in cytoplasmatic delivery of nanoparticle-based therapies. In fact, a failure of escape would result in a probable degradation of the cargo in the lysosome which merges with the late endosome, leading to a loss of therapeutic activity [176]. Several strategies have been proposed to overcome this problem, such as including positively charged or pH-sensitive moieties able to disrupt the endosomal membrane [177]. In this respect, it is to be noted that endosomal acidification, leading to the so-called proton sponge effect and osmotic rupture of polyamine-loaded endosomes, is slower and less robust in T cells as compared to epithelial cell lines [178]. In this view, the use of melittin, a pore-forming peptide, was hypothesized to yield more efficient endosomal escape. Melittin is a peptide derived from bee venom and consisting of 26 amino acids that has an inherent capacity to disrupt cell membranes also at acidic pH. Moreover, this peptide was shown to be effective as a delivery system for siRNA itself, being able to reach significant transfection efficiencies [179]. Additionally, a virus-inspired polymer for efficient *in vitro* and *in vivo* gene delivery, called VIPER [180], containing melittin, had been shown to efficiently mediate gene silencing in the lung of healthy mice and had been tolerated very well after pulmonary delivery [181]. Based on these observations, we decided to include melittin in our Tf-PEI conjugate to improve the endosomal escape. However, melittin was modified by 2,3-Dimethyl-maleic anhydride (DMMAAn) to reduce side effects by directing its activity to acidic pH and hence to the endosomal membrane only. Thus, general membrane activity was reduced, and this melittin derivative was conjugated to PEI and blended with different ratios of Tf-PEI.

As a result, we obtained a delivery system which retained its selectivity toward activated T cells due to the presence of transferrin at improved endosmolytic activity [182]. The new blend composed of Tf-PEI and Mel-PEI (Tf-Mel-PEI, 50:50) displayed optimal characterization parameters, showing particle sizes below 200 nm, low polydispersity indices and stability in lung lining fluids. In line with the results obtained with the Tf-PEI conjugate, we achieved significant cellular uptake results in both Jurkat and human primary activated T cells in comparison to both free siRNA and siRNA/lipofectamine. Moreover, after determining binding kinetics of the different formulations with CD71 using Surface Plasmon Resonance technique, we observed that Tf-Mel-PEI stably bound the transferrin receptor and also showed superior affinity over Tf-PEI [182].

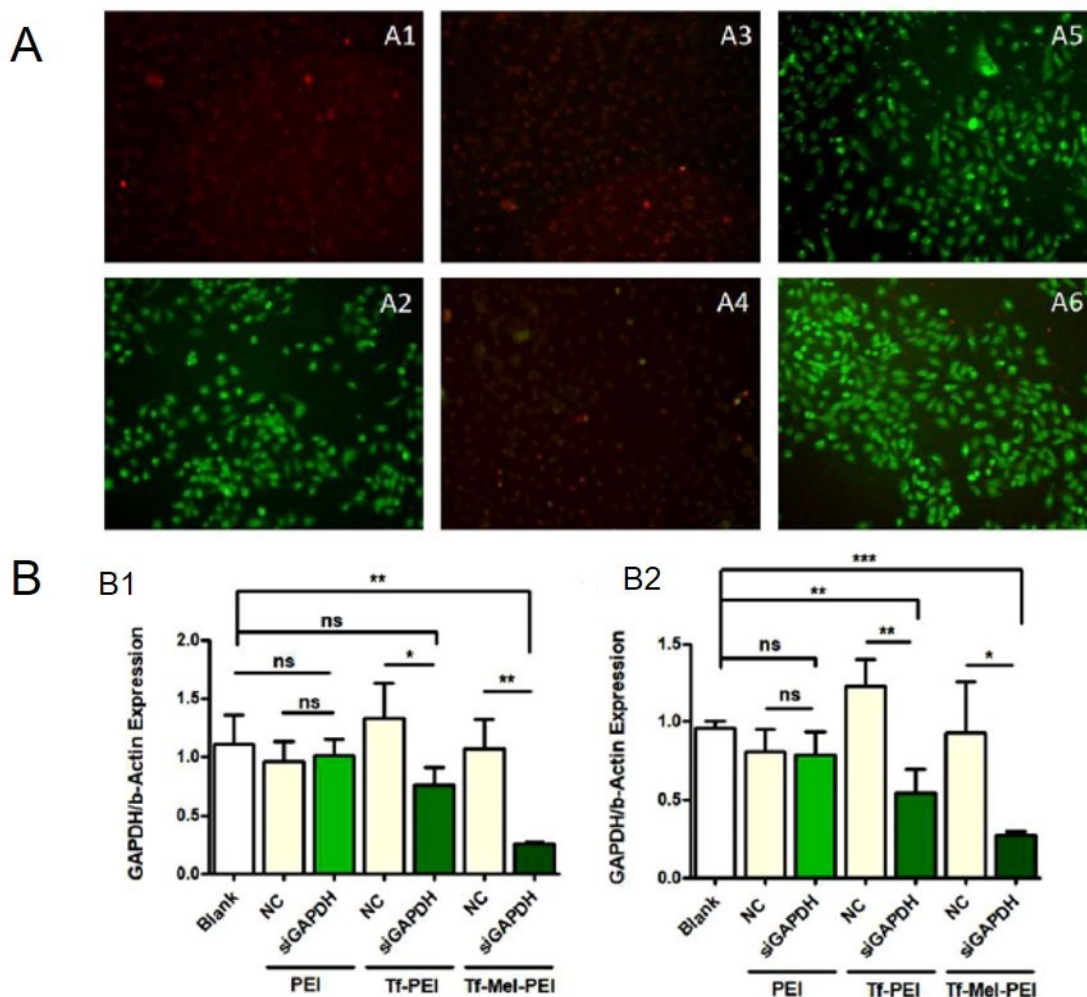


Figure VI.3. A) Acridine orange staining of untreated A549 cells (A1) and of A549 cells after incubation of polyplexes with Chloroquine (A2), PEI (A3), Tf-PEI (A4), Mel-PEI (A5) and Tf-Mel-PEI (A6). B) GAPDH knockdown in Jurkat cells (B1) and human primary activated T cells (B2) after treatment with GAPDH-siRNA or scrambled siRNA as negative control. Data points indicate mean \pm SD, n = 3; One-way ANOVA, *P<0.05, **P < 0.01, *** P < 0.001. Reproduced with permission from [32]. Copyright 2019 Wiley.

In the next step, the effect of melittin on the endosomal membrane was investigated via acridine orange staining of living cells. This technique is based on a differential fluorescence emission of the cell-permeable nucleic acid binding dye which emits red light if trapped in the endosome and green light if located within cytoplasmic pH. As shown in Figure VI.3.A., chloroquine, as positive control for successful endosomal release, as well as transfection with melittin-containing conjugates resulted in efficient endosomal escape, reflected in a color change of the dye from red to green. Positive and negative controls in fluorescence-based assays with chloroquine treatment are especially important as chloroquine is a mild base used to neutralize endosomal and lysosomal pH, and pH dependent dyes used to visualize these compartments can potentially render a negative result in the presence of this drug. After transfection with the Tf-PEI conjugate, only few green dots were detected while in PEI transfected cells, only red dye was found, supporting the findings by Olden et al. describing a lack of endosomal acidification in T cells [160] resulting in endosomal entrapment of PEI. Regarding endosomal escape, Tf-Mel-PEI clearly showed superior characteristics over the previously used Tf-PEI formulations [182].

To determine whether the effect of improved endosomal escape was also reflected on higher mRNA downregulation, the knockdown of GAPDH was evaluated via qRT-PCR (Figure VI.3B.). Indeed, in human primary activated T cells the Tf-Mel-PEI blend achieved higher gene silencing levels than Tf-PEI with 76% gene knockdown compared to 43%, respectively [182]. Most importantly, however, the increased endosomal escape was not paralleled by increased cytotoxicity or membrane destabilization [182].

Our published efforts so far describe a formulation of Tf-Mel-PEI polyplexes with optimal particle characteristics able to selectively target activated T cells and improved endosomal escape and gene silencing efficacy. Tf-Mel-PEI was therefore considered a suitable tool for follow up *in vivo* studies concerning *in vivo* specificity for activated T cells, biodistribution and therapeutic gene silencing efficiencies in a murine asthma model. Despite the fact that LMW-PEI and its Tf-PEI conjugate have been tolerated well in healthy and asthmatic mice [85], we are currently developing oligospermine derivatives to replace the PEI block in our approach [95]. It is expected that in the inflamed lung, even Tf-shielded LMW-PEI is not well tolerated, especially intracellularly where the disulfide bond between Tf and PEI will be reduced. Therefore, non-biodegradable PEI is not a promising approach for the treatment of

a chronic disease, and biodegradable alternatives are currently developed by us and others. By mimicking PEI with a polyamine that endogenously acts as nucleic acid condenser, we believe that similar condensation efficacy of siRNA will be obtained at reduced toxicity and immunogenicity but at increased biodegradability [95]. In parallel, inhalable dry powder formulations are being developed to pave the way for translation from bench to bed side.

VI.6. Pulmonary delivery of nucleic acids

Therapeutic approaches of delivering nucleic acids to the lung via inhalation benefit from direct accessibility and the ease of its administration route. However, several barriers, such as the architecture of the lung, the presence of mucus and surfactant, mucociliary clearance and phagocytosis by cells of the immune system, need to be overcome in the lung for successful delivery of nucleic acids to their target cells and sites of action [91, 183]. After carefully optimizing our formulations for gene silencing in T cells over the past years, we are currently assessing their efficacy in 3D cell culture models [184] and in mucus mobility assays based on Fluorescence Correlation Spectroscopy (FCS) [185]. Current clinical trials for inhalable gene-based therapies have been focused mainly on the use of viral and liposome-based vectors, such as in the case of cystic fibrosis, to deliver cDNA for the CFTR gene [186, 187]. However, the results obtained were not as good as expected in terms of transfection efficiency. The study and the development of new formulation strategies for inhalable gene therapies is therefore of paramount importance.

VI.7. Dry powder formulation

Spray drying (SD) is the most straight forward technique to produce inhalable particles. Although several groups have applied SD to obtain dry powder formulations of their nucleic acid formulations, analytics for characterizing nanoparticles before and after spray drying have been very scarce. However, an understanding of changes between freshly prepared and redispersed nanoparticles is needed to fully understand effects of tubing material, pump stress, shear forces and heat stress which are applied to the particles during production [96, 188]. Loss of nucleic acid and or polymer could ultimately lead to decreased *in vitro* and *in vivo* performance. Hence, we successfully developed and set up protocols for nucleic acid as well as amine based polymer quantification to easily quantify the components of dried formulations and redispersed suspensions [189]. Additionally, the effect of mannitol and trehalose on the redispersability of polyplexes consisting of 25k PEI and bulk DNA (bDNA) after SD was investigated. Both materials were chosen as they are generally recognized as safe (GRAS) substances, known for their lyo- and desicco-protection and commonly applied in SD [53]. We found that a distinct concentration of excipient was needed to preserve PEI-bDNA polyplex size and particle distribution, independent of the excipient's nature. Initial changes in zeta potentials of the formulations after SD and redispersion could also be eliminated. Furthermore, it was confirmed by cascade impaction analysis that particles were prepared with an aerodynamic diameter between 1 and 5 μm , which is a conducive size range for pulmonary administration. SEM revealed round smooth microparticles for mannitol-based formulations and also round but partly fused trehalose based microparticles. These findings were explained by the state of mannitol and trehalose via x-ray powder diffraction and differential scanning calorimetry revealing that mannitol crystallized upon spray drying while trehalose formulations dried without forming a crystalline but an amorphous state. This most probably led to the high residual moisture content of 3.2% of trehalose formulations compared to 0.4% of mannitol formulations and hence the fusion of trehalose microparticles. However, crystallinity and water content did not affect aerodynamic properties on short term. After establishing and ultimately applying the new set of analytical methods to SD powders, important changes to the initial formulations were detected: trehalose formulations showed ~32% nucleic acid loss at low N/P ratios reaching a plateau of ~20% at higher N/P ratios of the polymer/nucleic acid polyplexes, suggesting a stabilizing effect of excess polymer (Figure VI.4.A.).

Considering the measured polymer loss of the different formulations after SD (Figure VI.4.B.), N/P ratios of the redispersed formulations overall increased (Figure VI.4.C.). It was therefore hypothesized that the N/P increase at least partially explained the improved uptake and transfection efficiency of redispersed formulations *in vitro* compared to their freshly prepared counterparts with and without excipient as control (Figure VI.4.D. and VI.4.E.) [189].

Even if both DNA and RNA are nucleic acids, we have more than once shown that circular plasmid DNA, for example, behaves very differently from rigid, short double-stranded siRNA when condensed with cationic polymers [104]. Therefore, our current research on dry powder formulations focuses on the preparation of polyplexes consisting of siRNA and different PEI based delivery vectors with the goal of developing a platform technology for inhalable nucleic acid formulations.

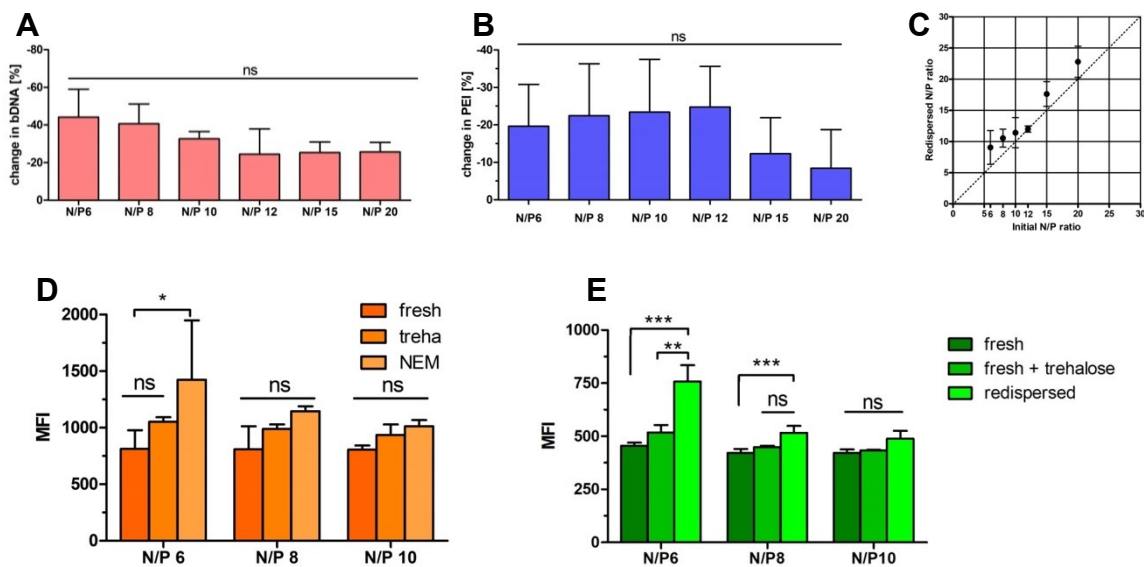


Figure VI.4. Polymer and nucleic acid quantification. Quantification of A) bulk DNA and B) PEI in the 10% trehalose nano in microparticle formulations following spray drying; C) Comparing the redispersed N/P ratio with the initial N/P ratio of the PEI polyplexes loaded with bulk DNA; D) Uptake and E) Transfection efficiency of redispersed nano in microparticle formulations in A549 cells. Median fluorescence intensity (MFI) was determined by flow cytometry to evaluate efficiency of D) fluorescently labeled bDNA or E) pEGFP in a human non-small cell lung carcinoma cell line (A549) of fresh or redispersed polyplexes from 10% trehalose NEM formulations at N/P ratios of 6, 8 and 10 with D) 0.5µg of bDNA or E) 0.75 µg of GFP plasmid in comparison to freshly prepared formulations in presence of trehalose. Blank samples consisted of A549 cells treated with 5% glucose only. Data points indicate mean ± SD (n=3). Two-way ANOVA, Bonferroni post-test, *P<0.05, **P < 0.01, *** P < 0.001, ns = non-significant. Reproduced with permission from [127]. Copyright 2019 Elsevier B.V.

VI.8. Conclusion

siRNA-based therapies offer the chance to potentially target any single mRNA specifically and efficiently and mediate its downregulation. In the treatment of asthma, this technique could be exploited to target GATA3 in activated T_H2 cells, one of the main factors involved in the pathogenesis of asthma. Almost 10 years ago, our group started a journey aimed to find a suitable delivery system able to downregulate GATA3 and to produce a final spray dried powder formulation to be administered to patients via inhalation. After identifying transferrin as a targeting ligand for activated T cells, we developed the Tf-PEI conjugate, a delivery system that displayed high cellular selectivity and intracellular uptake with high transfection efficiencies *ex vivo*. Due to insufficient *in vivo* gene silencing, however, this formulation was then improved in terms of endosomal escape by blending it with the Mel-PEI conjugate. The new formulation showed optimal particle characteristics and *ex vivo* parameters. In parallel, we have also focused on the development of a dry powder formulation, an essential step to produce a final formulation that could be transferred from bench to bedside. We successfully produced nano-in-micro particles with ideal characteristics while retaining high transfection efficacies after redispersion.

Current research is therefore focusing on the *in vivo* testing of Tf-Mel-PEI in a murine asthma model and the dry powder formulation of siRNA based polyplexes. Ultimately, both research fields will be combined and hopefully result in a new therapy for the treatment of severe, uncontrolled asthma.

VI.9. Funding Information

This project has received funding from the European Research Council (ERC) under the European Union's Horizon 2020 research and innovation programme (Grant agreement ERC-2014-StG637830)

VI.10. Acknowledgments

The authors like to thank all former and current lab members both in Detroit and Munich who made this research progress possible.

Chapter VII)

Successful Spray Drying of siRNA

evaluation of crystalline and amorphous substances on the drug quantity and quality of inhalable nano in microparticles

Tobias WM Keil, Domizia Baldassi, Friederike Adams, Wolfgang Friess, Aditi Mehta, Olivia M Merkel

The writing and main experiments were performed by myself. Domizia Baldassi helped with the PCR whereas Friederike Adams prepared the polymers. Wolfgang Frieß gave the idea of investigating the tubing material for adsorption effects whereas Aditi Mehta gave continuous support throughout the experimental section. Olivia Merkel did proof reading of this manuscript and supervised me at all stages of the research.

VII Successful Spray Drying of siRNA

VII.1. Abstract

Delivery of small interfering RNA can be achieved via viral vectors, lipid and polymer-based delivery. Amongst polymeric delivery, PEI and its derivatives are the most studied substances. For addressing severe pulmonary diseases which are difficult to control, the formulation of siRNA into inhalable dry powder formulation owns great potential. In this study we prepared spray dried formulations for dry powder inhalation of polyplexes at different temperatures consisting of siRNA and a PEI based block copolymer i.e. PEG-PCL-PEI (PPP) in presence of trehalose. We thereby investigated the effect of temperature on the recovery of siRNA after spray drying. We detected losses of ~40% at temperatures between 45°C and 90°C T-Out which increased significantly at a temperature of 100°C T-Out. It was shown in this study, that losses at low temperatures are not attributed to the spray drying process itself but rather to adsorption effects within the tubing material. Choosing a low abrasion silicon tubing resulted in a prevention of adsorption effects. Furthermore, mannitol and trehalose were chosen as matrix substances for the stabilization of polyplexes during the spray drying process forming crystalline and amorphous structures, respectively. For a

better understanding of excipient effects, mannitol and trehalose concentration were varied from 5 to 10% m/v and the spray drying temperature was set to 70 and 80° T-Out. It was shown that mannitol and trehalose formulations preserved siRNA integrity regardless of concentration and temperature. However, trehalose formulations showed full siRNA recovery whereas mannitol showed spray drying induced losses of ~20%. The effect of excipient on polymer recovery was even more pronounced. Whereas trehalose based formulations showed no changes, spray drying of mannitol formulations resulted in considerable losses of 50-60% PPP. These results were unaffected by the excipient concentration and T-Out. Despite the content changes, polyplex size and PDI were not influenced. Aerodynamic properties were confirmed by next generation impaction analysis based upon the amount of drug content. All formulations showed optimal aerodynamic characteristics enabling pulmonary delivery. Evaluation of transfection efficiency confirmed successful downregulation of GFP in a GFP expressing lung cancer cell line (H1299). These results were further transferred to a clinically more relevant model for downregulation of GATA3 overexpression in primary T-cells as potential novel therapeutic approach for the treatment of severe asthma. This study corroborated successful gene silencing of GATA3 in primary T-cells with spray dried powder formulations of transferrin-PEI/siRNA polyplexes intended for inhalation.

VII.2. Introduction

Application of drugs directly to their site of action is the optimal way to reduce doses and side effects. For lung diseases such as asthma, pulmonary delivery is therefore favored. [67] With a relatively low enzyme activity and a slow surface clearance [190], enzymatically prone substances are perfect candidates for this administration route. In addition, dry powder inhalers enable the delivery of drugs with a high shelf life and also provides an easy to use tool for patients along with high compliance. [84] Despite several available treatments for lung diseases, gene therapy is a promising new tool to address uncontrollable disease variants such as severe, uncontrolled asthma. [191] Small interfering RNA (siRNA) can silence the translation of messenger RNA into pathologically upregulated proteins and diminish disease symptoms. [30] However, siRNA therapeutics face several challenges associated with the delivery into cells and enzymatic stability. To address these issues, nanoparticles are

preferred to protect and encapsulate siRNA. Numerous vehicles are reported in literature to achieve uptake and transfection of cells with siRNA. [192] However, the only clinically approved siRNA drugs target the liver, and pulmonary delivery is still in the future. [35, 45]

Cationic polymers are one class of nucleic acid nanocarriers amongst which polyethyleneimine (PEI) is the most studied one. However, the use of PEI is limited due to its cytotoxicity profile. To overcome toxic characteristics of PEI our group has developed copolymers of PEI with better safety profiles. These copolymers combine the nucleic acid condensation and protection efficiency of PEI but also the transfection and stability effects of polycaprolactone (PCL) and polyethyleneglycol (PEG), respectively. It was shown that these copolymers of PEG-PCL-PEI (PPP) can form so called polyplexes with nucleic acids in the nanoscale by electrostatic interaction and successfully transfect cells *in vitro* and *in vivo* [97, 193, 194]. In order to deliver these nanoparticles to the lung, incorporation into microparticles with aerodynamic diameters between 1 and 5 μm is required. The matrices of these microparticles need to consist of excipients which readily dissolve upon impact on lung lining fluid and release their nano cargo. [127] The use of water-soluble substances is hence required.

A technique to produce such nano-in-microparticles (NIM) is spray drying. It is a widely applied method in food, cosmetic, chemical and pharmaceutical industry and allows gentle drying of small droplets. [2] In addition, it is much faster and less time and energy consumptive than spray freeze drying which is also used for the production of inhalable dry powder formulations of siRNA therapeutics. [77] However, spray drying applies heat to samples and might degrade or inactivate siRNA and/or PPP. [127] Also, pumping is a necessary step to process and ultimately spray samples. Here, adsorption based upon hydrophobic interactions between polyplexes and tubing surface could harm the formulation as was shown for DNA and a hydrophobized silica surface. [146] Furthermore, it is known that drying of biopharmaceuticals in combination with different excipients leads to amorphous or crystalline microparticles structures, depending on the nature of the excipient. This has tremendous effects on the stability and activity of the drug itself. [195, 196] We hypothesized, that similar processes can also affect polyplexes and their composition.

Therefore, the aim of this study was to evaluate the highest possible inlet temperature to dry siRNA-PPP polyplexes in respect to quantity and integrity. Importantly, quantification of siRNA upon polyplex redispersion after spray drying presents a novelty in the current literature. So far, this aspect has been disregarded in the siRNA formulation field, and we were the first to describe quantification of DNA upon polyplex redispersion of dry powders and transferred this knowledge within the work described here to siRNA polyplexes. [127] Additionally, we investigated absorption effects of standard silicon tubings in comparison to low abrasive silicon tubings, namely Pumpsil®. Furthermore, we observed the effects of two different excipients, mannitol and trehalose, which are known to crystallize or form an amorphous state during spray drying, respectively. We investigated their effect at two different concentrations, i.e. 5 and 10% m/V feeding solution, at the two highest possible temperatures where no effects on siRNA quantity and integrity were detected. All prepared formulations were tested regarding their nanoparticle size and content, microparticle size (geometric and aerodynamic), residual moisture and crystallinity. Also, this study presents for the first time the determination of aerodynamic characteristics via direct drug quantification as demanded by pharmacopoeias [51, 52] and not via surrogate parameters as done by various other groups. [55, 77, 96, 197, 198]

Ultimately, these formulations were also tested *in vitro* in an eGFP expressing cell line to confirm siRNA activity by downregulation of eGFP. Furthermore, these results were translated to a pharmacologically more relevant model i.e. GATA3 silencing in primary CD4+ T cells after spray dried formulations containing siRNA against GATA3 were produced and characterized.

VII.3. Materials and Methods

VII.3.1. Materials

Double stranded siRNA targeting green fluorescent protein (DsiRNA EGFP 1) (siGFP) and scrambled nonspecific control (siNC) were purchased from IDT (Integrated DNA Technologies, Inc., Leuven, Belgium). Hyper branched polyethyleneimine (PEI) (25kDa) was obtained from BASF (Ludwigshafen, Germany). Hetero-bifunctional polyethylene glycol (HO-PEG-COOH, 2.5 kDa) was acquired from JenKem Technologies (Plano, TX, USA). ϵ -Caprolactone, Heparin from porcine intestinal mucosa (H3393, >180units/mg, grade I-A), picrylsulfonic acid (TNBS) (P2297), TRIS EDTA Buffer Solution 1x (TE-buffer) (93283), TRIS EDTA Buffer Solution 100x for NGI analysis (T9285), tris borate EDTA buffer (TBE-buffer) (T 3913), RPMI-1640 Medium (R8758), fetal bovine serum (FBS) (F9665), Penicillin-Streptomycin (P/S) (P4333), G 418 disulfate salt solution (G8168), Dulbecco's Phosphate Buffered Saline (PBS) (D8537) and D-Mannitol were purchased from Merck KGaA (Darmstadt, Germany). D(+)-Trehalose dihydrate (28719.290) was acquired from VWR International GmbH (Darmstadt, Germany). Black 96 well plates (10307451), GeneRuler Ultra Low Range DNA Ladder (10400280), SYBR™ Safe™ DNA-Gel staining and polyacrylamide gels (Novex™ TBE Gels, 4-20%, EC62252BOX) were bought from Fisher Scientific (Schwerte, Germany). SYBR™ Gold dye was obtained from Life Technologies (Carlsbad, CA, U.S.A.). Pumpsil® tubings were received as a kind gift from Watson-Marlow GmbH (Rommerskirchen, Germany) and had an inner diameter and a thickness of 1.6 mm.

VII.3.2. PPP synthesis

Synthesis was performed as described before. [199] In brief, the triblock copolymer of polyethyleneimine-*graft*-polycaprolactone-*block*-polyethylene glycol (PEI-g-PCL-b-PEG) (PPP) was synthesized by coupling the heterobifunctional diblock copolymer acrylated-PCL-b-PEG-alkyne to PEI. Characterization was performed by ¹HNMR and UV Spectroscopy as described before [97].

VII.3.3. Polyplex preparation

Stock solutions of siGFP and PPP were prepared with a concentration of 100 μM and 1 mg/ml, respectively. Polyplexes were prepared with a total amount of 30 μg of siGFP. Therefore,

the amount of PPP (m_{PEI}) in μg was calculated as follows:

$$m_{\text{PPP}} = \left(\frac{m_{\text{siGFP}}}{17950,36 \text{ g/mol}} \right) \cdot 43.1 \cdot N/P \quad (\text{Eq. VII.1.})$$

The calculated amount of PPP was diluted up to 250 μL in a specified solvent (highly purified water (HPW), trehalose or mannitol) and 250 μL of the same solvent containing 30 μg siGFP was added. To allow polyplex formation, the mixture was incubated for 10 minutes. Then, 4500 μL of the same specified solvent was added and the polyplex suspension was incubated for another 10 minutes.

VII.3.4. Adsorption to tubing material

In order to test whether adsorption of polyplexes to tubing material takes place during pumping, different tubing materials were washed prior to experiments with pre-heated HPW and allowed to dry. After insertion into the Masterflex L/S (7520-47, Cole-Parmer GmbH, Wertheim, Germany), equipped with the Easy-Load II head module (77201-60), a pump rate of 1.2 ml/min was set. Polyplexes were prepared in HPW and pumped through the tubing and collected in a 5 ml tube for further analysis. This procedure was carried out in triplicates.

VII.3.4. Spray drying

For microparticle preparation a B-290 (Büchi Labortechnik, Essen, Germany) was used. As Pumpsil® tubings did not fit into the Büchi pre-installed pump, the Masterflex L/S (see 2.4.) was used with a pump rate of 1.2 ml/min. Nitrogen was used as atomizing gas, whereas drying gas was air. In order to avoid dust and other airborne particles, both nitrogen and air supply were filtered through a 0.22 μm pore. To ensure sufficient heating of the air supply and to avoid overheating of the Büchi vacuum pump, pressurized air was used. The aspirator was set to 70% and vacuum was set to -42 mbar by adjusting the level of pressurized air. The airflow was set to 40 mm corresponding to 473 NL/h. For particle collection, a high efficiency cyclone was attached. Polyplexes were prepared in 5 or 10% m/V

trehalose or mannitol. All formulations were prepared the same day to avoid inter-day differences related to ambient temperature and humidity, for example. For analysis three batches were produced on three different days. In the case of different inlet-temperatures (T-In), the measured outlet-temperatures (T-Out) were indicated next to T-In for a better understanding of the process. During the spray drying process, minor changes of T-Out were observed. Hence, T-Out was reported as mean with a deviation of $\pm 1.5^\circ \text{C}$.

VII.3.5. Z-Average and PDI measurements

To compare the effects of pumping and spray drying on polyplex content, 70 μL of freshly prepared polyplex suspension was compared to polyplexes after further processing. For pump adsorption experiments, 70 μL were taken after pumping. For redispersability of spray dried formulations, approximately 3.5 mg and 7.0 mg for 5% and 10% matrix formulations, respectively, were dissolved in 70 μL HPW. All samples were analyzed in disposable cuvettes (Brand GmbH, Wertheim, Germany) and analyzed with the Zetasizer Nano ZS (Malvern Instruments Inc., Malvern, U.K.). Therefore, the refractive index of water, mannitol or trehalose at 25°C for the indicated concentrations were set in the software, and detection was performed with the backscatter angle of 173° . For each experiment, measurements were taken in triplicates with 15 runs each and averaged afterwards.

VII.3.6 Static Light Scattering

A few μg of spray dried powder was suspended in about 2 ml of diethyl ether. About 30 minutes prior to measurements the HORIBA LA-950 (Retsch Technology GmbH, Haan, Germany) was switched on for equilibration. The cuvette was filled with diethyl ether, inserted into the device and acquisition and blank measurements were recorded. The sample suspension was mixed thoroughly by pipetting up and down and small amounts were added into the cuvette. Additionally, a small magnetic stir bar was inserted for sample stirring. The speed was adjusted to achieve light transmittance between 85 and 90% of red light and between 80 and 90% of blue light. The amount of powder in the cuvette was adjusted accordingly.

Following indices were used for measurements:

Real refractive index – mannitol: 1.330

Imaginary index – mannitol: 10.0

Real refractive index – trehalose: 1.652

Imaginary index – trehalose: 2.0

Refractive index diethyl ether: 1.352

Imaginary indices were chosen experimentally to obtain smallest possible R parameter (here $R < 0.08$ at all measurements). The quality of these measurement is given by the R parameter which decreases if the predicted scattering of the particle size distribution measurements fits with the detected scattering of the sample. [200] Measurements were executed on three different batches.

VII.3.7. Scanning Electron Microscopy

A small amount of powder was placed on top of a stub covered with double-sided carbon tape. Before analysis, the stub was coated with carbon under vacuum for 40 s. The morphology of particles was examined by scanning electron microscopy (SEM) using a FEI Helios G3 UC (Thermo Fisher Scientific, Schwerte, Germany).

VII.3.8. Residual water content

For trehalose and mannitol microparticles, approximately 5 mg and 15 mg were weighed into a 2R vial, respectively. Three different batches were measured in triplicates, each. Also, a 1% water standard was prepared with approximately 10 mg. After filling, a small piece of ceramic wool (Analytik Jena AG, Jena, Germany) was applied on top to avoid particle suction through the titrator. Vials were closed with a plastic stopper. Empty vials acting as blank values were treated accordingly. For coulometric measurements an Aqua 40.00 Karl Fischer Titrator with corresponding software from Analytik Jena AG (Jena, Germany) was used. First the oven was heated to 100°C and the system was cleared of residual humidity by inserting an empty closed vial and activating the pump until a final drift of less than 8.0 µg/min was reached. The specified drift was used and stop conditions were set to a total measurement time of 10 minutes or until the drift reached ≤ 2.0 µg/min of the initial drift. Blank measurements were executed and automatically subtracted from standard and

samples. Measurements were considered correct if the 1% water standard measurement resulted in a value between 0.9 and 1.1%.

VII.3.9. Differential Scanning Calorimetry

For calorimetric measurements 3 to 5 mg of sample were weighed into a concavus pan and closed. The reference was an empty closed concavus pan. Reference and sample were inserted into the oven at a set point of 25°C and the oven was closed. Measurements were taken with a DSC 214 Polyma (Erich NETZSCH GmbH & Co. Holding KG, Selb, Germany) starting from -10 °C with a ramp of 8° K/min until temperature reached 160°C for trehalose or 200°C for mannitol formulations. Data was analyzed using the Proteus Analysis software.

VII.3.10. XRPD

For identification of crystalline and or amorphous structures XRPD was executed with a 3,000 TT diffractometer (Seifert, Ahrensburg, Germany). Equipped with a copper anode with a voltage of 40 kV and a current of 30 mA, a wavelength of 0.154178 nm was used. The voltage of the scintillation detector was 1,000 V. Samples placed on the copper sample holder were analyzed in the range of 5-40° 2-theta in steps of 0.05° 2-theta.

VII.3.11. Aerodynamic properties

For analysis of aerodynamic properties apparatus E of the European Pharmacopoeia was used from Copley Scientific (Nottingham, UK). The next generation impactor (NGI) was fitted with a preseparator (PS) and an induction port (IP). The instrument was connected to a critical flow controller (TPK 2, ERWEKA GmbH, Langen, Germany) to ensure correct valve opening for a predetermined time to allow a total volume of 4 L air passing through the instrument for each measurement. Further on, the TPK was connected to a high-performance vacuum pump (HVP 1000, ERWEKA GmbH) generating a flow rate which was set to 30 L/min (volumetric L/min) by a TSI 4040 flowmeter (TSI Instruments Ltd., High Wycombe, UK). A stock of 0.167x Tris-EDTA (TE) solution was prepared by mixing 0.5 ml 100x TE with 299.5 ml HPW. Prior to each analysis, the preseparator was filled with 10 ml of Heparin-TE solution (23.3 mg Heparin in 60 ml 0.167x TE) (HTE) and cups were coated with 10 µL of a solution containing 83% glycerin, 14% ethanol and 3% Brij 35. [201] Cotton swabs pre-wetted with coating solution were used to distribute the coating solution across the

entire cup area. For analysis 4 or 8 hydroxypropylmethylcellulose capsules were loaded with approximately 45 mg of 5% or 10% m/V spray dried formulations, respectively. Each capsule was loaded into a Handihaler® (Boehringer Ingelheim Pharma GmbH & Co. KG, Ingelheim, Germany) and activated by piercing. According to the manufacturer's manual, the capsules were discharged twice with an interval between the two actuations of 5 s. After discharging the content of capsules into the impactor, the IP was carefully taken off and closed with two rubber stoppers after 10 ml of HTE were inserted. Also, the PS was carefully removed and both openings were closed with plastic stoppers. Both, IP and PS, were shaken vertically and horizontally for 1 minute. Finally, the NGI was disassembled and the small cups were filled with 2 ml HTE whereas the greater cups were filled with 4 ml HTE. All cups were covered with a plastic lid to avoid solvent evaporation. The cups were placed on a shaker for 5 to 10 minutes and the rotation speed was set in a fashion to avoid spilling but ensure complete dispersion of particles. Three aliquots of 100 µL from each stage including IP and PS were prepared for further analysis. The mass of siGFP deposited on each stage was analyzed as described under VII.3.12 with an extended standard point line towards the lower limit.

This experiment was carried out with three different batches. The mass median aerodynamic diameter (MMAD), geometric standard deviation (GSD), fine particle dose (FPD) and fine particle fraction (FPF) were calculated as described in the European Pharmacopoeia [51]. 'Fine particles' were considered all particles below 5 µm.

VII.3.12. siRNA and PPP quantification

Quantification assays were performed as described earlier. [127] In short, 50 mg for 5% and 100 mg for 10% matrix formulations, respectively, were transferred into a 2 ml volumetric flask and dissolved in HPW to release polyplexes. These solutions were used for the following assays:

TNBS assay

An aliquot of 100 μL of each sample was taken and mixed with 0.088% m/v TNBS in 0.1 M borax. After an incubation time of 1h, samples were analyzed with a quartz cuvette in a UV-1600PC spectrophotometer (VWR International GmbH, Darmstadt, Germany) at an absorbance of 405 nm. Results were compared with an equally treated standard dilution series (0.166 μg – 1.914 μg) where a corresponding amount of siGFP was added to avoid biases. Measurements were only considered for further analysis if an internal standard (iS), prepared as described in VII.3.3., showed a deviation of less than $\pm 10\%$ compared to the theoretical amount.

Heparin SYBR gold assay (HepSYBR)

An aliquot of 60 μL of each sample was taken and diluted with HPW to 150 μL . To dissociate siGFP from PPP, 75 μL of 2.33 mg/ml heparin solution in TE buffer was added and incubated for 2h. After dilution with HPW to 450 μL , triplicates of 100 μL were pipetted into a black 96 well plate. A dilution series starting at 0.09 $\mu\text{g}/100 \mu\text{L}$ was prepared and added in triplicates into the same 96 black well plate. To verify full dissociation of siGFP and PPP, an iS was prepared as described in VII.3.3, treated alike and analyzed in triplicates. A 4x SYBR gold solution in HPW was prepared for intercalation of double stranded RNA and 30 μL were added to each well with an 8-channel multi pipette. Fluorescence was measured at an excitation wavelength of 485/20 nm and an emission wavelength of 520/20 nm on a FLUOstar® Omega multi-mode microplate reader (BMG LABTECH GmbH, Ortenberg, Germany). Measurements were considered for further analysis if iS showed a deviation of less than $\pm 10\%$ compared to the theoretical amount.

VII.3.13. Integrity test

To achieve a final gel loading amount of 150 ng siGFP per lane ($m(\text{siGFP})_{\text{lane}}$), siRNA losses detected by HepSYBR were considered (recovery) and the following calculation was used to determine the amount of spray dried powder ($m(\text{NIM})$):

$$m(\text{NIM}) = m(\text{siGFP})_{\text{lane}} * \frac{m(\text{tsc})}{m(\text{siGFP})_{\text{sd}}} * \text{recovery} \quad (\text{Eq. VII.2.})$$

where $m(\text{tsc})$ is the total solid content of the spray dried powder and $m(\text{siGFP})_{\text{sd}}$ is the initial amount of siGFP used for spray drying i.e. 30 µg. Powder was weighed and reconstituted in 15 µL of HPW and 5 µL of Heparin (12 µg Heparin / 5 µL TE-buffer). After 30 minutes of incubation, 4 µL of the 6x loading dye was added and a 4-20% TBE gel (EC62252BOX, ThermoScientific, Germany) was loaded with 24 µL of each sample. For control, free siGFP and siGFP with heparin were loaded as well. The gel was run at a constant voltage of 200 V for up to 1 hour in Tris-Borate-EDTA buffer (TBE) until lanes separated. Gels were taken off the chamber and placed in 20 ml of a 1x SYBRsafe solution for 30 minutes under 50 rpm shaking. Gels were analyzed using a ChemiDoc fluorescence detector (Bio-Rad Laboratories GmbH, Feldkirchen, Germany).

VII.3.14. *In vitro* knockdown

For *in vitro* knockdown performance a non-small cell lung cancer line H1299 (ATCC CRL-5803) stably expressing enhanced green fluorescence protein (GFP) was used. Cells were cultivated in RPMI-1640 supplemented with FBS (10%), P/S (1%) and G418 (0.4%) for selection at 37°C with 5% CO₂. Cells were seeded into 24 well plates with a density of 2x10⁵ cells per well and a total volume of 500 µL medium. On the day of transfection, the medium was replaced by 400 µL fresh medium and 100 µL of samples were applied to obtain a final concentration of 100 nM siGFP or siNC. As different spray dried formulations at different concentrations were tested and taking detected losses into account, the amount of powder and hence of excipient had to be adjusted. Therefore, samples within the same group were treated to contain equal amounts of excipient for better comparability. After 72h, medium was discarded, cells were washed with PBS, trypsinized and collected. After centrifugation at 400 rcf for 5 minutes, supernatant was discarded and the cell pellet was resuspended in PBS. Samples were analyzed by flow cytometry (Attune® Acoustic Focusing Cytometer,

Life Technologies) and the median fluorescence intensity (MFI) was measured using 488 nm excitation and a 530/30 nm band pass emission filter set (BL-1H). Samples were run in triplicates for each batch, with each sample gated by morphology based on forward/sideward scattering for a set of 10,000 viable cells. Triplicates of each batch were summarized by generating the mean value.

VII.3.15. Tf-PEI and GATA3 formulation

Transferrin-PEI (Tf-PEI) was prepared as described in [32, 85]. To downregulate GATA3, two different siRNA sequences targeting GATA3 (siGATA3) were used from QIAGEN GmbH (Hilden, Germany) in a mixture of 1:1 (HS_GATA3_8 - SI04212446, and HS_GATA3_9 - SI04364101).

The formulation was spray dried as described in chapter VII.3.4. containing 1760 pmol / 5 ml of 5% v/v trehalose or mannitol. The powder was analyzed according to chapter VII.3.11. to ensure exact amounts of siGATA3 for transfection.

Transfection was executed with primary CD4⁺ T cells which were isolated from freshly obtained buffy coats (DRK, Berlin, Germany). Cells were cultured in RPMI medium supplemented with 10% FBS, 1% P/S, 10 mM HEPES, 1 mM sodium pyruvate and 4500 mg/L glucose.

For GATA3 knockdown 8×10^6 primary T cells were seeded in a 48 well plate containing 200 μ L medium. Primary T cell activation was executed by using Dynabeads™ Human T-Activator CD3/CD28 (11131D, Life Technologies) following the supplier's protocol of mixing beads and cells 1:1. Spray dried powder were redispersed in nuclease free water. Controls consisting of siGATA3 or siNC were prepared with Tf-PEI or LF. After two days of T cell activation samples were applied to cells thereby achieving a final concentration of 100 nM siRNA. Cells were incubated for 48h and after removal of Dynabeads lysed with the PureLink RNA mini kit according to the manufacturer's protocol (12183025, Thermo Fisher Scientific). In short, cells were washed, lysed, and RNA was isolated with an additional DNase digestion step. Afterwards, cDNA was synthesized using the high capacity cDNA Synthesis kit (#4368814, Applied Biosystems). After obtaining cDNA, the solution was diluted 1:10 and a qRT-PCR was run with custom synthesized GATA3 forward and reverse primers (Thermo Fisher) and β -actin primers (Qiagen, Hilden, Germany) for normalization.

Cycle thresholds were acquired by auto setting within the qPCRsoft software (Analytik Jena AG, Jena, Germany).

VII.3.16. Statistics

Experimental data was checked for significant difference by the GraphPad Prism 5 software using either One Way or Two-Way ANOVA repeated measurements, with either Bonferroni or Dunnetts post-hoc test with $p > 0.05$ considered not significant (ns) or significant when $*p < 0.05$, $**p < 0.01$, $***p < 0.001$.

VII.4. Results and Discussion

VII.4.1. Heat evaluation and integrity

Spray drying is the most straight-forward technique for preparing microparticles. However, heat is a central necessity which could have a tremendous effect on siRNA. Hence, we spray dried polyplexes in presence with trehalose (10% m/V) at various inlet-temperatures (T-In). As shown in Figure VII.1., increasing T-In up to 170°/89°C had no significant effect on the quantity of siGFP. At 200°C/100°C T-In/T-Out, a significant increase in siGFP loss was detected. As siRNA melts at around 90°C and switches from the double stranded to the single stranded form, it was important to avoid heating the siRNA formulation to this temperature for extended periods of time. The product temperature reached during the spray drying process is determined as the T-Out. [3] Hence, the temperature which affects the product is equal to T-Out and therefore crucial for stability and integrity. For T-In at 200°C and a subsequent T-Out of 100°C, melting of siRNA occurred and consequently resulted in higher susceptibility to degradation. [55, 202] Such high temperatures can potentially also lead to polyplex dissociation and siRNA release from the polyplexes. Protection of siRNA against heat and shear forces might therefore be hindered which could explain the greater loss at such elevated temperatures. However, the loss of siRNA is restricted as the exposure time of polyplexes to these temperatures is extremely low. Also, a large variation in siRNA recovery, reflected in a comparably great standard deviation, was observed for spray conditions at 170°/89°C T-In/T-Out. Here, T-Out with a small deviation ($89^\circ \pm 1.5^\circ \text{ C}$) just reached the melting temperature of siRNA. Again, this could induce melting in some cases, leading to greater siRNA losses. Therefore, the highest possible temperature which can be used for the preparation of siRNA via spray drying in our

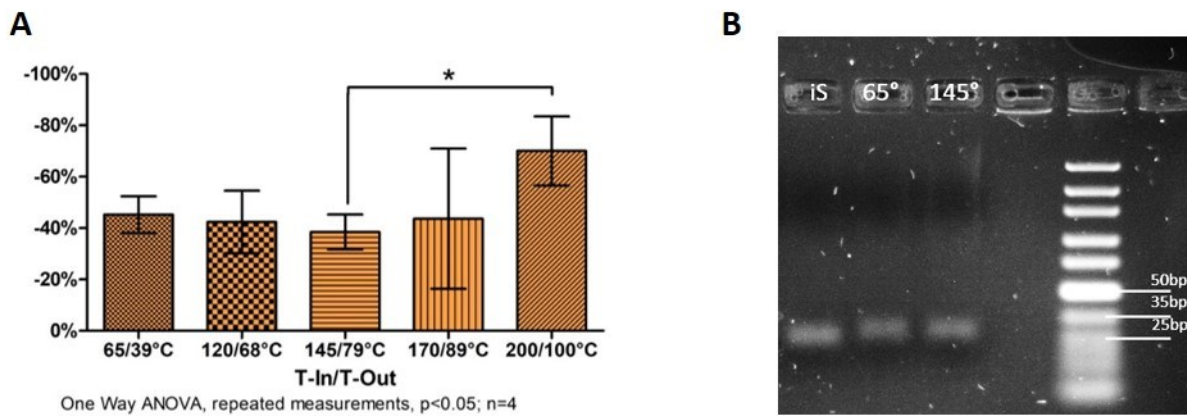


Figure VII.1. Influences of spray drying on siGFP

A) Quantification of siGFP after spray drying of polyplexes (N/P 5) at various T-In.

B) Agarose gel of redispersed polyplexes after spray drying with indicated T-In. siGFP was released from polyplexes upon incubation with heparin.

Lane 1: internal standard (iS),

Lane 2: redispersed spray dried powder at 65° T-In,

Lane 3: redispersed spray dried powder at 145° T-In,

Lane 5: low range DNA base pair ladder.

C) Quantification of siGFP after pumping polyplexes through standard silicon tubing and Pumpsil tubing.

(n=3)

case is determined at 145°C T-In and a subsequent T-Out of 79°C. Furthermore, we hypothesize that spray drying can also be successful without elevated losses at even higher T-In if the equipment is set up in a fashion that T-Out remains below 90°C. This could be achieved for example by increasing the feeding or aspirator rate when increasing T-In at the same time. [3] As the siRNA quantification described here relies on intercalation of a fluorescent dye which does not reflect the nucleic acid integrity, the latter has to be confirmed separately. This was achieved via gel retardation assay with samples obtained at the lowest T-In and the highest acceptable T-In (145°C). Figure VII.1.B. confirms the duplex length of about 25 bp for the internal standard as well as the spray dried samples obtained at both process parameters. Hence, siRNA integrity in the recovered material even at the highest applicable T-In was maintained. Although T-In/T-Out were reduced to minimize siRNA losses and duplex integrity was confirmed, nucleic acid losses were still rather high with approximately 40%. To further elucidate the reasons for these losses the effect of pumping polyplex suspensions from the sample container into the spray dryer was investigated. To test this effect, a polyplex suspension was pumped through the silicon tubing connected to the spray dryer and was collected afterwards. Interestingly,

quantification of siGFP after pumping with regular quality silicon tubing, which was used in the aforementioned experiments, revealed losses of around 40% (Figure VII.1.C.). These losses correspond to detected losses of redispersed polyplexes after spray drying. We therefore inferred that the measured losses during spray drying (Figure VII.1.A.) are not solemnly linked to the spray drying process itself but rather to the pumping step and the used tubing material. We further hypothesized that the source of adsorption of siGFP is due to hydrophobic interactions which was also shown for DNA. [146] Furthermore, we tested whether high quality silicon tubing would reduce siRNA adsorption. And indeed, siGFP losses were reduced to 0% when using Pumpsil tubing (Figure VII.1.C.). One explanation for the different adsorption behavior of siRNA polyplexes on high vs. regular quality silicon tubings might be abrasion which takes place in the latter tubing and results in cavities. These superficial changes lead to an increase and regeneration of surface area and hence to an increase of possible interactions between siGFP and the tubing material. Therefore, low abrasion tubings such as Pumpsil seem advantageous for the processing of polyplexes. The detailed mechanism for adsorption however is not within the scope of this article and will be addressed in future work.

VII.4.2. Nanoparticle Characteristics

Besides heat, spray drying exerts shear forces on nanoparticles and could disassemble polyplexes. Hence, DLS measurements were performed before and after spray drying to visualize any possible effects. Therefore, microparticles were dissolved in HPW for nanoparticle redispersion to mimic impaction and dissolution in the lung. As demonstrated in Figure VII.2., Z-average values of freshly prepared and redispersed polyplexes do not differ from each other statistically. Also, differences in PDI were not observed. However,

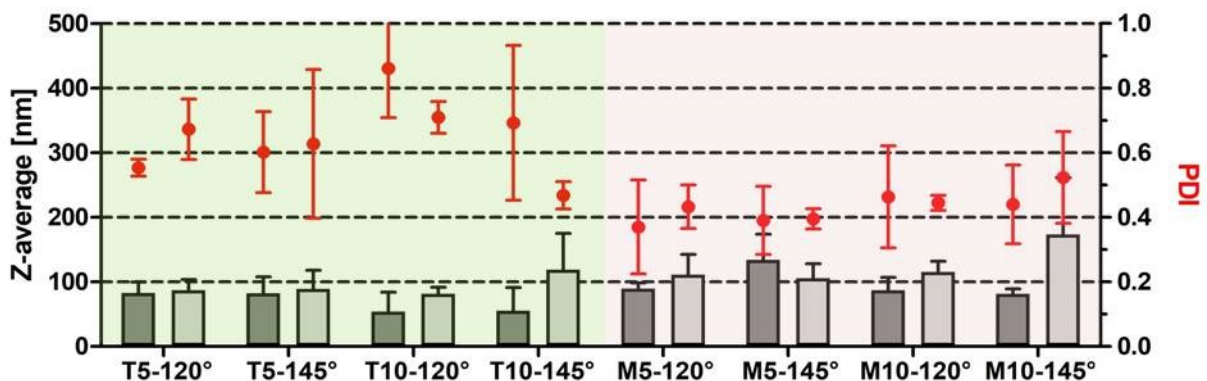


Figure VII.2 Dynamic Light Scattering measurements of freshly prepared (dark grey bars) and redispersed (light grey bars) polyplexes. PDI is indicated by red circles. (n=3)

we recognized high PDI values which might be explained to some extent by sugar/sugar alcohol monomers. It was shown by Weinbuch et al. that monomers of sugar and sugar alcohol are visible in highly concentrated solutions. [203] And indeed, we accordingly detected monomers at around 1 nm which are not visible if polyplexes are prepared solemnly in HPW (VII.SI-Figure1). This hypothesis is underlined by the fact that with increasing amount of excipient the peak at 1 nm increases (VII.SI-Figure1). This phenomenon also explains the trend of higher PDI values at higher concentrated excipient solutions. Nonetheless, z-averages and PDI did not differ significantly within one excipient group. However, trehalose formulated polyplexes showed higher PDI values than mannitol formulated polyplexes which might be again attributed to a higher monomer content. In summary, polyplex size and distribution were not affected by spray drying within each formulation. Furthermore, to confirm integrity and hence the base pair length of siRNA in all formulations, a gel assay was executed.

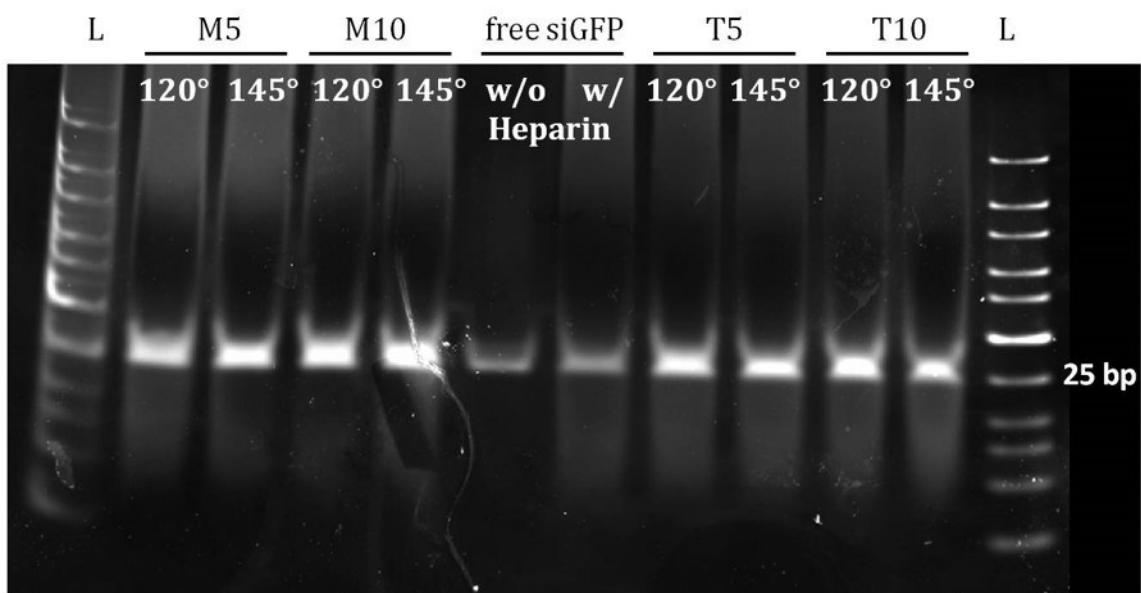


Figure VII.3. siGFP integrity

Agarose gel of redispersed polyplexes after spray drying with mannitol or trehalose at indicated T-In. siGFP was released from polyplexes upon incubation with heparin.

M5/T5: 5% m/V mannitol/trehalose formulation of siGFP-PPP; spray dried.

M10/T10: 10% m/V mannitol/trehalose formulation of siGFP-PPP; spray dried.

L: Ultra low range base pair ladder.

Figure VII.3. shows that independent of the chosen formulation and T-In, siRNA was intact in all cases reflected by all bands being detected at the same base pair length. Bands with a smaller molecular weight, which would indicate degradation of siRNA, were not detected. Smears accompanying all spray dried samples are attributed to heparin as shown by similar

effects in the sample containing free siRNA mixed with heparin but not in the sample containing free siRNA without heparin. Hence, we state that the base pair length of siRNA was not influenced by spray drying. However, Z-average, PDI and base pair length are considered qualitative approaches to determine successful spray drying whereas determination of siRNA and polymer content are quantitative and hence extremely relevant for correct dosing. Therefore, the content of siRNA was analyzed in redispersed particles and considerable losses were found when polyplexes were spray dried in the presence of mannitol (Figure VII.4.A.). Although not significant but worth mentioning is the fact that losses increased from approximately 17% to 21% when the temperature was increased. This is reasonable as a higher product temperature could lead to greater losses as explained earlier. These findings are also in line with a publication from Wu et al. where naked siRNA was spray dried in presence of mannitol at T-Out between 60 and 125°C. [55]

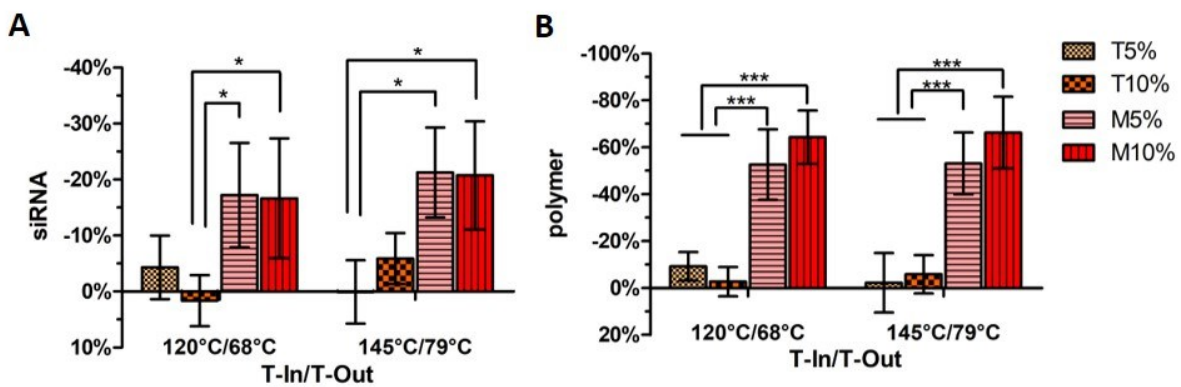


Figure VII.4. Effect of spray drying on polyplex composition quantitatively

Quantification of A) siRNA (siGFP) and B) polymer (PPP) after spray drying at two different temperatures with two different excipients at two different concentrations.

(n=4)

M5/T5: 5% w/v mannitol/trehalose formulation of siGFP-PPP; spray dried.

M10/T10: 10% w/v mannitol/trehalose formulation of siGFP-PPP; spray dried.

However, when polyplexes were spray dried with trehalose there was no significant change detectable compared to the applied amount of siRNA. Hence, statistically significant differences in regard to siRNA recovery after spray drying between the two different matrix formulations at both spray drying temperatures were observed. As analyzed by two-way ANOVA, the choice of excipient was identified as the source of variation accounting for 58.6% of total variation and a p-value of 0.0013 indicating a highly significant effect. Similarly, polymer quantification resulted in no difference in recovery after spray drying

when polyplexes were formulated with trehalose but showed losses of approximately 53% and 65% when formulated with 5% mannitol or 10% mannitol, respectively.

Here, no statistical differences between both temperatures and concentrations could be detected within each excipient group. However, all mannitol formulations showed significantly higher losses in polymer than their trehalose formulated counterparts. Hence, mannitol formulations were outperformed by their trehalose formulated counterpart in respect to siRNA and polymer recoveries. This observation might be explained by the fact that trehalose formulations form amorphous particles whereas mannitol crystallizes upon spray drying (see chapter VII.4.3). It was shown by several other publications that amorphous structures can stabilize bio macromolecules during drying. [204-207] Although this effect was not shown before in literature for polyplexes, it is not surprising that trehalose stabilizes polyplexes, also. One explanation for this phenomenon is the water replacement theory. [208] During desiccation trehalose stabilizes the structure of the entrapped molecules by forming hydrogen bonds and maintaining the three-dimensional structure. Also, higher residual moisture content of trehalose formulations (see chapter VII.4.3) might add to this fact enabling greater stabilization by forming additional hydrogen bonds and acting as a plasticizer. In contrast, crystalline mannitol was shown to inefficiently stabilize biopharmaceuticals and might not protect the formulation from a drying-stress induced strand dissociation or potential degradation of the double stranded siRNA. [209] The dissociation of double stranded siRNA due to temperatures close to the melting point could have led to the decreased detection of siRNA with the intercalation based fluorescence quantification as described in chapter VII.3.12 which does not detect single stranded short RNA. This proposed mechanism is reinforced by the fact that detection of smaller double stranded nucleic acid strains, which would be found if double strand breaks had occurred, could not be detected (Figure VII.3.).

VII.4.3. Microparticle Characteristics

Pulmonary delivery via dry powder formulation requires low residual moisture in order to avoid aggregation processes. Although it was discussed above that residual moisture may act as a plasticizer stabilizing polyplexes during the spray drying process, it could nonetheless cause microparticle aggregation and could be a source of microbiological instability and RNase contamination. Therefore, the water content of all formulations was measured by Karl Fischer titration. As reflected in Table VII.1, trehalose formulations exhibited between

	Residual moisture (%)
T5-120°	4.53 ± 0.20
T5-145°	3.85 ± 0.05
T10-120°	4.61 ± 0.17
T10-145°	3.82 ± 0.04
M5-120°	0.40 ± 0.03
M5-145°	0.27 ± 0.04
M10-120°	0.26 ± 0.02
M10-145°	0.19 ± 0.03

Table VII.1. Residual moisture
Residual moisture of polyplexes spray dried at 5 or 10% (w/v) with indicated excipient spray dried at 120° or 145° C T-In.
T: Trehalose
M: Mannitol

4.6 and 3.8% whereas mannitol formulations showed between 0.4 and 0.2% residual moisture. These results were expected and are in line with results from literature. [210-212] Trehalose commonly solidifies upon spray drying in an amorphous state which was confirmed via DSC (Figure VII.5.). In addition with the hygroscopic nature of trehalose, the reason for the formation of amorphous structures is the fast drying step which does not provide sufficient time for trehalose molecules to arrange within an ordered structure with subsequent crystal nucleation and growth. [213] All of the trehalose formulations showed glass transitions at temperatures between 38° and 53°C corresponding to their residual moisture content (Table VII.1). This temperature (T_g) is important for stability predictions during storage as amorphous solid

forms are thermodynamically unstable and tend to crystallize if stored close to or above T_g. [214] As discussed above regarding siRNA recovery after spray drying, the amorphous state of the formulation is favorable for polyplex preservation. Hence, for storing these products at room temperature or in the fridge for a longer period of time, high T_g values are necessary. This however is closely linked to the water content: the higher the residual moisture the lower T_g. [215] Also, with a lower residual moisture content degradation processes are less likely to occur. [215]

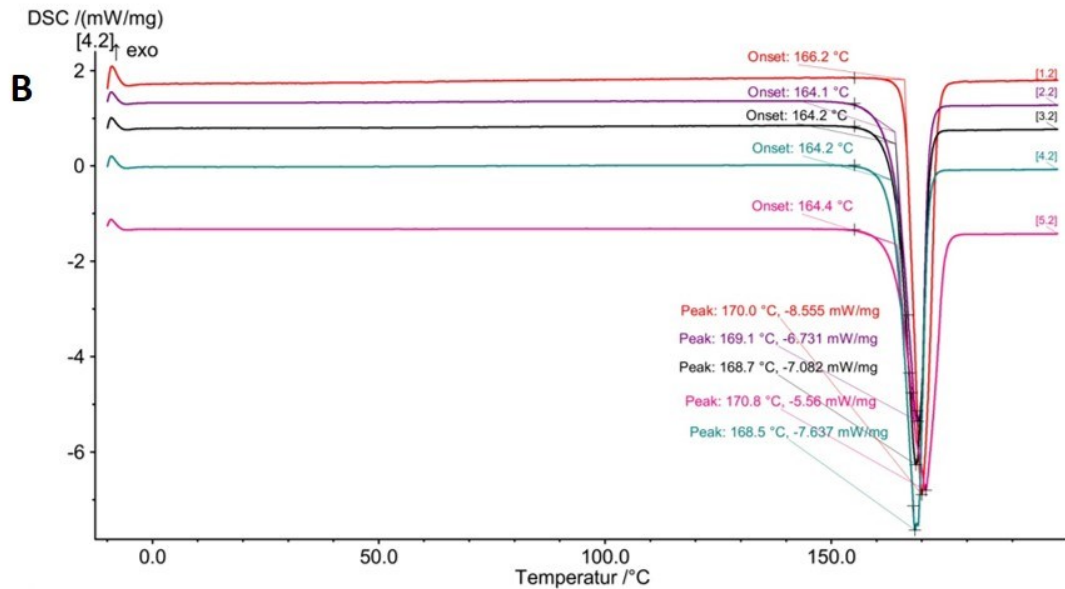
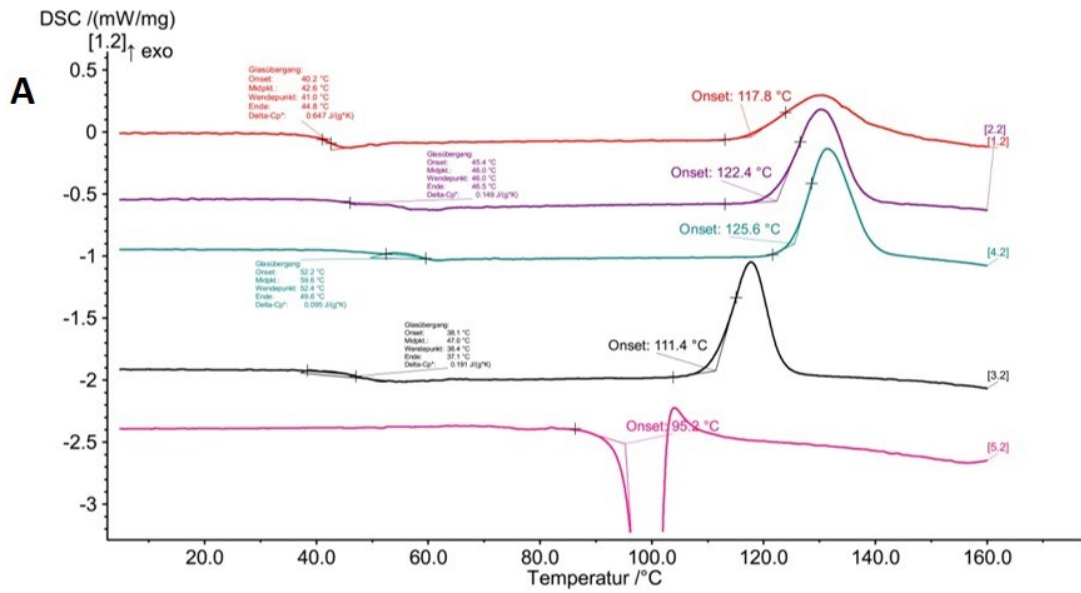


Figure VII.5. Differential Scanning Calorimetry

DSC measurements of A) Trehalose and B) Mannitol formulations:

A: 1.2) T5-120°, 2.2) T5-145°, 3.2) T10-120° 4.2) T10-145°, 5.2) trehalose dihydrate

B: 1.2) cryst. mannitol 2.2) T5-120°, 3.2) T5-145°, 4.2) T10-120°, 5.2) T10-145° .

It is therefore of great interest to further decrease the amount of residual moisture in trehalose formulations to avoid nucleation and degradation processes over time and in order to maintain the amorphous state of the formulation. While the impact of storage upon polyplex quality (size, PDI) and quantity has not yet been investigated, these aspects are currently under investigation in a greater scheme of optimizing formulation and process parameters. To confirm the amorphous state of trehalose, formulations were also tested by XRPD and typical amorphous halos were detected (Figure VII.6.A.). On the other hand, spray dried mannitol formulations exhibited the same temperature profile as the crystalline starting substance with a melting peak at 170°C as investigated by DSC (Figure VII.5.B.). This finding indicates a crystalline form of mannitol. For distinct differentiation between the mannitol polymorphs which could possibly appear, XRPD was performed on formulations prepared at T-In of 145°C. For both tested mannitol formulations, peaks at 14.6° and 16.8° 2-theta were detected which are both linked to the β form of mannitol (Figure VII.6.B.). [213, 216] Peaks specific for the α or δ form were not detected indicating that after spray drying β mannitol is the predominant polymorph. Although the drying time of spray dried formulations is very short and could have resulted in an amorphous state as obtained with trehalose, mannitol is less hygroscopic and less soluble. These characteristics lead to the fact that solutions of mannitol dry quicker and crystallize during spray drying. As the residual moisture content was lower for formulations prepared at higher temperatures and no significant differences in nanoparticle characteristics were found between formulations prepared at the two different temperatures, all following experiments were conducted with formulations produced at a T-In of 145°C.

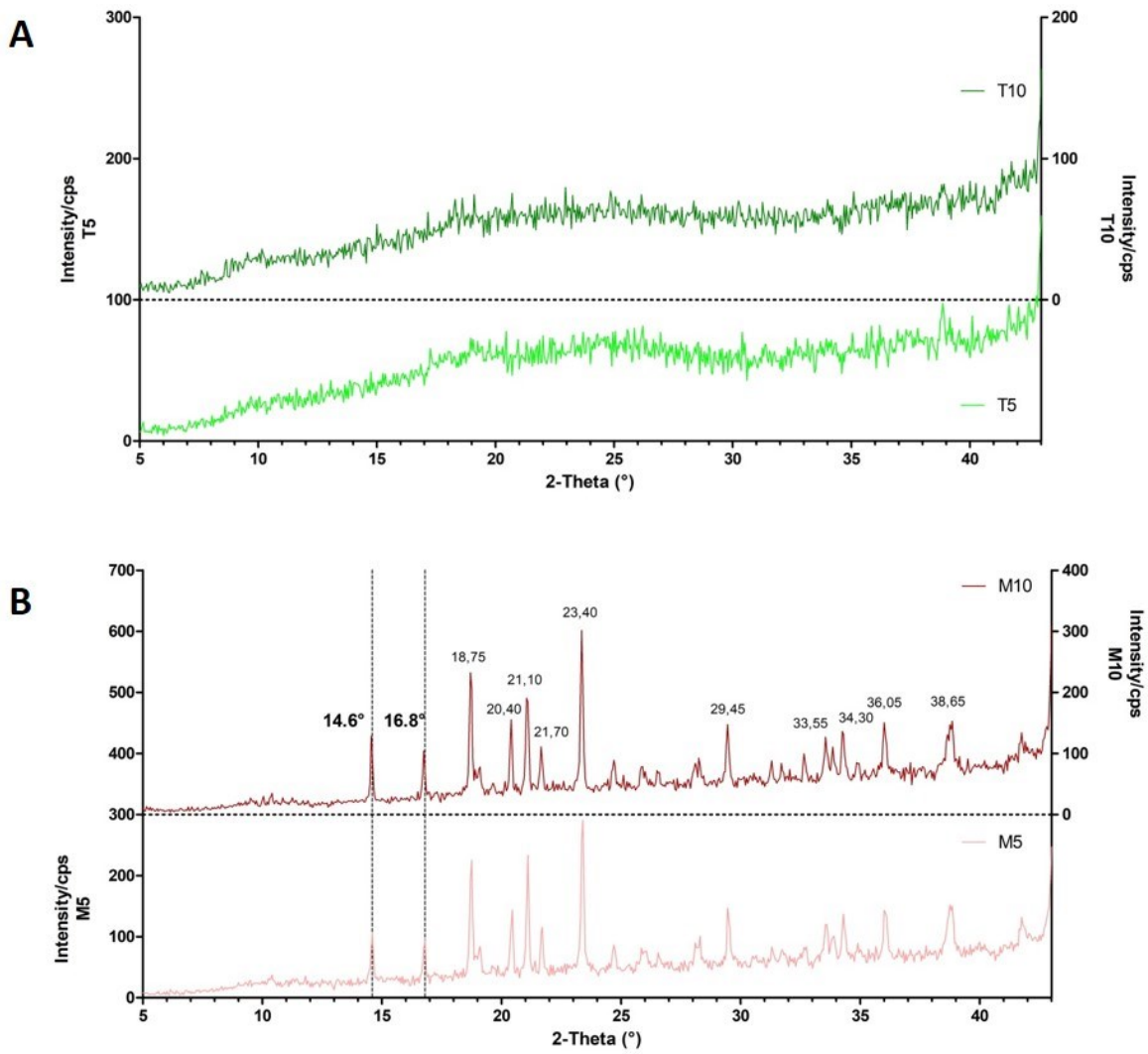


Figure VII.6. X-Ray Powder Diffraction

XRPD measurements of A) Trehalose and B) Mannitol formulations spray dried at 145°/79° T-In/T-Out. Each graph displays in the upper panel a 10% (w/v) formulated sample and in the lower panel a 5% (w/v) formulated sample in each graph, respectively.

To get a first understanding of microparticle size characteristics, static light scattering was performed in diethyl ether in which neither mannitol nor trehalose is soluble. As visualized in Figure VII.7. formulations differ from each other depending on the nature of excipient they are made of: both mannitol formulations show significantly lower values in the 10, 50 and 90 percentiles compared to the trehalose

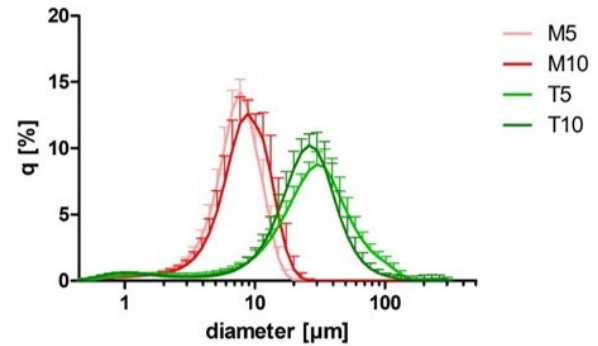


Figure VII.7. Static Light Scattering

Particle size distribution as measured by SLS of M5-145°, M10-145°, T5-145°, T10-145°.

formulations (data not shown). Mannitol formulations exhibited geometric median sizes of around 7 and 8 µm for 5 and 10% formulations, respectively, whereas trehalose formulations showed sizes of around 24 µm (Table VII.2). This can be explained by the fact, that amorphous trehalose particles with higher residual moisture show a tendency towards particle fusion through water bridges. [115] Hence, although in fact particles were produced with similar diameters as in the mannitol formulations, as confirmed by SEM (Figure VII.8.), these particles aggregate and may form greater secondary particles. This aggregation can be appreciated in the SEM micrographs (Figure VII.8.). Whereas recordings of mannitol particles confirm the findings of SLS measurements, trehalose particles show much smaller diameters. Additionally, water bridges can be observed as indicated by white arrows. Again, reductions in the water content of trehalose microparticles could considerably reduce this effect. Concerning the surface of the particles, mannitol formulations in general exhibited a very smooth round structure. Trehalose particles also showed nice smooth surfaces when formulated at 10% whereas 5% formulations indicated a somewhat roughened surface.

For pulmonary delivery aerodynamic sizes between 1 and 5 µm are crucial for successful delivery as discussed above. Although geometric median sizes were greater than 5 µm, the aerodynamic diameter also depends on the particle density and porosity and might therefore be lower as the geometric diameter. [217] In fact, measurements of impacted siRNA in the NGI revealed MMAD values close to or below 5 µm for trehalose and mannitol formulations indicating successful lung delivery. Also, calculation of GSD suggests a particle distribution which can be considered for pulmonary application. The FPF is considered as the percentage of drug that was delivered in particles below 5 µm compared to the overall impacted drug on all stages of the NGI.

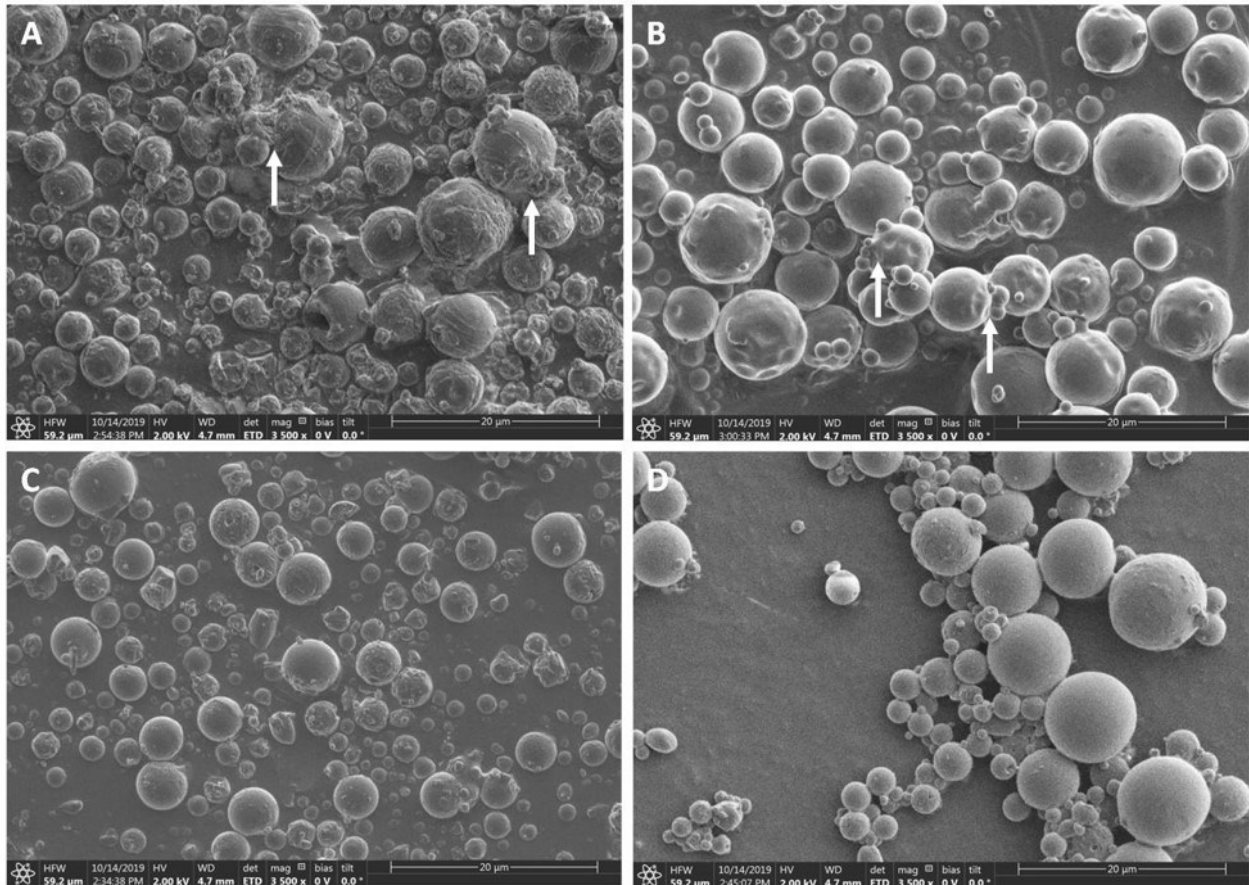


Figure VII.8. Scanning Electron Microscopy

SEM pictures of A) T5-145° B) T10-145° C) M5-145° D) M10-145°.

White arrows mark water bridges between single trehalose particles.

The higher the FPF the more drug could potentially be delivered to the site of action. Accordingly, fine particle fractions with approximately 27% for both trehalose and approximately 37% for both mannitol formulations, respectively, are considered very good. While only small amounts of particles collected in the NGI were below 5 µm and could potentially reach bronchioles and alveoli, asthma is a bronchial disease, and deposition in the larger airways may be achieved with particles larger than 5 µm also. However, to optimize the deposited dose and decrease side potential side effects, decreases in MMAD would be favorable. Compared to the FPF, the FPD is considered as the dose of drug in µg which was actually delivered in particles with less than 5 µm. It is therefore not a ratio but an exact dose which could be applied. Here, FPD differed between mannitol and trehalose formulations: whereas mannitol formulations could potentially deliver more than 0.5 µg, only less than 0.2 µg of siRNA could currently be delivered by trehalose formulations described above. Although the FPF in trehalose formulated polyplexes were much smaller, this finding cannot solely explain the discrepancy in FPD. To explain this phenomenon, it has

to be taken into account that for FPF calculations only the deposited amount of drugs inside the NGI is considered. Depositions in the pre-separator, induction port or even in the Handihaler device itself are not considered.

	Geometric median diameter (μm)	MMAD (μm)	GSD (μm)	FPF (%)	FPD (μg)
T5-145°	24.13 \pm 1.47	4.65 \pm 0.14	1.88 \pm 0.07	14.0 \pm 2.4	0.15 \pm 0.09
T10-145°	24.02 \pm 1.85	5.19 \pm 0.47	1.95 \pm 0.04	18.3 \pm 5.0	0.11 \pm 0.03
M5-145°	6.77 \pm 0.35	4.77 \pm 0.15	1.94 \pm 0.03	32.3 \pm 5.3	0.54 \pm 0.05
M10-145°	8.02 \pm 1.11	5.50 \pm 0.29	1.97 \pm 0.06	22.5 \pm 2.4	0.21 \pm 0.07

Table VII.2. Microparticle Characteristics

Microparticle characteristics of polyplexes spray dried at 5 or 10% m/V with indicated excipient at 145° C T-In.

T: Trehalose; M: Mannitol; MMAD: Mass Median Aerodynamic Diameter;

GSD: Geometric Standard Deviation; FPF: Fine Particle Fraction; FPD: Fine Particle Dose.

And indeed, a large amount of powder was found on the inner walls of the application device's capsule rack which unfortunately could not be quantified. This finding was noticed only for trehalose and not for mannitol formulations. The most reasonable explanation for this observation might be the amorphous structure of the powder and the higher residual moisture of trehalose formulations. After the release of powder from the capsule through the vacuum and the thus generated centrifugal forces, particles are forced to leave the Handihaler by following the airstream. Smaller and hence lighter particles can follow the airstream directly, whereas a great portion of particles which might be aggregated will follow the airstream only after impacting on and bouncing off the capsule rack's inner wall, thereby possibly disaggregating. However, due to the high residual water content and the subsequent plasticity of trehalose particles, a large amount of powder could adhere to the wall remaining within the device. This explains why suitable values were calculated for MMAD and GSD and FPF of ~27% based on the amount of drug deposited inside the NGI from the trehalose formulations. Mannitol powders, on the other hand, were not detected in the capsule rack and hence are suggested to be successfully introduced into the NGI without further losses.

From the overall assessment of the microparticle properties, we therefore conclude that crystalline structures outperform amorphous substances in all analyzed properties even if the amorphous state seemed favorable with regard to polyplex stability.

VII.4.4. *In Vitro* Performance

For siRNA delivery it is fundamental to maintain the molecule's bioactivity. Hence, spray dried powder was reconstituted, and enhanced green fluorescence protein expressing H1299 cells were transfected with redispersed polyplexes. Lipofectamine (LF) is a standard transfecting agent *in vitro* and is used as a positive control. [218] It is used to show the maximal possible effect of nucleic acids i.e. here siRNA downregulation of mRNA and subsequent protein expression (GFP). In all cases siRNA was active as the expression of GFP was significantly decreased (Figure VII.9.). Interestingly, lipofectamine-siGFP complexes used in the standard *in vitro* formulation with 5% glucose showed the highest downregulation observed in all five groups which is >95% in relative reduction (compared to LF-siNC containing a negative control siRNA sequence). Lipofectamine formulated with trehalose or mannitol with the respective concentration of excipient although successful in downregulation, only showed a relative reduction between 70 and 80%. One possible mechanism for this discrepancy might be explained by the fact, that transfection is a process which is energy consuming and factors which provide energy to cells such as glucose are therefore favorable. [219] Exchanging glucose for trehalose or mannitol might therefore lower this positive effect and cells might take up particles less efficiently than in the glucose reference group. Whether this effect or the viscosity of the matrix solutions used here causes the decreased transfection remains unclear and is part of future research.

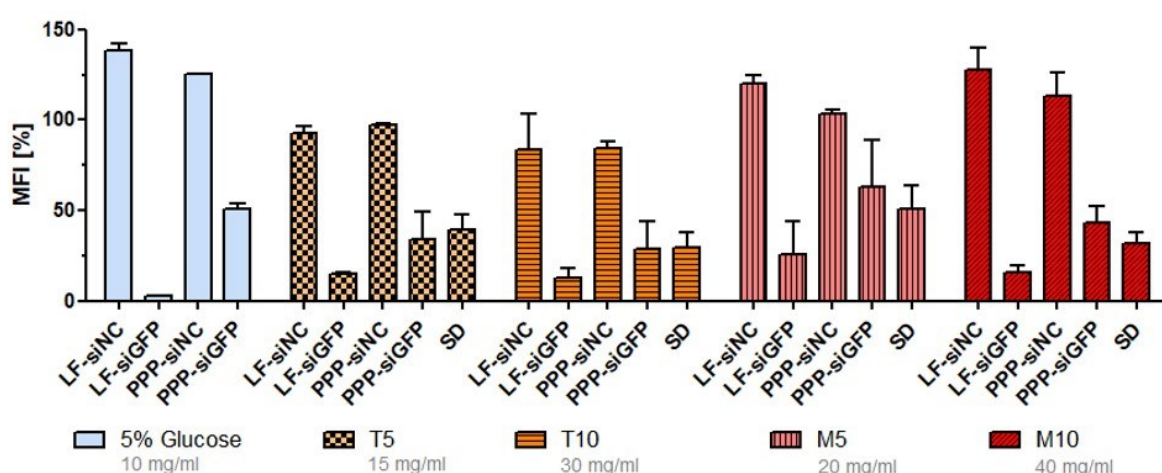


Figure VII.9. GFP Knockdown

In vitro knockdown of GFP within a H1299 cell line stably expressing eGFP. Within each group, samples contain the same amount of excipient as indicated by the legend.

LF: Lipofectamine, PPP: PEG-PCL-PEI block copolymer, siNC: negative control siRNA, siGFP: siRNA sequence against eGFP, SD: spray dried polyplexes consisting of PPP and siGFP at 5% (w/v) total solid content at 145°C T-In.

In previous studies polyplexes made of PPP and siRNA already showed knockdown efficiencies of ~50% *in vitro* [220] and even >70% *in vivo* where Lipofectamine is not stable and too toxic. [193] Hence, it is of great importance to retain transfection ability and efficiency during spray drying for *in vitro* experiments and follow up studies *in vivo*. As demonstrated in Figure VII.9., polyplexes formed of siGFP and PPP performed better than their negative control formulations (PPP-siNC). Importantly, all spray dried polyplexes (SD) performed as well as their freshly prepared counterparts. This effect is independent of the excipient's nature and its concentration (marked in grey).

After confirming bioactivity, this knowledge was transferred towards a clinically more relevant model in which GATA binding protein 3 (GATA3) was attempted to be downregulated in CD4+ T cells. In severe uncontrolled asthma, Th2 cells play a crucial role in the activation of downstream effects which orchestrate the full manifestation of asthma which is caused by a upregulated expression of GATA3. [156] Downregulation of such overexpressed proteins could lead to a significant improvement and thus benefit in therapy and administration frequency as shown for other siRNA based therapies. [34] Therefore, the delivery system our group has optimized for T cell transfection of siRNA, namely transferrin-coupled PEI (Tf-PEI), [32] was spray dried in combination with two siRNA

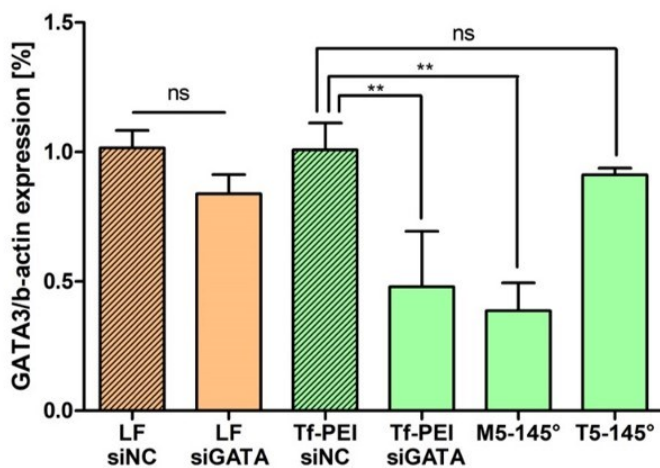


Figure VII.10. GATA3 Knockdown

Ex vivo knockdown of GATA3 within primary CD4+ T cells

LF: Lipofectamine,

Tf-PEI: Transferrin conjugated PEI,

siNC: negative control siRNA,

siGATA: siRNA sequence against GATA3,

M5-145°/T5-145°: spray dried polyplexes of Tf-PEI and

siGATA at 145°C T-In with 5% (w/v) Mannitol or 5% (w/v)

Trehalose.

sequences targeting GATA3.

The amount of siGATA was quantified as described earlier to ensure the amount for transfection. After two days of incubation, the amount of GATA3 mRNA was analyzed and normalized to β -actin. As expected, Lipofectamine showed no significant difference between the negative control siRNA and siGATA (Figure VII.10.). Freshly prepared polyplexes consisting of Tf-PEI and siGATA however, mediated a significant reduction in the

expression of GATA3, and most of all polyplexes of Tf-PEI and siGATA which were spray dried with 5% mannitol (M5-145°) showed identical effects. Importantly, the gene silencing efficacy of M5-145° did not differ significantly from that of freshly prepared siGATA containing polyplexes confirming retained bioactivity and transfection efficiency. Polyplexes spray dried with 5% trehalose however, showed no transfection at all. This is surprising as it was expected that amorphous substances such as trehalose would stabilize transferrin, a 79 kDa protein, to a greater extent than the crystalline mannitol especially because the latter excipient is known to induce protein aggregation upon spray drying. [8] However, here, mannitol formulations stabilized transferrin just as well and allowed successful transfection. One plausible reason for the lack of gene silencing of the trehalose formulation might be redispersion problems in rather small volumes used for transfection considering their aggregation tendency shown in Figure VII.8. Successful stabilization of transferrin in the mannitol formulations could potentially be achieved by PEI in the polyplexes. PEI participates in the formation of polyplexes but could also interact within transferrin directly. And indeed, as was shown, PEI is able to physically crosslink a protein and increase its stability during stresses induced by pH shifts and stirring. [221] This could explain the maintained stability and conformation of Tf enabling recognition of Tf-receptors of T cells with the Tf decorated polyplexes. Further research will focus on the formation of protein aggregates, the secondary structure and binding kinetics of Tf when spray dried alone, in mixture with PEI and as a Tf-PEI conjugate in either mannitol or trehalose for a better understanding of the processes underlying these findings.

VII.5. Conclusions & Outlook

In summary, we showed that spray drying above T-Out of 90°C results in significant changes in the quantity of siRNA recovered after spray drying. Spray drying at temperatures below 90°C showed no significant differences in respect to recovered quantity and base pair length. Furthermore, we were able to show that the tubing material can have a tremendous effect on the preparation and processing of spray dried polyplexes as interactions between the tubing material and siRNA may occur.

We demonstrated that spray drying did not affect polyplex size and PDI independent of the different excipients and their concentration used in this study. This was also shown for siRNA integrity. Quantitative analysis revealed significant losses of siGFP and PPP after spray drying

when formulated with mannitol, a representative for crystalline substances. However, no changes regarding the recovery of both polyplex components were observed when spray dried with trehalose, the typical matrix used for amorphous microparticles. Therefore, we hypothesize that for nanoparticle properties amorphous substances are crucial to minimize losses through processing.

Concerning microparticle characteristics, mannitol formulations significantly outperformed trehalose formulations with regard to particle characteristics. Due to crystalline structure and subsequent lower residual moisture, mannitol particles exhibited smaller geometric median sizes and showed favorable aerodynamic characteristics.

For in vitro analysis, both formulations showed efficient downregulation of GFP in an eGFP expressing cell line indicating preserved bioactivity with all tested formulations. These findings were translated towards primary CD4⁺ T cells which play a central role in the pathogenesis of inflammatory diseases such as asthma where GATA3 upregulation can be observed.

We demonstrated that spray drying of polyplexes had no negative effect on the efficiency when formulated with mannitol, and successful transfection of primary T cells *ex vivo* was achieved with the spray dried mannitol formulation for dry powder inhalation as reflected by efficient and sequence specific GATA3 silencing.

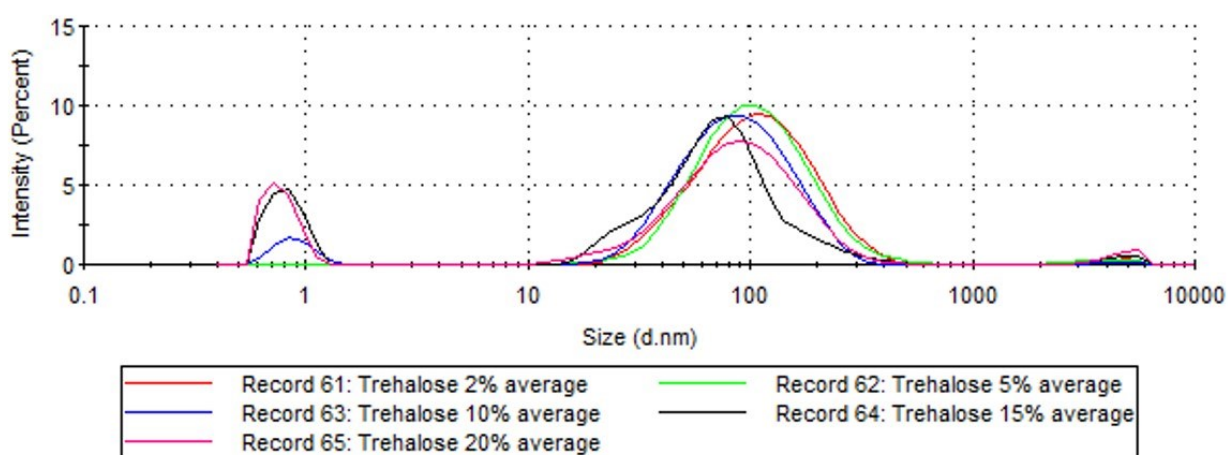
For future research, we are eager to combine beneficial properties of both crystalline and amorphous particles for stabilization through the amorphous matrix and optimal microparticle characteristics through the crystalline material. This approach is based on findings in the freeze drying research of biopharmaceuticals where crystalline and amorphous forming substances are combined to achieve full stabilization with optimal cake appearances [195, 222-224]. Furthermore, studies will be carried out where spray drying will be performed at higher airflow to produce smaller particles and improve aerodynamic properties. Also, trehalose formulations will be prepared and investigated after a secondary drying step which is expected to decrease the residual moisture content and possibly improve microparticle characteristics without lowering nanoparticle stability.

VII.6. Acknowledgements

This project has received funding from the European Research Council (ERC) under the European Union's Horizon 2020 research and innovation programme (Grant agreement No. 637830).

The authors like to thank Dr. Mathias Keil for the NGI set up and Actarmo Medical GmbH, in specific Dr. Sybille Welzhofer, for NGI training. We also like to acknowledge Christian Minke for his work with the SEM and the support from Christoph Zimmermann.

VII.7. Supplementary Data



S-Figure VII.1: DLS of polyplexes with monomer content

DLS measurements of polyplexes in trehalose at various concentrations (m/V). Each record represents an average of three independent measurements and depicts the size distribution by intensity

Chapter VIII)

New Characterization Technique of Polyplexes by TRPS

This chapter was submitted on June 5th, 2020, to the European Journal of Pharmaceutics and Biopharmaceutics:

Tobias WM Keil, Olivia M Merkel, Characterization of Positively Charged Polyplexes by Tunable Resistive Pulse Sensing

VIII New Characterization Technique of Polyplexes by TRPS

VIII.1. Abstract

With the approval of the first siRNA-based drugs, non-viral siRNA delivery has gained special interest in industry and academia in the last two years. For non-viral delivery, positively charged lipid and polymer formulations play a central role in research and development. However, nanoparticle size characterization, particularly of polydisperse formulations, can be very challenging. Tunable resistive pulse sensing for particle by particle measurements of size, polydispersity, zeta potential and a direct concentration promises better assessment of nanoparticle formulations. However, the current application is not optimized for positively charged particles. A supplier-provided coating solution for difficult-to-measure samples does not allow for successful measurements of positively charged nanoparticles. This article describes a new coating solution based on choline-chloride. Coating is verified by current-voltage (I-V) recordings and ultimately tested on a positively charged nanoparticle formulation comprising of siRNA and PEG-PCL-PEI polymer. This coating allows for the first time successful size, PDI and concentration measurement by tunable resistive pulse sensing of positively charged polyplexes. This article provides the foundation for further polyplex research as well as other positively charged nanoparticle formulations based on particle by particle measurements.

VIII.2. Introduction

Cationic lipids and polymers are often used as non-viral vectors and are developed to serve as efficient delivery vehicles for plasmids, small interfering RNA (siRNA) and other new promising nucleic acid-based therapeutics. [225] Especially polyethyleneimine (PEI) and its derivatives are widely studied due to their high positive charge density and hence their ability to form so-called polyplexes with negatively charged macromolecules such as nucleic acids (e.g. siRNA) by electrostatic self-assembly. Particulate formulations of nucleic acids are currently under investigation for therapeutic approaches, and in 2018 the first siRNA containing drug, Patisiran[®], a lipid nanoparticle formulation was approved. To characterize nucleic acid-containing nanoparticles it is of great interest to the scientific community to better understand particle by particle size, surface charge and also the concentration of the formulation.

Tunable resistive pulse sensing (TRPS) has recently attracted interest in particle characterization in the nano meter range and has become accessible with benchtop instruments such as the qNano developed and distributed by iZON-Ltd [226]. This technique enables particle by particle size measurements with simultaneous particle counting and zeta potential measurements when suspended in electrolyte solution. Measurements are based on the Coulter principle in nanoscale: A tunable conical shaped pore made of polyurethane is placed between two fluid chambers containing electrolyte solutions. Voltage can be applied between two electrodes through the pore which are located on each side of the pore resulting in a baseline current. Passing particles lead to a quick decrease in current and enable single particle counting. The magnitude of this blocking is thereby relative to particle size. The frequency of blockings leads to the calculation of the sample concentration. By stretching or relaxing the nanopore an ideal pore size can be obtained to detect a broad range of particle sizes and to provide precise information about size distribution/polydispersity index by standard deviation and PDI. To adapt the frequency of particles passing through the pore, pressure or vacuum of 20 mm Hg at maximum can be applied to accelerate or slow down the measurement. Currently, TRPS is successfully applied to detect sizes of a wide range of nanoparticles and their concentrations as well as zeta potentials. [227] For some applications, iZON Science Ltd. suggests a coating procedure based on their proprietary coating solution consisting of a polyvinylpyrrolidone solution in order to minimize non-specific interactions between particles and the negative surface

charge of the pore membrane [228] facilitating measurements [229]. This coating procedure successfully shifts the surface charge of the pore to a less negative potential. [228] Wilmott et al [230] demonstrated that positively charged particles and even neutral charged particles cannot be measured with the qNano as the particle blockage rate decreases to zero. This is underlined by the fact that all publications reporting measurements with the IZON qNano Gold until today measured samples with a negative surface charge. There is only one publication describing measurements of positively charged particles which were, however, shielded by a large hydrophobic component and is, hence, not representable for positive particles, in general. [231] Even with adapting the coating procedure by exchanging PVP with PEI, to the best of our knowledge, no one has been able to successfully measure positively charged particles nor any other particles e.g. calibration particles after the coating procedure [228, 232].

Hence, the aim of this work was the establishment of a new coating solution to enable reproducible measurements of particles with positive charges with the qNano system for particle by particle size and concentration measurements without hindering calibration measurements nor minimizing pore shelf life.

VIII.3. Materials

L-Histidine monohydrochloride monohydrate (H4036), Choline chloride (C1879), 800 Da low molecular weight branched PEI (LMW-PEI) (408719), 750 kDa high molecular weight branched PEI (HMW-PEI) (P3143) and potassium chloride (P9333) were purchased from Sigma-Aldrich (Sigma-Aldrich Chemie GmbH, Germany).

25 kDa hyperbranched PEI (hy-PEI) was obtained from BASF (Germany). PEI-g-PCL-b-PEG (PPP) polymer was synthesized according to Jones et al. [97]. siRNA as sodium salt against EGFP (siGFP) was obtained from Integrated DNA Technologies (IDT, Coralville, IA, U.S.A.) and prepared as 100 μ M solution in RNase-free DEPC water. Solutions of 32% sodium hydroxide and 37% hydrochloric acid were used from in house supply. Millex-GV filters with a pore diameter of 0.22 μ m were purchased from Merck Millipore Ltd. (SLGV004SL). Coating solutions were prepared and tested as depicted in table VIII.1.

Coating agent	Concentration of coating agent (m/v)	Concentration of KCl (mM)
LMW-PEI	0.1%	100
LMW-PEI	5.0%	100
HMW-PEI	0.1%	100
HMW-PEI	5.0%	100
Hy-PEI	0.1%	100
Hy-PEI	0.9%	100
PPP	0.1%	100
PPP	0.9%	100
PVP*	10%	100
Choline-Chloride	10%	100

Table VIII.1. Coating Solutions

composition of different coating solutions of PEI, PEG-PCL-PEI (PPP), PVP and choline-chloride.

LMW: low molecular weight

HMW: high molecular weight

Hy: hyperbranched

*iZON proprietary coating solution

VIII.4. Methods

Polyplex preparation

siGFP stock solution was diluted in a histidine buffered saline (30 mM histidine, 100mM KCl) at pH 6.4 (HBS) to a concentration of 2.22 μ M. The amount of PPP (m(Polymer)) was calculated based on its PEI content with following formula:

$$m(\text{polymer}) = n(\text{siRNA}) * 52 * MW (\text{protonable units}) * N/P \text{ ratio} \quad (\text{Eq.VIII.1.}),$$

where n(siRNA) is the amount of siRNA, whereas the N/P ratio is defined as the ratio between nitrogen groups of the polymer (N) and phosphate groups of the nucleic acid (P). For all measurements a ratio of 8 was chosen. HBS solutions were filtered through 0.22 μ m filters prior to polyplex preparation. Once calculated, PPP was diluted in HBS and the same volume containing 2.22 μ M siRNA was added to achieve a final concentration of 1.11 μ M siRNA resulting in the formation of polyplexes. This suspension was incubated for 20 min at room temperature.

TRPS measurements

Measurements were executed with the qNano Gold system and analyzed with the iZON Control Suite 3.3.2.2001 software (iZON Science LTD). Calibration particles, iZON coating solution and nanopores were purchased from the same supplier. For instrument setup, the lower electrode was wetted with HBS for 1-2 min. The solution was removed with a pipet, and the nanopore was installed. The pore was stretched, and the stretch was calibrated at approximately 46 mm. Before attaching the upper fluid chamber and placing 35 μL of HBS inside, the lower fluid chamber was filled with 75 μL of HBS. By applying maximum pressure for 5 min, the pore was wetted which was verified by the detection of an increased current.

Coating procedure was executed for 20 min by applying the respective coating solution in the lower and upper fluid chamber and applying a maximum possible voltage. Thereafter the coating solutions were replaced by fresh coating solutions and a maximum vacuum of 20 mm Hg was applied for another 20 min. To clean the pore of remaining coating substances, HBS was applied in both chambers and maximum pressure was applied for 10 min. Afterwards, all solutions were refreshed.

For sample changeover, the upper chamber was emptied and washed 3 times with 35 μL of HPW followed by detaching the upper chamber, rinsing it three times with 500 μL of water and consecutive air drying. After wiping the surface of the nanopore free of remaining liquid with light duty non-lint tissue and reattaching the upper fluid chamber, the system was prepared for a new sample.

For current-voltage (I-V) measurements, a current was established with a 5% HBS solution for about 10 min. A certain stretch was applied and the voltage was set to 1.6 V and decreased in 0.1 V steps to -1.6 V. Data points were read when the current was stable or when a time limit of 30 s was reached.

PDI values of TRPS measurements were calculated as follows:

$$PDI = \left(\frac{\text{standard deviation}}{\text{mean diameter}} \right)^2 \quad (\text{Eq.VIII.2.})$$

Dynamic Light Scattering (DLS) measurements

Aliquots of 70 μL were taken per sample in HBS and inserted into a DTS1070 cuvette (Brand GmbH Co KG, Germany) and measured in triplicates with 15 runs each in the Zetasizer Nano ZS from Malvern Panalytika GmbH (Kassel, Germany) at 173° backscatter angle and processed via Zetasizer Software Version 7.03.

VIII.5. Results and Discussion

I-V measurements

In a conical shaped pore the flow of cations runs preferably from the small opening towards the wide opening when a positive potential is applied [233]. In case of a negative surface charge of the pore which was described in case of the iZON's pore by Weatherall [232], the concentration of cations at the smaller pore opening is higher than at the wider opening side. This is due to the two characteristic factors contributing to the flow i.e. translocation of ions close to the pore walls and across the centre of the pore. Cations are present close to the walls according to their charge due to ionic interactions with the negative surface charge of the pore and form highly concentrated areas where the pore diameter is the smallest. Anions on the other hand, are less likely to pass this region and are more likely to be rejected. When positive potentials are applied, i.e. with the cathode at the smaller opening and anode on the wider opening, the cations' flow is directed towards the anode. As anions flow towards the smaller pore opening under rejection, this results in a buildup of charge inside the conically shaped pore and hence an increased current. When negative potentials are applied, this phenomenon is reversed, and cations flow towards the small opening. In this case, the anions' flow is directed towards the wider opening but are rejected at the smaller opening leading to a decreased current as a result of charge buildup outside the pore [233]. These effects are specific to pH and ionic strength as the electrolyte concentration changes and are reversed when the pore surface charge is changed from negative to positive. This can especially be observed when the pore is coated and the surface charge of the pore is shifted while keeping pH and ionic strength constant.

As shown in Figure VIII.1., uncoated pores exhibit the expected current rectification. After coating pores with a 10% choline solution, the current of coated pores changes slightly when negative voltages are applied and is significantly greater (less negative) compared to

uncoated pores. When applying a positive potential, the current of coated pores increases but does not reach current values as great as uncoated pores.

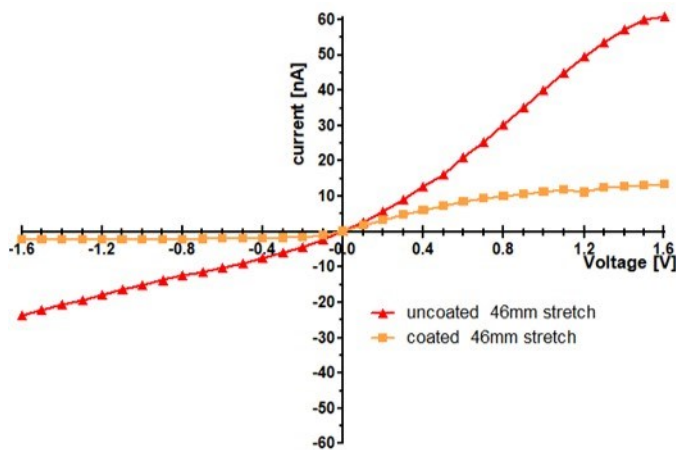


Figure VIII.1. I-V measurement

I-V measurements of a NP 200 at a stretch of 46 mm of an uncoated (red) and a 10 % (m/v) choline-chloride solution coated pore (yellow).

With increased current values at all tested voltages Blundell et al [234] suggested a positive surface charge. This conclusion was comprehensible as in the reported experiment the pore was coated with positively charged PEI [234]. Similar effects were also observed when applying PEI based coating solutions from table 1 but did not result in stable measurements (data not shown). However, in case of choline, we experienced increased

currents only at negative voltages but smaller currents at positive voltages. Whether this can be interpreted as a rather neutral surface charge needs to be evaluated in further studies. An optimal tool to do so is the usage of a streaming potential analyzer which could detect exact potentials. Nonetheless, these modifications showed a successful coating of the polyurethane pore with choline.

Polyplex measurements

Polyplexes were prepared and measured by DLS after an incubation time of 20 minutes. While DLS measurement took place, an aliquot of 35 μ L was taken for TRPS measurement. Although DLS results showing suitable sizes and polydispersity indices (PDIs), measurements with uncoated pores were not executable or only for a few seconds followed by an irreversible blocking of the pore (data not shown). As suggested earlier this might be caused by the charge of polyplexes. Here, PPP-siRNA polyplexes had zeta potentials of 15.6 ± 6.0 mV.

Following iZON's guideline, measurements with the proprietary PVP coating solution [229] were not successful either. Despite varying concentration and type of PEI (Table VIII.1) to extent first experiments [234], measurements were still not possible. Additionally, the usage

of a coating substance which is chemically different from the polymer used in the polyplex formulation might influence size and PDI of the dynamic polyplex system where free and complexed polymers exchange constantly. To avoid such effects, PPP was used for pore coating, and different concentrations were tested. However, improvements in performance were not achieved. To avoid biased measurements due to decreased currents, for all tested coating procedures increased currents were applied but failed again in successful measurements of polyplexes and even calibration standards. Despite vigorous cleaning and flushing, reconditioning of the pores was not achievable suggesting a partial blocking allowing ionic but not particle flow.

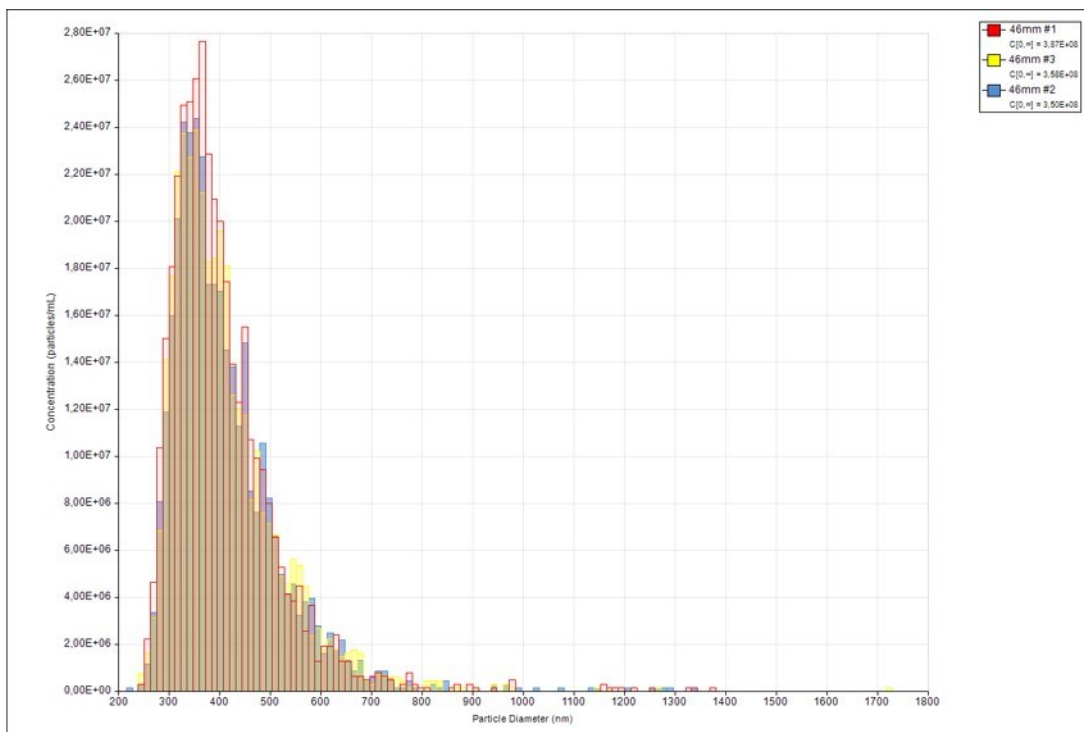


Figure VIII.2. TRPS results

Size distribution of siGFP-PPP polyplexes measured via TRPS with a 10 % (m/v) choline-chloride solution coated NP 200 at a stretch of 46.0 mm.

Eventually, after all these different procedures were tested, measurements were possible for an unlimited period of time after coating the pore with a 10% (m/V) choline-chloride solution in combination with 100 mM KCl. As shown in Figure VIII.2., a polyplex suspension was measured in triplicates at 46.00 mm stretch resulting in comparable sizes, d90/d10 distribution as well as particle concentration (see Table VIII.2 and Figure VIII.2.). The measurement of triplicates with comparable results underlines the fact that detection was independent of time and consistent measurements were made possible. In addition, we also reduced the stretch to 44.30 mm which decreases the pore diameter enabling the detection of smaller particles in general. According to this new range of detectable particles, we indeed found smaller particles not measured at 46.00 nm stretch (Figure VIII.3.). Subsequently, a reduced mean diameter, increased particle concentration and increased d90/d10 ratio was found (Table VIII.1). Although the minimum particle count of 500 particles for further analysis was achieved, the number of particles evaluated for this measurement is still low (768 particles) considering other measurements (>2000 particles) (Table VIII.2). This limitation might lead to a biased size distribution, mean diameter and particle concentration which is more efficiently balanced when the recommended 1000 particles are evaluated [235].

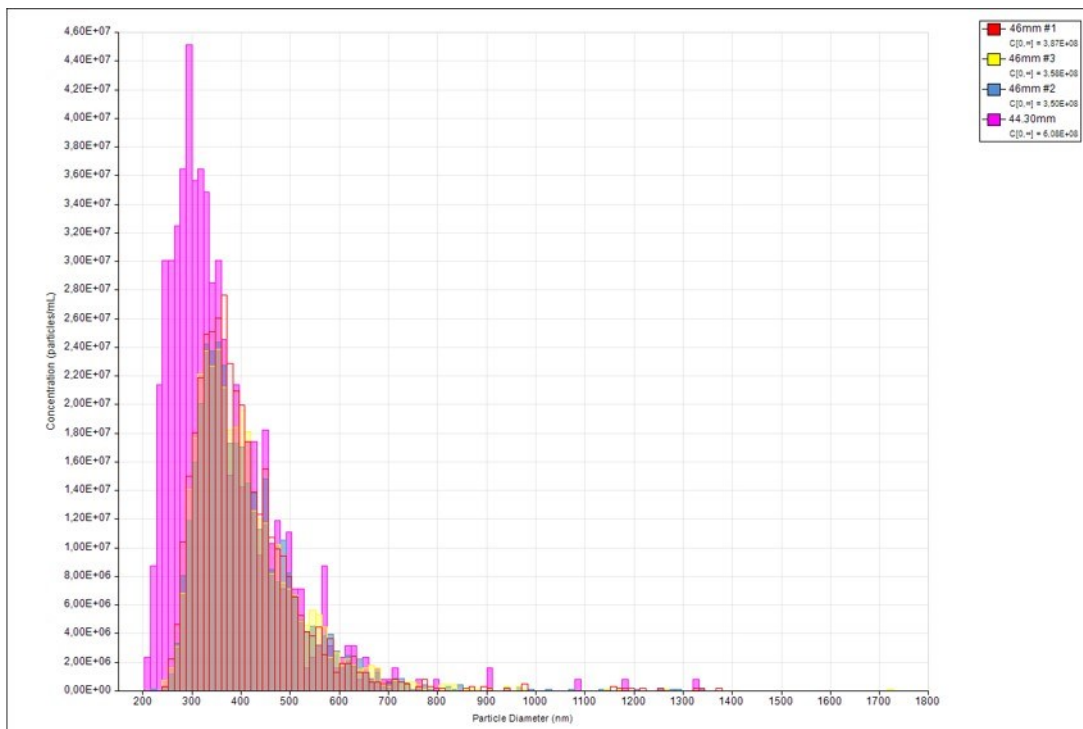


Figure VIII.3. Comparison of TRPS measurements of polyplexes recorded at different stretches with a 10% (m/v) choline-chloride solution coated NP 200.

However, a smaller particle count was expected as decreasing the pore opening is accompanied by an increased pore blocking frequency caused by greater particles and a subsequently prolonged measurement time. To avoid biases in the measurement of dynamic systems such as polyplexes, a maximum time limit of 10 minutes was individually set which explains the decreased

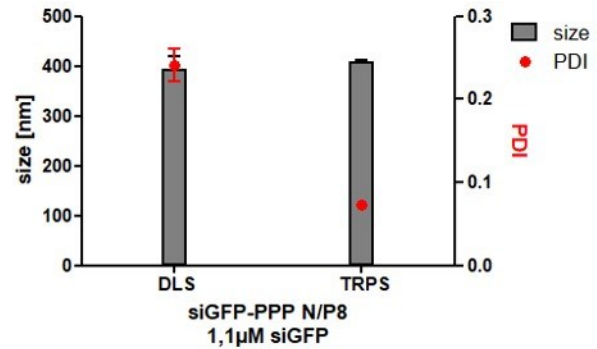


Figure VIII.4. DLS vs. TRPS

Comparison of size and PDI of siGFP-PPP polyplexes at N/P 8 measured by DLS and TRPS

particle count. Nonetheless, these findings underline a successful coating procedure with choline which enables polyplex measurements on the one side without affecting the measurement method itself on the other. For future and more accurate polyplex analysis, polyplex preparation methods, such as microfluidic mixing [193], should be applied which result in a more narrow particle size distribution and allow an even higher consistent analysis via TRPS. [236] When comparing DLS measurements with TRPS data of choline-chloride coated NP at a stretch of 46.0 mm, we observed slightly smaller size values but with greater deviation (Table VIII.2) and greater PDIs (Figure VIII.4.) when measurements are performed by DLS. It is known that DLS measurements tend to overestimate hydrodynamic sizes and polydispersities due to the basis of calculation [237]. However, here we also demonstrate that TRPS measurements do not entirely reflect the presence of all particles since smaller particles which were detected with a decreased stretch were neglected in measurements with a larger pore stretch. Sufficient measurements at smaller stretches however, were not possible due to frequent blocking caused by greater particles. Improved polyplex preparation, for example via microfluidics, is suggested as described above. Nonetheless, these results confirm that TRPS can be applied successfully for characterizing positively charged particles in general and polyplexes specifically.

VIII.6. Conclusions

This work demonstrated the successful coating of polyurethane pores for TRPS resulting in an increased surface charge. To the best of our knowledge this allowed TRPS characterization of highly positively charged polyplexes for the first time.

Despite the greater ability of polymers to form interactions with the nanopore due to greater structures and hence greater availability of interactions, i.e. Van-der-Waals forces and hydrogen-bonds, we found a successful coating substance of much smaller size.

Instead of using temporarily charged structures which strongly depend on pH such as PEI, we used a permanently charged structure independent of pH. This has the additional benefit of enabling measurements at different pH values in various buffers broadening the applicability of the technique itself even further and allows for measuring more complex polyplex formulations and positively charged molecules in general.

VIII.7. Acknowledgements:

The authors thank Gabriella Costabile for expert advice and Eduard Trenkenschuh and Andreas Stelzl for scientific exchange. This work was supported by ERC-2014-StG – 637830 "Novel Asthma Therapy" to Olivia Merkel.

Chapter IX)

Summary and Outlook

IX Summary and Outlook

Within this thesis, the successful preparation of DNA based polyplexes inside of microparticles for pulmonary delivery was shown. Our tested formulations showed ideal properties for pulmonary delivery with MMAD's below 5 μm and GSD's below 2 μm . The determination of MMAD and related aerodynamic parameters was shown by quantification of the mass of the active ingredient (here DNA) as required by FDA and EMA [51, 52]. To the best of our knowledge, this was described for the first time for nucleic acid related pulmonary delivery. [50, 54, 56, 89, 96, 109, 238] This success was enabled by the establishment of polyplex analytics namely quantification of nucleic acid and polymer. This also allowed the recalculation of the N/P ratio between polymer and DNA characterizing the spray dried nanoparticle formulation. It was shown that upon higher losses of DNA compared to PEI, the ratio increased. Although the N/P ratio strongly correlates with the efficiency in *in vitro* experiments, uptake and transfection results of fluorescently labeled DNA or plasmid DNA with PEI, respectively, were not influenced. Also, losses of DNA detected in Chapter III could successfully be attributed to interactions of polyplexes with the tubing surface. During spray drying in chapter III losses of approximately 30% of DNA were detected which correlates with losses after a single pump cycle with a silicon tubing of regular quality as shown in chapter VI. By exchanging the style of pump and hence avoiding the usage of tubings, losses of DNA could be successfully minimized. It was also shown, that the choice of pump was irrelevant for losses of DNA but the choice of tubing material was significant. Hence, shear stresses applied through peristaltic pumps are negligible. As a conclusion, DNA losses during spray drying observed in chapter III are rather attributed to adsorption effects within the tubing than to the pumping or the spray drying process itself.

Furthermore, the methods established for the quantification of the composition and the determination of aerodynamic properties were successfully transferred from DNA based formulations to siRNA formulations (Chapter VII). Based on the established analytics, it was shown that one of the most pronounced effects of spray drying on siRNA polyplexes was heat. Process temperatures which resulted in product temperatures of 90°C and higher had a significant effect on the amount of siRNA recovered after spray drying. This effect is most likely caused by melting of siRNA double strands which is known to happen at a temperature of ~90°C. Temperatures applied during the spray drying process which resulted in lower product temperatures (i.e. below 90°C) did not negatively affect recovery. Besides, the excipient solid form was shown to impact the recovery of siRNA and polymer during spray drying. It was shown, that trehalose, solidifying in an amorphous structure, stabilized siRNA and polymer significantly better than the mannitol which crystallizes even during a fast drying step. Despite these differences, size and PDI of redispersed nanoparticles from spray dried formulations were not significantly changed compared to nanoparticles characterized before spray drying. Also, the in vitro performance was shown to be conserved. Investigations of microparticle characteristics such as residual moisture, geometric size and aerodynamic properties, showed that mannitol formulations outperformed trehalose formulations. Nonetheless, both excipients resulted in satisfying aerodynamic characteristics (MMAD $\leq 5 \mu\text{m}$; GSD $\leq 2 \mu\text{m}$) ideal for pulmonary delivery. Encouraged by these findings, a promising bioconjugate for transfecting activated T_H2-cells, i.e. Tf-PEI, complexed with siGATA3 was spray dried with mannitol or trehalose, respectively, and evaluated for GATA3 knockdown in primary human T-cells. Despite our expectations, mannitol formulations achieved significant knockdown whereas trehalose formulations did not. One explanation might be the insufficient rehydration/resuspension of polyplexes after spray drying of trehalose formulations.

With the development of tunable resistive pulse sensing, particle by particle measurements of size and zeta potentials of nanoparticles has become accessible. [226, 239-247] However, this method has so far only been described for negatively charged particles. In fact, measurements of hydrophilic positively charged particles were not possible. [248] Within this thesis, a coating method based on choline-chloride was developed enabling the successful measurement of positively charged polyplexes. It is further hypothesized that this

coating technique can also enable the measurement of other positively charged nanoparticles, hence, broadening the applicability of TRPS to additional applications.

In future experiments, spray drying of Tf-PEI based formulations must be investigated in more detail. Especially the structure of Tf should be ascertained after spray drying. This could be achieved by investigating the binding kinetics of Tf-PEI before and after processing via surface plasmon resonance. [32] Other techniques which confirm the Tf structure specifically such as fluorescently labeled antibodies against Tf could also be applied. In case the glycoprotein's structure is negatively affected, methods have to be applied identifying the source of change. Such techniques involve the identification of protein denaturation: as high temperatures are applied during the spray drying process, protein unfolding is a potential risk. [249] Such high temperatures can also accelerate chemical reactions such as oxidation and deamidation. [250, 251] To test for these degradation reactions ion-exchange chromatography, size exclusion chromatography and peptide mapping are suggested. [252]

Furthermore, dry powders which were prepared with trehalose as matrix excipient showed greater residual moisture contents than mannitol formulations. For better comparison between both formulations and for improvement of microparticle characteristics, techniques which reduce the amount of water should be applied. Such techniques include drying under room or elevated temperatures while applying vacuum but also prolonged exposure times to heat in the spray drying process are possible [18, 253]: after spray drying the product remains in the sample collector while the pump is turned off. As a result of missing water evaporation and the consequently absent cooling, T-Out rises. The hot air is thereby guided through the whole system passing the dried powder further removing moisture. This method could improve microparticle characteristics such as geometric size and aerodynamic properties of trehalose formulations which are influenced by the residual moisture.

Another approach to improve the dry powder formulation for siRNA could be a combination of mannitol and trehalose. In the lyophilization process of biopharmaceuticals beneficial effects were shown for a ratio of 1:4 trehalose:mannitol. [222-224] Formulations were able to stabilize the protein and maintaining optimal cake performances. For spray drying such

combinations have not been tried. Trehalose could exert its stabilization properties shown in chapter VII whereas mannitol could contribute to the optimal microparticle characteristics.

Also, aerodynamic diameters of reported formulations herein were on the upper limit i.e. 5 μm . A decrease in size by increasing the airflow is hypothesized to consequently show beneficial effects on the MMAD. [3] Also, particle engineering is another aspect to consider for improving aerodynamic properties [53]: upon addition of leucine or tri-leucine, it was shown that particles exert surrogated surface structures as a function of the chosen additive concentration resulting in smaller aerodynamic diameters. Furthermore, a reduction in MMAD leads consequently to an increase of FPF and FPD, bringing the formulation from the benchtop closer to the clinic and the patient.

Chapter X)

Publication list

X Publication list

Peer Reviewed Articles:

T-cell targeted pulmonary siRNA delivery for the treatment of asthma, T.W.M. Keil, D. Baldassi, O.M. Merkel, Wiley Interdiscip. Rev.: Nanomed. Nanobiotechnol., (2020) e1634

Characterization of spray dried powders with nucleic acid-containing PEI nanoparticles, T.W.M. Keil, D.P. Feldmann, G. Costabile, Q. Zhong, S. da Rocha, O.M. Merkel, Eur. J. Pharm. Biopharm., 143 (2019) 61-69.

Dry powder inhalation of siRNA, T.W.M. Keil, O.M. Merkel, Ther. Delivery, 10 (2019) 265-267

Distinct Parameters in the EEG of the PLP α -SYN Mouse Model for Multiple System Atrophy Reinforce Face Validity, L. Härtner, T.W.M. Keil, M. Kreuzer, E.M. Fritz, G.K. Wenning, N. Stefanova, T. Fenzl, Front. Behav. Neurosci., 10 (2017) 252.

Oral Presentations:

Successful Spray Drying of Polyplexes, T.W.M. Keil, O.M. Merkel, International Conference on Nanomedicine and Nanobiotechnology 2019 (ICONAN 2019), Munich, Germany, October 16th – 18, 2019

Pulmonary delivery of spray dried polyplexes with retained in vitro efficiencies designed for siRNA therapy, T. W. M. Keil, D. Feldmann, A. Mehta, G. Costabile, O. M. Merkel, 22nd Annual Meeting, CRS Local Chapter Germany, Halle, Germany, March 1-2, 2018

- ***awarded with the 'Best Oral Presentation Award'*** -

Poster Presentations:

New insight in the aggregation processes of polyplexes after spray drying, T.W.M. Keil, O. M. Merkel, APS Pharmsci 2019, Greenwich, United Kingdom, September 11-13, 2019

Spray dried polyplexes with retained uptake and transfection efficiencies designed for pulmonary delivery, T.W.M. Keil, D. Feldmann; A. Mehta; G. Costabile; O.M. Merkel, PBP World Meeting, Granada, Spain, March 19-22 2018

Formulation of Polyplex Systems For Pulmonary Therapy, T.W.M. Keil, D. Feldmann, A. Mehta, O.M. Merkel, 4th Annual Meeting SFNano, Bordeaux, France, Dec 5-8, 2017

Stabilising Nanoparticles In Microparticles for Pulmonary siRNA Delivery, T.W.M. Keil, I. Chong, D.-A. Kronberger, D. Feldman, A. Mehta, O.M. Merkel, NIM Workshop "Young Ideas in Nanoscience", Munich, Germany, May 2, 2017

Chapter XI)

Reference List

XI Reference List

- [1] S. R. Percy, *Improvement in drying and concentrating liquid substances by atomizing*, US Patent 125,406, **1872**.
- [2] K. Cal and K. Sollohub, *Spray drying technique. I: Hardware and process parameters*, J. Pharm. Sci., **2010**, 575-586.
- [3] Büchi-Labortechnik-AG, *Training Papers Spray Drying*, https://static1.buchi.com/sites/default/files/downloads/Set_3_Training_Papers_Spray_Drying_en_01.pdf?996b2db24007502bd69c913b675467cfc63880ba, **1997 - 2002**.
- [4] J. Broadhead, S. Edmond Rouan and C. Rhodes, *The spray drying of pharmaceuticals*, Drug Dev. Ind. Pharm., **1992**, 1169-1206.
- [5] S. M. Wong, I. W. Kellaway and S. Murdan, *Enhancement of the dissolution rate and oral absorption of a poorly water soluble drug by formation of surfactant-containing microparticles*, Int. J. Pharm., **2006**, 61-68.
- [6] K. G. Desai and H. J. Park, *Encapsulation of vitamin C in tripolyphosphate cross-linked chitosan microspheres by spray drying*, J. Microencapsulation, **2005**, 179-192.
- [7] T. Yi, J. Wan, H. Xu and X. Yang, *A new solid self-microemulsifying formulation prepared by spray-drying to improve the oral bioavailability of poorly water soluble drugs*, Eur. J. Pharm. Biopharm., **2008**, 439-444.
- [8] S. Schüle, W. Frieß, K. Bechtold-Peters and P. Garidel, *Conformational analysis of protein secondary structure during spray-drying of antibody/mannitol formulations*, Eur. J. Pharm. Biopharm., **2007**, 1-9.
- [9] S. Schüle, T. Schulz-Fademrecht, P. Garidel, K. Bechtold-Peters and W. Frieß, *Stabilization of IgG1 in spray-dried powders for inhalation*, Eur. J. Pharm. Biopharm., **2008**, 793-807.
- [10] G. Lee, *Spray-drying of proteins*, in: C. J.F. and M. M.C. (Eds.) *Rational Design of Stable Protein Formulations*, *Pharmaceutical Biotechnology*, vol 13. Springer, Boston, MA, **2002**, pp. 135-158.
- [11] S. White, D. B. Bennett, S. Cheu, P. W. Conley, D. B. Guzek, S. Gray, J. Howard, R. Malcolmson, J. M. Parker and P. Roberts, *EXUBERA®: pharmaceutical development of a novel product for pulmonary delivery of insulin*, Diabetes Technol. Ther., **2005**, 896-906.
- [12] J. S. Skyler, *Pulmonary insulin delivery—state of the art 2007*, Diabetes Technol. Ther., **2007**, S-1-S-3.
- [13] J. Brange and L. Langkjær, *Insulin structure and stability*, in: W. Y.J. and P. R. (Eds.) *Stability and Characterization of Protein and Peptide Drugs*, *Pharmaceutical Biotechnology*, vol 5. Springer, Boston, MA, **1993**, pp. 315-350.
- [14] T. K. Mandal, *Inhaled insulin for diabetes mellitus*, Am. J. Health-Syst. Pharm., **2005**, 1359-1364.
- [15] A. H. Barnett, *Exubera inhaled insulin: a review*, Int. J. Clin. Pract., **2004**, 394-401.
- [16] J. R. White and R. K. Campbell, *Inhaled insulin: an overview*, Clinical Diabetes, **2001**, 13-16.
- [17] W. L. Hulse, R. T. Forbes, M. C. Bonner and M. Getrost, *Influence of protein on mannitol polymorphic form produced during co-spray drying*, Int. J. Pharm., **2009**, 67-72.
- [18] L. C. Foster, M.-C. Kuo and S. R. Billingsley, *Stable glassy state powder formulations*, US Patent 6,258,341, **2001**.

- [19] B. C. Hancock and G. Zografi, *The relationship between the glass transition temperature and the water content of amorphous pharmaceutical solids*, Pharm. Res., **1994**, 471-477.
- [20] S. Yoshioka, Y. Aso and S. Kojima, *The effect of excipients on the molecular mobility of lyophilized formulations, as measured by glass transition temperature and NMR relaxation-based critical mobility temperature*, Pharm. Res., **1999**, 135-140.
- [21] A. H. Chow, H. H. Tong, P. Chattopadhyay and B. Y. Shekunov, *Particle engineering for pulmonary drug delivery*, Pharm. Res., **2007**, 411-437.
- [22] T. B. Martonen and I. M. Katz, *Deposition patterns of aerosolized drugs within human lungs: effects of ventilatory parameters*, Pharm. Res., **1993**, 871-878.
- [23] D. Groneberg, C. Witt, U. Wagner, K. Chung and A. Fischer, *Fundamentals of pulmonary drug delivery*, Respir. Med., **2003**, 382-387.
- [24] P. A. Jaques and C. S. Kim, *Measurement of total lung deposition of inhaled ultrafine particles in healthy men and women*, Inhalation Toxicology, **2000**, 715-731.
- [25] A. Fire, D. Albertson, S. W. Harrison and D. G. Moerman, *Production of antisense RNA leads to effective and specific inhibition of gene expression in *C. elegans* muscle*, Development, **1991**, 503-514.
- [26] R. L. Setten, J. J. Rossi and S.-P. Han, *The current state and future directions of RNAi-based therapeutics*, Nat. Rev. Drug Discovery, **2019**, 421-446.
- [27] A. Fire, S. Q. Xu, M. K. Montgomery, S. A. Kostas, S. E. Driver and C. C. Mello, *Potent and specific genetic interference by double-stranded RNA in *Caenorhabditis elegans**, Nature, **1998**, 806-811.
- [28] L. Jones, F. Ratcliff and D. Baulcombe, *RNA-directed transcriptional gene silencing in plants can be inherited independently of the RNA trigger and requires Met1 for maintenance*, Curr. Biol., **2001**, 747-757.
- [29] S. M. Elbashir, J. Martinez, A. Patkaniowska, W. Lendeckel and T. Tuschl, *Functional anatomy of siRNAs for mediating efficient RNAi in *Drosophila melanogaster* embryo lysate*, EMBO J., **2001**, 6877-6888.
- [30] G. J. Hannon, *RNA interference*, Nature, **2002**, 244-251.
- [31] P. D. Zamore, T. Tuschl, P. A. Sharp and D. P. Bartel, *RNAi: double-stranded RNA directs the ATP-dependent cleavage of mRNA at 21 to 23 nucleotide intervals*, Cell, **2000**, 25-33.
- [32] R. Kandil, Y. Xie, R. Heermann, L. Isert, K. Jung, A. Mehta and O. M. Merkel, *Coming in and Finding Out: Blending Receptor-Targeted Delivery and Efficient Endosomal Escape in a Novel Bio-Responsive siRNA Delivery System for Gene Knockdown in Pulmonary T Cells*, Adv. Ther. (Weinheim, Ger.), **2019**, 1900047.
- [33] F. Czauderna, M. Fechtner, S. Dames, H. Aygun, A. Klippel, G. J. Pronk, K. Giese and J. Kaufmann, *Structural variations and stabilising modifications of synthetic siRNAs in mammalian cells*, Nucleic Acids Res., **2003**, 2705-2716.
- [34] S. M. Hoy, *Patisiran: First Global Approval*, Drugs, **2018**, 1625-1631.
- [35] S. S. Titze-de-Almeida, P. R. P. Brandao, I. Faber and R. Titze-de-Almeida, *Leading RNA Interference Therapeutics Part 1: Silencing Hereditary Transthyretin Amyloidosis, with a Focus on Patisiran*, Mol. Diagn. Ther., **2019**, 1-11.
- [36] P. R. Cullis and M. J. Hope, *Lipid Nanoparticle Systems for Enabling Gene Therapies*, Mol. Ther., **2017**, 1467-1475.
- [37] J. A. Kulkarni, M. M. Darjuan, J. E. Mercer, S. Chen, R. van der Meel, J. L. Thewalt, Y. Y. C. Tam and P. R. Cullis, *On the Formation and Morphology of Lipid Nanoparticles Containing Ionizable Cationic Lipids and siRNA*, ACS Nano, **2018**, 4787-4795.
- [38] J. A. Kulkarni, P. R. Cullis and R. van der Meel, *Lipid Nanoparticles Enabling Gene Therapies: From Concepts to Clinical Utility*, Nucleic Acid Ther., **2018**, 146-157.
- [39] L. L. Cummins, S. R. Owens, L. M. Risen, E. A. Lesnik, S. M. Freier, D. McGee, C. J. Guinosso and P. D. Cook, *Characterization of fully 2'-modified oligoribonucleotide hetero- and homoduplex hybridization and nuclease sensitivity*, Nucleic Acids Res., **1995**, 2019-2024.
- [40] M. Takahashi, N. Minakawa and A. Matsuda, *Synthesis and characterization of 2'-modified-4'-thioRNA: a comprehensive comparison of nuclease stability*, Nucleic Acids Res., **2009**, 1353-1362.

- [41] C. Allerson, N. Sioufi, R. Jarres, T. Prakash, N. Naik, A. Berdeja, L. Wanders, R. Griffey, E. Swayze and B. Bhat, *Fully 2'-modified oligonucleotide duplexes with improved in vitro potency and stability compared to unmodified small interfering RNA*, *J. Med. Chem.*, **2005**, 901-904.
- [42] J. M. Layzer, A. P. McCaffrey, A. K. Tanner, Z. Huang, M. A. Kay and B. A. Sullenger, *In vivo activity of nuclease-resistant siRNAs*, *RNA*, **2004**, 766-771.
- [43] J. K. Nair, J. L. Willoughby, A. Chan, K. Charisse, M. R. Alam, Q. Wang, M. Hoekstra, P. Kandasamy, A. V. Kel'in, S. Milstein, N. Taneja, J. O'Shea, S. Shaikh, L. Zhang, R. J. van der Sluis, M. E. Jung, A. Akinc, R. Hutabarat, S. Kuchimanchi, K. Fitzgerald, T. Zimmermann, T. J. van Berkel, M. A. Maier, K. G. Rajeev and M. Manoharan, *Multivalent N-acetylgalactosamine-conjugated siRNA localizes in hepatocytes and elicits robust RNAi-mediated gene silencing*, *J. Am. Chem. Soc.*, **2014**, 16958-16961.
- [44] J. K. Nair, H. Attarwala, A. Sehgal, Q. Wang, K. Aluri, X. Zhang, M. Gao, J. Liu, R. Indrakanti and S. Schofield, *Impact of enhanced metabolic stability on pharmacokinetics and pharmacodynamics of GalNAc-siRNA conjugates*, *Nucleic Acids Res.*, **2017**, 10969-10977.
- [45] P. de Paula Brandão, S. Titze-de-Almeida and R. Titze-de-Almeida, *Leading RNA Interference Therapeutics Part 2: Silencing Delta-Aminolevulinic Acid Synthase 1, with a Focus on Givosiran*, *Mol. Diagn. Ther.*, **2019**, 1-8.
- [46] Q. Ge, L. Filip, A. Bai, T. Nguyen, H. N. Eisen and J. Chen, *Inhibition of influenza virus production in virus-infected mice by RNA interference*, *Proc. Natl. Acad. Sci. U. S. A.*, **2004**, 8676-8681.
- [47] S. M. Tompkins, C. Y. Lo, T. M. Tumpey and S. L. Epstein, *Protection against lethal influenza virus challenge by RNA interference in vivo*, *Proc. Natl. Acad. Sci. U. S. A.*, **2004**, 8682-8686.
- [48] V. Bitko, A. Musiyenko, O. Shulyayeva and S. Barik, *Inhibition of respiratory viruses by nasally administered siRNA*, *Nat. Med.*, **2005**, 50-55.
- [49] A. G. Rosas-Taraco, D. M. Higgins, J. Sanchez-Campillo, E. J. Lee, I. M. Orme and M. Gonzalez-Juarrero, *Intrapulmonary delivery of XCL1-targeting small interfering RNA in mice chronically infected with Mycobacterium tuberculosis*, *Am. J. Respir. Cell Mol. Biol.*, **2009**, 136-145.
- [50] M. Y. T. Chow, Y. S. Qiu, F. F. K. Lo, H. H. S. Lin, H. K. Chan, P. C. L. Kwok and J. K. W. Lam, *Inhaled powder formulation of naked siRNA using spray drying technology with L-leucine as dispersion enhancer*, *Int. J. Pharm.*, **2017**, 40-52.
- [51] European-Pharmacopoeia-Commission, *Aerodynamic Assessment of Fine Particles*, in: 2.9.18 Preparations for Inhalation, Ph.Eur. 9.0, **2017**, pp. 440-454.
- [52] United-States-Pharmacopoeial-Convention, *Particle Size - Aerodynamic Size Distribution*, in: 601 Aerosols, Nasal Sprays, Metered-Dose Inhalers, and Dry Powder Inhalers, USP 35, **2012**, pp. 232-252.
- [53] R. Vehring, *Pharmaceutical particle engineering via spray drying*, *Pharm Res*, **2008**, 999-1022.
- [54] M. Y. T. Chow, Y. Qiu, Q. Liao, P. C. L. Kwok, S. F. Chow, H. K. Chan and J. K. W. Lam, *High siRNA loading powder for inhalation prepared by co-spray drying with human serum albumin*, *Int. J. Pharm.*, **2019**, 118818.
- [55] J. Wu, L. Wu, F. Wan, J. Rantanen, D. Cun and M. Yang, *Effect of thermal and shear stresses in the spray drying process on the stability of siRNA dry powders*, *Int. J. Pharm.*, **2019**, 32-39.
- [56] D. M. Jensen, D. Cun, M. J. Maltesen, S. Frokjaer, H. M. Nielsen and C. Foged, *Spray drying of siRNA-containing PLGA nanoparticles intended for inhalation*, *J. Control. Release*, **2010**, 138-145.
- [57] L. B. Jensen, J. Griger, B. Naeye, A. K. Varkouhi, K. Raemdonck, R. Schifflers, T. Lammers, G. Storm, S. C. de Smedt and B. S. Sproat, *Comparison of polymeric siRNA nanocarriers in a murine LPS-activated macrophage cell line: gene silencing, toxicity and off-target gene expression*, *Pharm. Res.*, **2012**, 669-682.
- [58] T. K. Endres, M. Beck-Broichsitter, O. Samsonova, T. Renette and T. H. Kissel, *Self-assembled biodegradable amphiphilic PEG-PCL-IPEI triblock copolymers at the borderline between micelles and nanoparticles designed for drug and gene delivery*, *Biomaterials*, **2011**, 7721-7731.
- [59] A. Raup, H. Wang, C. Synatschke, V. Jerome, S. Agarwal, D. Pergushov, A. Mueller and R. Freitag, *Compaction and transmembrane delivery of pDNA: differences between I-PEI and two types of amphiphilic block copolymers*, *Biomacromolecules*, **2017**.
- [60] S. M. Zou, P. Erbacher, J. S. Remy and J. P. Behr, *Systemic linear polyethylenimine (L-PEI)-mediated gene delivery in the mouse*, *J. Gene Med.*, **2000**, 128-134.

- [61] B. Urban-Klein, S. Werth, S. Abuharbeid, F. Czubyko and A. Aigner, *RNAi-mediated gene-targeting through systemic application of polyethylenimine (PEI)-complexed siRNA in vivo*, Gene Ther., **2005**, 461.
- [62] O. Boussif, F. Lezoualc'h, M. A. Zanta, M. D. Mergny, D. Scherman, B. Demeneix and J.-P. Behr, *A versatile vector for gene and oligonucleotide transfer into cells in culture and in vivo: polyethylenimine*, Proc. Natl. Acad. Sci. U. S. A., **1995**, 7297-7301.
- [63] D. Adams, A. Gonzalez-Duarte, W. D. O'Riordan, C.-C. Yang, M. Ueda, A. V. Kristen, I. Tournev, H. H. Schmidt, T. Coelho and J. L. Berk, *Patisiran, an RNAi therapeutic, for hereditary transthyretin amyloidosis*, N Engl J Med, **2018**, 11-21.
- [64] M. J. R. Ruigrok, H. W. Frijlink and W. L. J. Hinrichs, *Pulmonary administration of small interfering RNA: The route to go?*, J Control Release, **2016**, 14-23.
- [65] K. Thanki, K. G. Blum, A. Thakur, F. Rose and C. Foged, *Formulation of RNA interference-based drugs for pulmonary delivery: challenges and opportunities*, Ther Deliv, **2018**, 731-749.
- [66] A. Aigner and D. Kögel, *Nanoparticle/siRNA-based therapy strategies in glioma: which nanoparticles, which siRNAs?*, Nanomedicine, **2018**, 89-103.
- [67] S. Weber, A. Zimmer and J. Pardeike, *Solid Lipid Nanoparticles (SLN) and Nanostructured Lipid Carriers (NLC) for pulmonary application: a review of the state of the art*, Eur. J. Pharm. Biopharm., **2014**, 7-22.
- [68] M. L. Levy, A. Hardwell, E. McKnight and J. Holmes, *Asthma patients' inability to use a pressurised metered-dose inhaler (pMDI) correctly correlates with poor asthma control as defined by the global initiative for asthma (GINA) strategy: a retrospective analysis*, NPJ Prim. Care Respir., **2013**, 406-411.
- [69] I. Y. Saleem, F. Diez, B. E. Jones, N. Kayali and L. Polo, *Investigation on the aerosol performance of dry powder inhalation hypromellose capsules with different lubricant levels*, Int. J. Pharm., **2015**, 258-263.
- [70] P. Demoly, P. Hagedoorn, A. H. de Boer and H. W. Frijlink, *The clinical relevance of dry powder inhaler performance for drug delivery*, Respir. Med., **2014**, 1195-1203.
- [71] J. S. Patil and S. Sarasija, *Pulmonary drug delivery strategies: A concise, systematic review*, Lung India, **2012**, 44-49.
- [72] M. Y. Yang, J. G. Chan and H. K. Chan, *Pulmonary drug delivery by powder aerosols*, J. Control. Release, **2014**, 228-240.
- [73] A. S. Barham, F. Tewes and A. M. Healy, *Moisture diffusion and permeability characteristics of hydroxypropylmethylcellulose and hard gelatin capsules*, Int. J. Pharm., **2015**, 796-803.
- [74] W. Liang, A. Y. Chan, M. Y. Chow, F. F. Lo, Y. Qiu, P. C. Kwok and J. K. Lam, *Spray freeze drying of small nucleic acids as inhaled powder for pulmonary delivery*, Asian J. Pharm, **2018**, 163-172.
- [75] D. Leng, K. Thanki, C. Foged and M. Yang, *Formulating Inhalable Dry Powders Using Two-Fluid and Three-Fluid Nozzle Spray Drying*, Pharm. Res., **2018**, 247-257.
- [76] W. Liang, M. Y. Chow, S. F. Chow, H.-K. Chan, P. C. Kwok and J. K. Lam, *Using two-fluid nozzle for spray freeze drying to produce porous powder formulation of naked siRNA for inhalation*, Int J Pharm, **2018**, 67-75.
- [77] T. Okuda, M. Morishita, K. Mizutani, A. Shibayama, M. Okazaki and H. Okamoto, *Development of spray-freeze-dried siRNA/PEI powder for inhalation with high aerosol performance and strong pulmonary gene silencing activity*, J. Control. Release, **2018**, 99-113.
- [78] O. M. Merkel, I. Rubinstein and T. Kissel, *siRNA delivery to the lung: what's new?*, Adv. Drug Delivery Rev., **2014**, 112-128.
- [79] M. Hoppentocht, P. Hagedoorn, H. W. Frijlink and A. H. de Boer, *Technological and practical challenges of dry powder inhalers and formulations*, Adv. Drug Delivery Rev., **2014**, 18-31.
- [80] A. Ziaee, A. B. Albadarin, L. Padrela, T. Femmer, E. O'Reilly and G. Walker, *Spray drying of pharmaceuticals and biopharmaceuticals: Critical parameters and experimental process optimization approaches*, Eur. J. Pharm. Sci., **2019**, 300-318.
- [81] M. Y. T. Chow, Y. Qiu, F. F. K. Lo, H. H. S. Lin, H.-K. Chan, P. C. L. Kwok and J. K. W. Lam, *Inhaled powder formulation of naked siRNA using spray drying technology with L-leucine as dispersion enhancer*, Int J Pharm, **2017**.

- [82] N. R. Labiris and M. B. Dolovich, *Pulmonary drug delivery. Part I: physiological factors affecting therapeutic effectiveness of aerosolized medications*, Br. J. Clin. Pharmacol., **2003**, 588-599.
- [83] J. S. Patton and P. R. Byron, *Inhaling medicines: delivering drugs to the body through the lungs*, Nat. Rev. Drug Discovery, **2007**, 67-74.
- [84] G. K. Crompton, *Dry powder inhalers: advantages and limitations*, J. Aerosol Med., **1991**, 151-156.
- [85] Y. R. Xie, N. H. Kim, V. Nadithe, D. Schalk, A. Thakur, A. Kilic, L. G. Lum, D. J. P. Bassett and O. M. Merkel, *Targeted delivery of siRNA to activated T cells via transferrin-polyethylenimine (Tf-PEI) as a potential therapy of asthma*, J. Control. Release, **2016**, 120-129.
- [86] J. Soutschek, A. Akinc, B. Bramlage, K. Charisse, R. Constien, M. Donoghue, S. Elbashir, A. Geick, P. Hadwiger, J. Harborth, M. John, V. Kesavan, G. Lavine, R. K. Pandey, T. Racie, K. G. Rajeev, I. Rohl, I. Toudjarska, G. Wang, S. Wuschko, D. Bumcrot, V. Koteliansky, S. Limmer, M. Manoharan and H. P. Vornlocher, *Therapeutic silencing of an endogenous gene by systemic administration of modified siRNAs*, Nature, **2004**, 173-178.
- [87] R. M. Seguin and N. Ferrari, *Emerging oligonucleotide therapies for asthma and chronic obstructive pulmonary disease*, Expert Opin. Inv. Drug., **2009**, 1505-1517.
- [88] M. Klinger-Strobel, C. Lautenschlager, D. Fischer, J. G. Mainz, T. Bruns, L. Tuchscher, M. W. Pletz and O. Makarewicz, *Aspects of pulmonary drug delivery strategies for infections in cystic fibrosis--where do we stand?*, Expert Opin Drug Deliv, **2015**, 1351-1374.
- [89] M. Y. Chow and J. K. Lam, *Dry powder formulation of plasmid DNA and siRNA for inhalation*, Curr. Pharm. Des., **2015**, 3854-3866.
- [90] M. S. Draz, B. A. Fang, P. Zhang, Z. Hu, S. Gu, K. C. Weng, J. W. Gray and F. F. Chen, *Nanoparticle-mediated systemic delivery of siRNA for treatment of cancers and viral infections*, Theranostics, **2014**, 872-892.
- [91] O. M. Merkel, M. Zheng, H. Debus and T. Kissel, *Pulmonary gene delivery using polymeric nonviral vectors*, Bioconjugate Chem., **2012**, 3-20.
- [92] F. Alexis, J. Zeng and W. Shu, *PEI Nanoparticles for Targeted Gene Delivery*, Cold Spring Harb., **2006**.
- [93] J. Heyder, *Deposition of inhaled particles in the human respiratory tract and consequences for regional targeting in respiratory drug delivery*, Proc. Am. Thorac. Soc., **2004**, 315-320.
- [94] R. S. Heyder, Q. Zhong, R. C. Bazito and S. R. P. da Rocha, *Cellular internalization and transport of biodegradable polyester dendrimers on a model of the pulmonary epithelium and their formulation in pressurized metered-dose inhalers*, Int. J. Pharm., **2017**, 181-194.
- [95] M. Elsayed, V. Corrand, V. Kolhatkar, Y. Xie, N. H. Kim, R. Kolhatkar and O. M. Merkel, *Influence of oligospermines architecture on their suitability for siRNA delivery*, Biomacromolecules, **2014**, 1299-1310.
- [96] J. Schulze, S. Kuhn, S. Hendriks, M. Schulz-Siegmund, T. Polte and A. Aigner, *Spray-Dried Nanoparticle-in-Microparticle Delivery Systems (NiMDS) for Gene Delivery, Comprising Polyethylenimine (PEI)-Based Nanoparticles in a Poly(Vinyl Alcohol) Matrix*, Small, **2018**, e1701810.
- [97] S. K. Jones, V. Lizzio and O. M. Merkel, *Folate Receptor Targeted Delivery of siRNA and Paclitaxel to Ovarian Cancer Cells via Folate Conjugated Triblock Copolymer to Overcome TLR4 Driven Chemotherapy Resistance*, Biomacromolecules, **2016**, 76-87.
- [98] J. Schindelin, I. Arganda-Carreras, E. Frise, V. Kaynig, M. Longair, T. Pietzsch, S. Preibisch, C. Rueden, S. Saalfeld, B. Schmid, J. Y. Tinevez, D. J. White, V. Hartenstein, K. Eliceiri, P. Tomancak and A. Cardona, *Fiji: an open-source platform for biological-image analysis*, Nat. Methods, **2012**, 676-682.
- [99] S. L. Snyder and P. Z. Sobocinski, *An improved 2,4,6-trinitrobenzenesulfonic acid method for the determination of amines*, Anal. Biochem., **1975**, 284-288.
- [100] V. Naini, P. R. Byron and E. M. Phillips, *Physicochemical stability of crystalline sugars and their spray-dried forms: Dependence upon relative humidity and suitability for use in powder inhalers*, Drug Dev. Ind. Pharm., **1998**, 895-909.
- [101] P. C. Seville, H. Y. Li and T. P. Learoyd, *Spray-dried powders for pulmonary drug delivery*, Crit. Rev. Ther. Drug Carrier Syst., **2007**, 307-360.

- [102] D. S. Conti, D. Brewer, J. Grashik, S. Avasarala and S. R. da Rocha, *Poly(amidoamine) Dendrimer Nanocarriers and Their Aerosol Formulations for siRNA Delivery to the Lung Epithelium*, Mol. Pharmaceutics, **2014**, 1808-1822.
- [103] S. Boeckle, K. von Gersdorff, S. van der Piepen, C. Culmsee, E. Wagner and M. Ogris, *Purification of polyethylenimine polyplexes highlights the role of free polycations in gene transfer*, J. Gene Med., **2004**, 1102-1111.
- [104] M. Zheng, G. M. Pavan, M. Neeb, A. K. Schaper, A. Danani, G. Klebe, O. M. Merkel and T. Kissel, *Targeting the blind spot of polycationic nanocarrier-based siRNA delivery*, ACS Nano, **2012**, 9447-9454.
- [105] D. A. Kuhn, D. Vanhecke, B. Michen, F. Blank, P. Gehr, A. Petri-Fink and B. Rothen-Rutishauser, *Different endocytotic uptake mechanisms for nanoparticles in epithelial cells and macrophages*, Beilstein J. Nanotechnol., **2014**, 1625-1636.
- [106] Y. Takashima, R. Saito, A. Nakajima, M. Oda, A. Kimura, T. Kanazawa and H. Okada, *Spray-drying preparation of microparticles containing cationic PLGA nanospheres as gene carriers for avoiding aggregation of nanospheres*, Int. J. Pharm., **2007**, 262-269.
- [107] E. Bielski, Q. Zhong, H. Mirza, M. Brown, A. Molla, T. Carvajal and S. R. da Rocha, *TPP-dendrimer nanocarriers for siRNA delivery to the pulmonary epithelium and their dry powder and metered-dose inhaler formulations*, Int. J. Pharm., **2017**, 171-183.
- [108] W. Abdelwahed, G. Degobert, S. Stainmesse and H. Fessi, *Freeze-drying of nanoparticles: formulation, process and storage considerations*, Adv. Drug Delivery Rev., **2006**, 1688-1713.
- [109] M. Agnoletti, A. Bohr, K. Thanki, F. Wan, X. H. Zeng, J. P. Boetker, M. Yang and C. Foged, *Inhalable siRNA-loaded nano-embedded microparticles engineered using microfluidics and spray drying*, Eur. J. Pharm. Biopharm., **2017**, 9-21.
- [110] W. Yang, J. I. Peters and R. O. Williams, 3rd, *Inhaled nanoparticles--a current review*, Int. J. Pharm., **2008**, 239-247.
- [111] C. Nunes, R. Suryanarayanan, C. E. Botez and P. W. Stephens, *Characterization and crystal structure of D-mannitol hemihydrate*, J. Pharm. Sci., **2004**, 2800-2809.
- [112] M. G. Cares-Pacheco, G. Vaca-Medina, R. Calvet, F. Espitalier, J. J. Letourneau, A. Rouilly and E. Rodier, *Physicochemical characterization of D-mannitol polymorphs: the challenging surface energy determination by inverse gas chromatography in the infinite dilution region*, Int. J. Pharm., **2014**, 69-81.
- [113] A. Burger, J. O. Henck, S. Hetz, J. M. Rollinger, A. A. Weissnicht and H. Stottner, *Energy/temperature diagram and compression behavior of the polymorphs of D-mannitol*, J. Pharm. Sci., **2000**, 457-468.
- [114] L. Yu, *Amorphous pharmaceutical solids: preparation, characterization and stabilization*, Adv Drug Deliv Rev, **2001**, 27-42.
- [115] L. Weng, S. Ziaei and G. D. Elliott, *Effects of Water on Structure and Dynamics of Trehalose Glasses at Low Water Contents and its Relationship to Preservation Outcomes*, Sci. Rep., **2016**, 28795.
- [116] N. Y. Chew, P. Tang, H. K. Chan and J. A. Raper, *How much particle surface corrugation is sufficient to improve aerosol performance of powders?*, Pharm. Res., **2005**, 148-152.
- [117] W. Wang, *Lyophilization and development of solid protein pharmaceuticals*, Int. J. Pharm., **2000**, 1-60.
- [118] H. Nagase, T. Endo, H. Ueda and M. Nakagaki, *An anhydrous polymorphic form of trehalose*, Carbohydr. Res., **2002**, 167-173.
- [119] L. Yu, D. S. Mishra and D. R. Riggsbee, *Determination of the glass properties of D-mannitol using sorbitol as an impurity*, J. Pharm. Sci., **1998**, 774-777.
- [120] N. R. Rabbani and P. C. Seville, *The influence of formulation components on the aerosolisation properties of spray-dried powders*, J. Control. Release, **2005**, 130-140.
- [121] J. Fahrmeir, M. Gunther, N. Tietze, E. Wagner and M. Ogris, *Electrophoretic purification of tumor-targeted polyethylenimine-based polyplexes reduces toxic side effects in vivo*, J. Control. Release, **2007**, 236-245.

- [122] L. Chen, J. D. Simpson, A. V. Fuchs, B. E. Rolfe and K. J. Thurecht, *Effects of Surface Charge of Hyperbranched Polymers on Cytotoxicity, Dynamic Cellular Uptake and Localization, Hemotoxicity, and Pharmacokinetics in Mice*, Mol. Pharmaceutics, **2017**, 4485-4497.
- [123] S. Srinivasachari, Y. Liu, G. Zhang, L. Prevet and T. M. Reineke, *Trehalose click polymers inhibit nanoparticle aggregation and promote pDNA delivery in serum*, J. Am. Chem. Soc., **2006**, 8176-8184.
- [124] H. Yin, R. L. Kanasty, A. A. Eltoukhy, A. J. Vegas, J. R. Dorkin and D. G. Anderson, *Non-viral vectors for gene-based therapy*, Nat. Rev. Genet., **2014**, 541.
- [125] M. J. R. Ruigrok, H. W. Frijlink and W. L. J. Hinrichs, *Pulmonary administration of small interfering RNA: The route to go?*, J. Control. Release, **2016**, 14-23.
- [126] D. Cun, D. K. Jensen, M. J. Maltesen, M. Bunker, P. Whiteside, D. Scurr, C. Foged and H. M. Nielsen, *High loading efficiency and sustained release of siRNA encapsulated in PLGA nanoparticles: quality by design optimization and characterization*, Eur. J. Pharm. Biopharm., **2011**, 26-35.
- [127] T. W. M. Keil, D. P. Feldmann, G. Costabile, Q. Zhong, S. da Rocha and O. M. Merkel, *Characterization of spray dried powders with nucleic acid-containing PEI nanoparticles*, Eur. J. Pharm. Biopharm., **2019**, 61-69.
- [128] A. K. Tyagi, T. W. Randolph, A. Dong, K. M. Maloney, C. Hitscherich, Jr. and J. F. Carpenter, *IgG particle formation during filling pump operation: a case study of heterogeneous nucleation on stainless steel nanoparticles*, J. Pharm. Sci., **2009**, 94-104.
- [129] A. Nayak, J. Colandene, V. Bradford and M. Perkins, *Characterization of subvisible particle formation during the filling pump operation of a monoclonal antibody solution*, J. Pharm. Sci., **2011**, 4198-4204.
- [130] M. E. Cromwell, E. Hilario and F. Jacobson, *Protein aggregation and bioprocessing*, AAPS J., **2006**, E572-579.
- [131] W. G. Whitford, *Single-use systems as principal components in bioproduction*, BioProcess Int., **2010**, 34-42.
- [132] A. H. Gray, J. Wright, L. Bruce and J. Oakley, *Clinical pharmacy pocket companion*, 2nd Edition ed., Pharmaceutical Press, **2015**.
- [133] C. Her and J. F. Carpenter, *Effects of Tubing Type, Formulation, and Postpumping Agitation on Nanoparticle and Microparticle Formation in Intravenous Immunoglobulin Solutions Processed With a Peristaltic Filling Pump*, J. Pharm. Sci., **2020**, 739-749.
- [134] S. Altenor, B. Carene, E. Emmanuel, J. Lambert, J. J. Ehrhardt and S. Gaspard, *Adsorption studies of methylene blue and phenol onto vetiver roots activated carbon prepared by chemical activation*, J. Hazard. Mater., **2009**, 1029-1039.
- [135] G. Ström, M. Fredriksson and P. Stenius, *Contact angles, work of adhesion, and interfacial tensions at a dissolving hydrocarbon surface*, J. Colloid Interface Sci., **1987**, 352-361.
- [136] N. B. Bam, J. L. Cleland, J. Yang, M. C. Manning, J. F. Carpenter, R. F. Kelley and T. W. Randolph, *Tween protects recombinant human growth hormone against agitation-induced damage via hydrophobic interactions*, J. Pharm. Sci., **1998**, 1554-1559.
- [137] T. Arakawa, D. B. Dix and B. S. Chang, *The effects of protein stabilizers on aggregation induced by multiple-stresses*, Yakugaku Zasshi, **2003**, 957-961.
- [138] V. Saller, *Interactions of formulation and disposables in biopharmaceutical drug product manufacturing*, in: *Pharmaceutical Technology and Bioharmaceutics*, LMU München: Fakultät für Chemie und Pharmazie, **2015**, pp. 201.
- [139] D. K. Owens and R. C. Wendt, *Estimation of the surface free energy of polymers*, J. Appl. Polym. Sci., **1969**, 1741-1747.
- [140] E. G. Shafrin and W. A. Zisman, *Upper limits to the contact angles of liquids on solids*, in: F. Fowkes (Ed.) *Contact Angle, Wettability, and Adhesion*, ACS Publications, **1964**, pp. 145-157.
- [141] E. Wolfram, *Adhäsion von Flüssigkeiten an Kunststoffoberflächen*, Kolloid-Zeitschrift und Zeitschrift für Polymere, **1962**, 75-85.
- [142] F. Ganachaud, A. Elaïssari, C. Pichot, A. Laayoun and P. Cros, *Adsorption of single-stranded DNA fragments onto cationic aminated latex particles*, Langmuir, **1997**, 701-707.

- [143] V. Chan, S. E. McKenzie, S. Surrey, P. Fortina and D. J. Graves, *Effect of hydrophobicity and electrostatics on adsorption and surface diffusion of DNA oligonucleotides at liquid/solid interfaces*, J. Colloid Interface Sci., **1998**, 197-207.
- [144] V. Ballardur, A. Theretz and B. Mandrand, *Determination of the Main Forces Driving DNA Oligonucleotide Adsorption onto Aminated Silica Wafers*, J. Colloid Interface Sci., **1997**, 408-418.
- [145] X. Zhao and J. K. Johnson, *Simulation of adsorption of DNA on carbon nanotubes*, J. Am. Chem. Soc., **2007**, 10438-10445.
- [146] M. Cardenas, A. Braem, T. Nylander and B. Lindman, *DNA compaction at hydrophobic surfaces induced by a cationic amphiphile*, Langmuir, **2003**, 7712-7718.
- [147] K. Eskilsson, C. Leal, B. Lindman, M. Miguel and T. Nylander, *DNA– Surfactant Complexes at Solid Surfaces*, Langmuir, **2001**, 1666-1669.
- [148] Z. Bengali, A. K. Pannier, T. Segura, B. C. Anderson, J. H. Jang, T. A. Mustoe and L. D. Shea, *Gene delivery through cell culture substrate adsorbed DNA complexes*, Biotechnol. Bioeng., **2005**, 290-302.
- [149] T. Segura and L. D. Shea, *Surface-tethered DNA complexes for enhanced gene delivery*, Bioconjugate Chem., **2002**, 621-629.
- [150] *The Global Asthma Report 2018*, in, Auckland, New Zealand, **2018**.
- [151] M. Weckmann, A. Collison, J. L. Simpson, M. V. Kopp, P. A. Wark, M. J. Smyth, H. Yagita, K. I. Matthaei, N. Hansbro and B. Whitehead, *Critical link between TRAIL and CCL20 for the activation of TH2 cells and the expression of allergic airway disease*, Nat. Med., **2007**, 1308-1315.
- [152] M. Wegmann, H. Fehrenbach, A. Fehrenbach, T. Held, C. Schramm, H. Garn and H. Renz, *Involvement of distal airways in a chronic model of experimental asthma*, Clin. Exp. Allergy, **2005**, 1263-1271.
- [153] S. Sel, M. Wegmann, T. Dicke, S. Sel, W. Henke, A. Ö. Yildirim, H. Renz and H. Garn, *Effective prevention and therapy of experimental allergic asthma using a GATA-3–specific DNase*, J. Allergy Clin. Immunol., **2008**, 910-916. e915.
- [154] J. C. de Groot, A. Ten Brinke and E. H. Bel, *Management of the patient with eosinophilic asthma: a new era begins*, ERJ Open Res., **2015**, 00024-02015.
- [155] J. A. Walker, J. L. Barlow and A. N. McKenzie, *Innate lymphoid cells—how did we miss them?*, Nat. Rev. Immunol., **2013**, 75.
- [156] A. Ray and L. Cohn, *Th2 cells and GATA-3 in asthma: new insights into the regulation of airway inflammation*, J. Clin. Invest., **1999**, 985-993.
- [157] N. Krug, J. M. Hohlfeld, R. Buhl, J. Renz, H. Garn and H. Renz, *Blood eosinophils predict therapeutic effects of a GATA3-specific DNase in asthma patients*, J. Allergy Clin. Immunol., **2017**, 625-628 e625.
- [158] T. N. Lively, K. Kossen, A. Balhorn, T. Koya, S. Zinnen, K. Takeda, J. J. Lucas, B. Polisky, I. M. Richards and E. W. Gelfand, *Effect of chemically modified IL-13 short interfering RNA on development of airway hyperresponsiveness in mice*, J. Allergy Clin. Immunol., **2008**, 88-94.
- [159] Y. Liu, J. Nguyen, T. Steele, O. Merkel and T. Kissel, *A new synthesis method and degradation of hyper-branched polyethylenimine grafted polycaprolactone block mono-methoxyl poly (ethylene glycol) copolymers (hy-PEI-g-PCL-b-mPEG) as potential DNA delivery vectors*, Polymer, **2009**, 3895-3904.
- [160] B. R. Olden, Y. Cheng, J. L. Yu and S. H. Pun, *Cationic polymers for non-viral gene delivery to human T cells*, J. Control. Release, **2018**, 140-147.
- [161] T. W. M. Keil and O. M. Merkel, *Dry powder inhalation of siRNA*, Ther Deliv, **2019**, 265-267.
- [162] F. T. Ishmael, *The inflammatory response in the pathogenesis of asthma*, J. Am. Osteopath. Assoc., **2011**, S11-17.
- [163] P. J. Barnes, *Cytokine modulators as novel therapies for asthma*, Annu. Rev. Pharmacol. Toxicol., **2002**, 81-98.
- [164] M. Wegmann, *Th2 cells as targets for therapeutic intervention in allergic bronchial asthma*, Expert Rev. Mol. Diagn., **2009**, 85-100.
- [165] B. K. Kaletas, I. M. van der Wiel, J. Stauber, L. J. Dekker, C. Guzel, J. M. Kros, T. M. Luider and R. M. A. Heeren, *Sample preparation issues for tissue imaging by imaging MS*, Proteomics, **2009**, 2622-2633.

- [166] T. Dicke, M. Wegmann, S. Sel, H. Renz and H. Garn, *Gata-3-specific Dnazyme As An Approach For Asthma-therapy*, *J. Allergy Clin. Immunol.*, **2007**, S1.
- [167] C. Montixi, C. Langlet, A. M. Bernard, J. Thimonier, C. Dubois, M. A. Wurbel, J. P. Chauvin, M. Pierres and H. T. He, *Engagement of T cell receptor triggers its recruitment to low-density detergent-insoluble membrane domains*, *The EMBO journal*, **1998**, 5334-5348.
- [168] N. C. Thomson, M. Patel and A. D. Smith, *Lebrikizumab in the personalized management of asthma*, *Biologics*, **2012**, 329-335.
- [169] L. M. Neckers and J. Cossman, *Transferrin receptor induction in mitogen-stimulated human T lymphocytes is required for DNA synthesis and cell division and is regulated by interleukin-2 (TCGF)*, in: *Thymic Hormones and Lymphokines*, Springer, **1984**, pp. 383-394.
- [170] R. M. Galbraith, P. Werner, P. Arnaud and G. M. Galbraith, *Transferrin binding to peripheral blood lymphocytes activated by phytohemagglutinin involves a specific receptor. Ligand interaction*, *J. Clin. Invest.*, **1980**, 1135-1143.
- [171] N. H. Kim, V. Nadithe, M. Elsayed and O. M. Merkel, *Tracking and treating activated T cells*, *J. Drug Deliv. Sci. Tec.*, **2013**, 17-21.
- [172] S. Ramishetti, R. Kedmi, M. Goldsmith, F. Leonard, A. G. Sprague, B. Godin, M. Gozin, P. R. Cullis, D. M. Dykxhoorn and D. Peer, *Systemic Gene Silencing in Primary T Lymphocytes Using Targeted Lipid Nanoparticles*, *ACS Nano*, **2015**, 6706-6716.
- [173] M. Saraiva and A. O'garra, *The regulation of IL-10 production by immune cells*, *Nat. Rev. Immunol.*, **2010**, 170-181.
- [174] I. M. Chu, A. M. Michalowski, M. Hoenerhoff, K. M. Szauter, D. Luger, M. Sato, K. Flanders, A. Oshima, K. Csiszar and J. E. Green, *GATA3 inhibits lysyl oxidase-mediated metastases of human basal triple-negative breast cancer cells*, *Oncogene*, **2012**, 2017-2027.
- [175] R. Kandil, D. P. Feldmann, Y. Xie and O. M. Merkel, *Evaluating the Regulation of Cytokine Levels After siRNA Treatment in Antigen-Specific Target Cell Populations via Intracellular Staining*, *Nanotechnology for Nucleic Acid Delivery*, **2019**, 323-331.
- [176] S. A. Smith, L. I. Selby, A. P. R. Johnston and G. K. Such, *The Endosomal Escape of Nanoparticles: Toward More Efficient Cellular Delivery*, *Bioconjug Chem*, **2019**, 263-272.
- [177] L. I. Selby, C. M. Cortez-Jugo, G. K. Such and A. P. R. Johnston, *Nanoescapology: progress toward understanding the endosomal escape of polymeric nanoparticles*, *Wiley Interdiscip. Rev.: Nanomed. Nanobiotechnol.*, **2017**, e1452.
- [178] B. R. Olden, E. Cheng, Y. Cheng and S. H. Pun, *Identifying key barriers in cationic polymer gene delivery to human T cells*, *Biomaterials Science*, **2019**, 789-797.
- [179] K. K. Hou, H. Pan, G. M. Lanza and S. A. Wickline, *Melittin derived peptides for nanoparticle based siRNA transfection*, *Biomaterials*, **2013**, 3110-3119.
- [180] Y. Cheng, R. C. Yumul and S. H. Pun, *Virus-Inspired Polymer for Efficient In Vitro and In Vivo Gene Delivery*, *Angew. Chem., Int. Ed.*, **2016**, 12013-12017.
- [181] D. P. Feldmann, Y. Cheng, R. Kandil, Y. Xie, M. Mohammadi, H. Harz, A. Sharma, D. J. Peeler, A. Moszczynska, H. Leonhardt, S. H. Pun and O. M. Merkel, *In vitro and in vivo delivery of siRNA via VIPER polymer system to lung cells*, *J. Control. Release*, **2018**, 50-58.
- [182] Kandil, Y. Xie, R. Heermann, L. Isert, K. Jung, A. Mehta and O. M. Merkel, *Coming in and Finding Out: Blending Receptor-Targeted Delivery and Efficient Endosomal Escape in a Novel Bio-Responsive siRNA Delivery System for Gene Knockdown in Pulmonary T Cells*, *Advanced Therapeutics*, **2019**, 1900047.
- [183] O. M. Merkel and T. Kissel, *Nonviral Pulmonary Delivery of siRNA*, *Acc Chem Res*, **2012**, 961-970.
- [184] K. Zscheppang, J. Berg, S. Hedtrich, L. Verheyen, D. E. Wagner, N. Suttorp, S. Hippenstiel and A. C. Hocke, *Human Pulmonary 3D Models For Translational Research*, *Biotechnol. J.*, **2018**, 1700341.
- [185] O. M. Merkel, D. Librizzi, A. Pfestroff, T. Schurrat, K. Buyens, N. N. Sanders, S. C. De Smedt, M. Behe and T. Kissel, *Stability of siRNA polyplexes from poly(ethylenimine) and poly(ethylenimine)-g-poly(ethylene glycol) under in vivo conditions: effects on pharmacokinetics and biodistribution measured by Fluorescence Fluctuation Spectroscopy and Single Photon Emission Computed Tomography (SPECT) imaging*, *J Control Release*, **2009**, 148-159.

- [186] U. Griesenbach, D. M. Geddes and E. W. Alton, *Gene therapy for cystic fibrosis: an example for lung gene therapy*, Gene Ther., **2004**, S43-50.
- [187] N. J. Caplen, E. W. Alton, P. G. Middleton, J. R. Dorin, B. J. Stevenson, X. Gao, S. R. Durham, P. K. Jeffery, M. E. Hodson, C. Coutelle and et al., *Liposome-mediated CFTR gene transfer to the nasal epithelium of patients with cystic fibrosis*, Nat. Med., **1995**, 39-46.
- [188] D. M. K. Jensen, D. Cun, M. J. Maltesen, S. Frokjaer, H. M. Nielsen and C. Foged, *Spray drying of siRNA-containing PLGA nanoparticles intended for inhalation*, J Control Release, **2010**, 138-145.
- [189] T. W. M. Keil, D. P. Feldmann, G. Costabile, Q. Zhong, S. da Rocha and O. M. Merkel, *Characterization of spray dried powders with nucleic acid-containing PEI nanoparticles*, Eur J Pharm Biopharm, **2019**.
- [190] A. Ray, A. Mandal and A. K. Mitra, *Recent Patents in Pulmonary Delivery of Macromolecules*, Recent Pat Drug Deliv Formul, **2015**, 225-236.
- [191] P. Hematti, E. G. Schmuck, J. A. Kink and A. N. Raval, *Generation of therapeutic cells using extracellular components of target organs*, in, US Patent US20180282698A1 **2018**.
- [192] H. J. Kim, A. Kim, K. Miyata and K. Kataoka, *Recent progress in development of siRNA delivery vehicles for cancer therapy*, Adv. Drug Delivery Rev., **2016**, 61-77.
- [193] D. P. Feldmann, Y. Xie, S. K. Jones, D. Yu, A. Moszczynska and O. M. Merkel, *The impact of microfluidic mixing of triblock micelleplexes on in vitro / in vivo gene silencing and intracellular trafficking*, Nanotechnology, **2017**, 224001.
- [194] T. Endres, M. Zheng, M. Beck-Broichsitter and T. Kissel, *Lyophilised ready-to-use formulations of PEG-PCL-PEI nano-carriers for siRNA delivery*, Int. J. Pharm., **2012**, 121-124.
- [195] J. Horn, J. Schanda and W. Friess, *Impact of fast and conservative freeze-drying on product quality of protein-mannitol-sucrose-glycerol lyophilizates*, Eur. J. Pharm. Biopharm., **2018**, 342-354.
- [196] M. T. Cicerone, M. J. Pikal and K. K. Qian, *Stabilization of proteins in solid form*, Adv. Drug Delivery Rev., **2015**, 14-24.
- [197] W. Liang, M. Y. Chow, P. N. Lau, Q. T. Zhou, P. C. Kwok, G. P. Leung, A. J. Mason, H. K. Chan, L. L. Poon and J. K. Lam, *Inhalable dry powder formulations of siRNA and pH-responsive peptides with antiviral activity against H1N1 influenza virus*, Mol. Pharmaceutics, **2015**, 910-921.
- [198] W. L. Liang, M. Y. T. Chow, S. F. Chow, H. K. Chan, P. C. L. Kwok and J. K. W. Lam, *Using two-fluid nozzle for spray freeze drying to produce porous powder formulation of naked siRNA for inhalation*, Int. J. Pharm., **2018**, 67-75.
- [199] L. Liu, M. Zheng, D. Librizzi, T. Renette, O. M. Merkel and T. Kissel, *Efficient and Tumor Targeted siRNA Delivery by Polyethylenimine-graft-polycaprolactone-block-poly (ethylene glycol)-folate (PEI-PCL-PEG-Fol)*, Mol. Pharmaceutics, **2015**, 134-143.
- [200] HORIBA, *Understanding the Chi Square and R Parameter - Calculations in the LA-950 Software*, <https://www.horiba.com/fileadmin/uploads/Scientific/Documents/PSA/TN153.pdf>, 4.
- [201] S. Claus, C. Weiler, J. Schiewe and W. Friess, *Optimization of the fine particle fraction of a lyophilized lysozyme formulation for dry powder inhalation*, Pharm. Res., **2013**, 1698-1713.
- [202] M. Terrazas and E. T. Kool, *RNA major groove modifications improve siRNA stability and biological activity*, Nucleic Acids Res., **2009**, 346-353.
- [203] D. Weinbuch, J. K. Cheung, J. Ketelaars, V. Filipe, A. Hawe, J. den Engelsman and W. Jiskoot, *Nanoparticulate Impurities in Pharmaceutical-Grade Sugars and their Interference with Light Scattering-Based Analysis of Protein Formulations*, Pharm. Res., **2015**, 2419-2427.
- [204] N. K. Jain and I. Roy, *Effect of trehalose on protein structure*, Protein Sci., **2009**, 24-36.
- [205] I. Vollrath, W. Friess, A. Freitag, A. Hawe and G. Winter, *Comparison of ice fog methods and monitoring of controlled nucleation success after freeze-drying*, Int. J. Pharm., **2019**, 18-28.
- [206] J. H. Gitter, R. Geidobler, I. Presser and G. Winter, *A comparison of controlled ice nucleation techniques for freeze-drying of a therapeutic antibody*, J. Pharm. Sci., **2018**, 2748-2754.
- [207] J. H. Crowe, L. M. Crowe and D. Chapman, *Preservation of membranes in anhydrobiotic organisms: the role of trehalose*, Science, **1984**, 701-703.
- [208] J. H. Crowe, F. A. Hoekstra and L. M. Crowe, *Anhydrobiosis*, Annu. Rev. Physiol., **1992**, 579-599.
- [209] K. Izutsu and S. Kojima, *Excipient crystallinity and its protein-structure-stabilizing effect during freeze-drying*, J. Pharm. Pharmacol., **2002**, 1033-1039.

- [210] M. Adler and G. Lee, *Stability and surface activity of lactate dehydrogenase in spray-dried trehalose*, *J. Pharm. Sci.*, **1999**, 199-208.
- [211] M. Maury, K. Murphy, S. Kumar, L. Shi and G. Lee, *Effects of process variables on the powder yield of spray-dried trehalose on a laboratory spray-dryer*, *Eur. J. Pharm. Biopharm.*, **2005**, 565-573.
- [212] N. Y. Chew and H.-K. Chan, *Influence of particle size, air flow, and inhaler device on the dispersion of mannitol powders as aerosols*, *Pharm. Res.*, **1999**, 1098-1103.
- [213] Y. Y. Lee, J. X. Wu, M. Yang, P. M. Young, F. van den Berg and J. Rantanen, *Particle size dependence of polymorphism in spray-dried mannitol*, *Eur. J. Pharm. Sci.*, **2011**, 41-48.
- [214] K. J. Geh, M. Hubert and G. Winter, *Progress in formulation development and sterilisation of freeze-dried oligodeoxynucleotide-loaded gelatine nanoparticles*, *Eur. J. Pharm. Biopharm.*, **2018**, 10-20.
- [215] E. Y. Shalaev and G. Zografi, *How does residual water affect the solid-state degradation of drugs in the amorphous state?*, *J. Pharm. Sci.*, **1996**, 1137-1141.
- [216] J. H. Gitter, R. Geidobler, I. Presser and G. Winter, *Significant Drying Time Reduction Using Microwave- Assisted Freeze- Drying for a Monoclonal Antibody*, *J. Pharm. Sci.*, **2018**, 2538-2543.
- [217] I. Gonda and A. F. Abdelkhalik, *On the Calculation of Aerodynamic Diameters of Fibers*, *Aerosol Sci. Technol.*, **1985**, 233-238.
- [218] F. Cardarelli, L. Digiacomio, C. Marchini, A. Amici, F. Salomone, G. Fiume, A. Rossetta, E. Gratton, D. Pozzi and G. Caracciolo, *The intracellular trafficking mechanism of Lipofectamine-based transfection reagents and its implication for gene delivery*, *Sci. Rep.*, **2016**, 25879.
- [219] J. S. Kim, T. J. Yoon, K. N. Yu, M. S. Noh, M. Woo, B. G. Kim, K. H. Lee, B. H. Sohn, S. B. Park and J. K. Lee, *Cellular uptake of magnetic nanoparticle is mediated through energy-dependent endocytosis in A549 cells*, *J. Vet. Sci.*, **2006**, 321-326.
- [220] Y. Liu, O. Samsonova, B. Sproat, O. Merkel and T. Kissel, *Biophysical characterization of hyper-branched polyethylenimine-graft-polycaprolactone-block-mono-methoxyl-poly (ethylene glycol) copolymers (hy-PEI-PCL-mPEG) for siRNA delivery*, *J. Control. Release*, **2011**, 262-268.
- [221] C. Garcia-Galan, O. Barbosa and R. Fernandez-Lafuente, *Stabilization of the hexameric glutamate dehydrogenase from Escherichia coli by cations and polyethyleneimine*, *Enzyme Microb Technol*, **2013**, 211-217.
- [222] J. Horn, E. Tolardo, D. Fissore and W. Friess, *Crystallizing amino acids as bulking agents in freeze-drying*, *Eur. J. Pharm. Biopharm.*, **2018**, 70-82.
- [223] R. E. Johnson, C. F. Kirchoff and H. T. Gaud, *Mannitol–sucrose mixtures—versatile formulations for protein lyophilization*, *J. Pharm. Sci.*, **2002**, 914-922.
- [224] A. Hawe and W. Friess, *Physicochemical characterization of the freezing behavior of mannitol-human serum albumin formulations*, *AAPS PharmSciTech*, **2006**, 94.
- [225] O. M. Merkel, M. Zheng, H. Debus and T. Kissel, *Pulmonary gene delivery using polymeric nonviral vectors*, *Bioconjug Chem*, **2012**, 3-20.
- [226] J. A. Van Der Voorn, R. Vogel and B. M. Glossop, *Characterization of particles*, in, US Patents US9664643B2, **2017**.
- [227] E. Weatherall and G. R. Willmott, *Applications of tunable resistive pulse sensing*, *Analyst*, **2015**, 3318-3334.
- [228] E. L. Blundell, *Measuring zeta potential using tunable resistive pulse sensing: applications in biosensing*, in: Department of Chemistry, Loughborough University, **2017**, pp. 262.
- [229] iZON-Science-Ltd., *What is nanopore coating? Why is it important?*, in, <https://izon.com>, **2017**.
- [230] G. Willmott, R. Vogel, S. Yu, L. Groenewegen, G. Roberts, D. Kozak, W. Anderson and M. Trau, *Use of tunable nanopore blockade rates to investigate colloidal dispersions*, *Journal of Physics: Condensed Matter*, **2010**, 454116.
- [231] N. Hartl, F. Adams, G. Costabile, L. Isert, M. Döblinger, X. Xiao, R. Liu and O. M. Merkel, *The Impact of Nylon-3 Copolymer Composition on the Efficiency of siRNA Delivery to Glioblastoma Cells*, *Nanomaterials*, **2019**, 986.
- [232] E. Weatherall, *Advancement of Measurement Techniques for Tunable Resistive Pulse Sensing*, in: Chemistry, Victoria University of Wellington **2017**, pp. 368.

- [233] Z. S. Siwy, *Ion-Current Rectification in Nanopores and Nanotubes with Broken Symmetry*, *Adv. Funct. Mater.*, **2006**, 735-746.
- [234] E. L. Blundell, L. J. Mayne, M. Lickorish, S. D. Christie and M. Platt, *Protein detection using tunable pores: resistive pulses and current rectification*, *Faraday Discuss.*, **2016**, 487-505.
- [235] iZON-Science-Ltd., *How do I deal with a partial nanopore blockage during a recording?*, in: iZON Support, <https://support.izon.com/how-do-i-deal-with-a-partial-nanopore-blockage-during-a-recording>, **2017**.
- [236] S. Damiati, U. B. Kompella, S. A. Damiati and R. Kodzius, *Microfluidic devices for drug delivery systems and drug screening*, *Genes*, **2018**, 103.
- [237] S. Bhattacharjee, *DLS and zeta potential—What they are and what they are not?*, *J. Control. Release*, **2016**.
- [238] D. K. Jensen, L. B. Jensen, S. Koocheki, L. Bengtson, D. Cun, H. M. Nielsen and C. Foged, *Design of an inhalable dry powder formulation of DOTAP-modified PLGA nanoparticles loaded with siRNA*, *J. Control. Release*, **2012**, 141-148.
- [239] S. J. Sowerby, M. F. Broom and G. B. Petersen, *Dynamically resizable nanometre-scale apertures for molecular sensing*, *Sensors and Actuators B-Chemical*, **2007**, 325-330.
- [240] S. J. Sowerby, G. B. Petersen, M. F. Broom and M. D. Jones, *Detecting, measuring and controlling particles and electromagnetic radiation*, in, US Patents US8247214B2, **2012**.
- [241] E. Garza-Licudine, D. Deo, S. Yu, A. Uz-Zaman and W. B. Dunbar, *Portable nanoparticle quantization using a resizable nanopore instrument—the IZON qNano™*, in: Engineering in Medicine and Biology Society (EMBC), 2010 Annual International Conference of the IEEE, IEEE, **2010**, pp. 5736-5739.
- [242] G. S. Roberts, S. Yu, Q. Zeng, L. C. Chan, W. Anderson, A. H. Colby, M. W. Grinstaff, S. Reid and R. Vogel, *Tunable pores for measuring concentrations of synthetic and biological nanoparticle dispersions*, *Biosens. Bioelectron.*, **2012**, 17-25.
- [243] E. L. Blundell, R. Vogel and M. Platt, *Particle-by-particle charge analysis of DNA-modified nanoparticles using tunable resistive pulse sensing*, *Langmuir*, **2016**, 1082-1090.
- [244] E. L. Blundell, R. Vogel and M. Platt, *Determination of zeta potential via nanoparticle translocation velocities through a tunable nanopore: using DNA-modified particles as an example*, **2016**.
- [245] R. Vogel, W. Anderson, J. Eldridge, B. Glossop and G. Willmott, *A variable pressure method for characterizing nanoparticle surface charge using pore sensors*, *Anal. Chem.*, **2012**, 3125-3131.
- [246] R. Vogel, A. K. Pal, S. Jambhrunkar, P. Patel, S. S. Thakur, E. Reátegui, H. S. Parekh, P. Saá, A. Stassinopoulos and M. F. Broom, *High-Resolution Single Particle Zeta Potential Characterisation of Biological Nanoparticles using Tunable Resistive Pulse Sensing*, *Sci. Rep.*, **2017**, 17479.
- [247] R. Vogel, G. Willmott, D. Kozak, G. S. Roberts, W. Anderson, L. Groenewegen, B. Glossop, A. Barnett, A. Turner and M. Trau, *Quantitative sizing of nano/microparticles with a tunable elastomeric pore sensor*, *Anal. Chem.*, **2011**, 3499-3506.
- [248] G. R. Willmott, R. Vogel, S. S. C. Yu, L. G. Groenewegen, G. S. Roberts, D. Kozak, W. Anderson and M. Trau, *Use of tunable nanopore blockade rates to investigate colloidal dispersions*, *J. Phys.: Condens. Matter*, **2010**, 454116.
- [249] S. J. Shire, *Stability of Monoclonal Antibodies (mAbs)*, Woodhead Publishing, Monoclonal Antibodies, **2015**.
- [250] W. Wang, *Protein aggregation and its inhibition in biopharmaceutics*, *Int. J. Pharm.*, **2005**, 1-30.
- [251] H. C. Mahler, W. Friess, U. Grauschopf and S. Kiese, *Protein aggregation: pathways, induction factors and analysis*, *J. Pharm. Sci.*, **2009**, 2909-2934.
- [252] Y. Le Basle, P. Chennell, N. Tokhadze, A. Astier and V. Sautou, *Physicochemical Stability of Monoclonal Antibodies: A Review*, *J. Pharm. Sci.*, **2020**, 169-190.
- [253] M. J. Pikal, S. Shah, M. L. Roy and R. Putman, *The secondary drying stage of freeze drying: drying kinetics as a function of temperature and chamber pressure*, *Int. J. Pharm.*, **1990**, 203-217.

XII Acknowledgements

I like to thank my supervisor, Prof. Dr. Olivia Merkel, for all her efforts, trouble shootings, ideas and time she spent with me and this work. Thank you for giving me the opportunity to work on this thesis and the fascinating topic.

I also like to thank Prof. Dr. Frieß and Prof. Dr. Winter who supplied me with excellent feedback and ideas and created a great working atmosphere amongst all groups.

Further scientific exchange was provided by Christoph Marshall and Eduard Trenkenschuh who always had time for discussing current results and techniques. In line, I am gratefully thankful for the help of Julian Gitter who introduced me to residual moisture measurements and freeze drying in theory and practice. Immeasurable thanks go out to Dr. Aditi Mehta who provided me with guidance and superb expertise and knowledge in cell culture work but also with fun from the start of this thesis as my first lab mate.

I like to appreciate both of my current lab mates, Bettina Schwarz and Domizia Baldassi, two of the nicest people I have met, always caring and always with a smile on their faces.

I like to point out all current and former members of the Department of Pharmaceutical Technology and Biopharmaceutics. With all events we had, we had grown together into a proper squad giving each other a hand if help was needed. I am sure that together as a group we all enjoyed our theses to the fullest. Big thanks again to all the PI's who made this possible.

Thanks to my best friend who always reminded me that life also includes laughter and hop.

I also noticed how important it is to have people behind you who back you up when time gets rough. These people are not with me all day but they are there when I need them. Thank you, Mama and Papa, for your support and motivation throughout my studies and this whole thesis. Thanks to my older brother who has been like an idol to me since I was little.

Thanks to my little sister who is always able to cheer me up. This is the best family.

I am also very grateful that during the time of this thesis I have met the person who means the world to me. Thank you, my love, for always being there when research did not work out and things seemed to go crazy. And thank you so much for all the joy and fun you brought with you.

